MATHEMATICAL SOLUTIONS OF ELECTRIC POTENTIAL AND MAGNETIC FIELD RESPONSE FROM HETEROGENEOUS MEDIA

By

Warin Sripanya

A Thesis Submitted in Partial Fulfillment of the Requirements for the Degree
DOCTOR OF PHILOSOPHY
Program of MATHEMATICS
Graduate School
SILPAKORN UNIVERSITY
2011

MATHEMATICAL SOLUTIONS OF ELECTRIC POTENTIAL AND MAGNETIC FIELD RESPONSE FROM HETEROGENEOUS MEDIA

By

Warin Sripanya

A Thesis Submitted in Partial Fulfillment of the Requirements for the Degree
DOCTOR OF PHILOSOPHY
Program of MATHEMATICS
Graduate School
SILPAKORN UNIVERSITY
2011

The Graduate School, Silpakorn University has approved and accredited the Thesis title of "Mathematical Solutions of Electric Potential and Magnetic Field Response from Heterogeneous Media" submitted by Mr.Warin Sripanya as a partial fulfillment of the requirements for the degree of Doctor of Philosophy in MATHEMATICS.

....

(Assistant Professor Panjai Tantatsanawong, Ph.D.)

Dean of Graduate School

........../.............../..........

The Thesis Advisor

Associate Professor Suabsagun Yooyuanyong, Ph.D.

The Thesis Examination Committee

.... Chairman

(Sawanya Sakuntasathien, Ph.D.)

........../.............../..........

.... Member

(Associate Professor Sanoe Koonprasert, Ph.D.)

........../.............../..........

.... Member

(Associate Professor Suabsagun Yooyuanyong, Ph.D.)

........../.............../..........

50305804 : MAJOR : MATHEMATICS
KEY WORDS : MAGNETIC FIELD/ ELECTRIC POTENTIAL/ DIRECT CURRENT
WARIN SRIPANYA : MATHEMATICAL SOLUTIONS OF ELECTRIC POTENTIAL AND MAGNETIC FIELD RESPONSE FROM HETEROGENEOUS MEDIA. THESIS ADVISOR : ASSOC. PROF. SUABSAGUN YOOYUANYONG, Ph.D. 96 pp.

Magnetic field and electric potential resulting from the injection of electric current into the ground can be used to explore the earth's structures. We derive analytical solutions of the steady state magnetic field due to a direct current source on four types of multilayered earth structures including layers having constant, exponentially, linearly and binomially varying conductivities. The Hankel transform is introduced to our problems and analytical results are obtained. Our solutions are achieved by solving a boundary value problem in the wave number domain and then transforming the solution back to the spatial domain. The propagator matrix technique is used to formulate recurrence relations for solving the problems. One of these relations is applicable to general cases in which the layers have either constant or exponentially varying conductivities. Another one is generalized in all cases where the layers have constant, linearly or binomially varying conductivities. The effects of magnetic fields obtained from the DC and MMR methods are plotted and compared to show the behavior in response to different ground structures at many depths while some parameters are approximately given. The ground structures of rice paddy field and marine shrimp aquaculture farm are used to investigate the magnetic field responses. The magnetic fields obtained from different ground structures and methods of investigation are very much different, especially for the first 5 metres of source-receiver spacing. The curves of magnetic fields show some significance to the depth of overburden layer. An inverse problem via the use of the Newton-Raphson optimization technique is introduced for finding a conductivity parameter of the ground. The method leads to very good results and has high speed of convergence. Analytical solutions of the electric potential are derived for the problem of a buried current source and a buried receiver. The models of a layered earth are developed for source and receiver electrodes buried anywhere within transitional ground structures including layers having linearly and binomially varying conductivities. The propagator matrix technique is also applied to make upward and downward recurrences for solving the problems. Our solutions can be used to interpret hole-to-hole, hole-to-surface and conventional surface array data. The inversion processes, using the Newton-Raphson and quasi-Newton methods, are conducted to estimate the conductivity variation parameters. A regularization technique can also be applied to inverse problems arising in geoelectrical resistivity sounding. We propose here to use a regularized inversion scheme for interpretation of magnetic field data gathered from a horizontally stratified layered earth. The iterative scheme using the regularized conjugate gradient method is applied to estimate the conductivity parameters of the ground. The L-curve criterion is used to determine a suitable value of the regularization parameter. The final inverted model obtained is qualitatively in good agreement with the real model from synthetic data. A comparison of inversion results obtained from our scheme, conventional conjugate gradient and Levenberg-Marquardt methods on a test data set clearly demonstrates an edge over the other two stated schemes as far as the robustness is concerned. The scheme described here has been successfully used for geophysical inversion of magnetic field data.

Department of Mathematics   Graduate School, Silpakorn University   Academic Year 2011
Student's signature ....
Thesis Advisor's signature ....

Acknowledgements

First and foremost, I would like to express my deepest sense of gratitude to my thesis supervisor, Assoc. Prof. Dr. Suabsagun Yooyuanyong, whose expertise, understanding, and patience, added considerably to my graduate experience. I appreciate his vast knowledge and skill in many areas (e.g., vision, aging, ethics, interaction with participants), and his assistance in writing reports (i.e., grant proposals, scholarship applications and this thesis).

I would also like to express my thanks and appreciation to the other members of my thesis committee, Dr. Sawanya Sakuntasathien and Assoc. Prof. Dr. Sanoe Koonprasert, whose helpful suggestions, increased readability and reduced ambiguity.

A very special thanks goes out to Dr. Noppadol Chumchob, without whose motivation and encouragement, I would not have considered a graduate career in geophysical research. He provided me with direction and technical support.

I take this opportunity to express the profound gratitude from my deep heart to my beloved parents and my siblings for their love and continuous support, both spiritually and materially. I must also acknowledge my best friend, Pakamas Pawong for the support and encouragement whenever I was in need.

Last but not least, I recognize that this thesis would not have been possible without the financial assistance of the Nakhon Pathom Rajabhat University (Graduate Scholarship), and express my gratitude to this agency.

Contents

Chapter 1

Introduction

1.1 DC Electrical Methods and Their Applications

While both electromagnetic and DC electrical methods first came into use in the early part of the 20th century, the DC methods gained early acceptance because of less demanding theoretical and instrumentation considerations. DC methods have become the most widely used geoelectrical method. These techniques have been standardized, and the capabilities and limitations of the methods are widely understood and accepted.

In fact, it is important to realize that direct current is not used in DC electrical surveys. The DC techniques could better be described as employing time varying direct current. This phrase may well be considered to be an oxymoron, but it is useful in pointing out that when we speak of a DC geoelectrical method, we mean that theory based on DC behavior is used, not direct current. There are many sources of nearly DC voltage in the earth, and it is not easily possible to identify the DC voltage caused by current that we inject into the ground from all the other DC voltages. We make our contribution detectable by causing it to vary with time in a specified way, so that the signature of the signal can be recognized. The signature can be of any form, so long as the frequency is low enough that the term $-\partial\mathbf{B}/\partial t$ in Maxwell's equations can be ignored.

A particularly important group of DC electrical techniques includes those known as vertical electrical sounding (VES). In traditional soundings, an assumption is made that the geoelectrical structure in the area of exploration is one-dimensional, with resistivity in the earth varying only with depth. The concept of one-dimensionality is often extended to include geoelectrical structures which are obviously other than one-dimensional. In such cases, representation of a more complicated earth structures by a series of one-dimensional resistivity-depth functions along a profile is used as a first step towards a more exact two- or three-dimensional interpretation.

Another approach to the use of DC surveys is in horizontal profiling.

In this application, we assume that the geoelectrical structure is one in which electrical resistivity in the earth changes laterally. Surveys are then carried out by moving electrode arrays along a profile, attempting to determine the location of changes in ground resistivity along the profile.

A third approach to using DC surveys is the electrical mapping method. In such a survey, a single source of current flow in the ground is established, and thus, the electric field or the potential is mapped over the surface of the earth around the source in an area of exploration interest. Mapping the spatial behavior of the DC field is useful in that interpretations can be made fairly readily in terms of two- and three-dimensional earth structures.

A highly important time-varying electrical method is the induced polarization (IP) method. In this method, it is recognized that the current flow in the earth can cause chemical reactions with some minerals, in particular the metal oxides and sulfides, causing some of the energy to be stored as chemical energy. As the level of the current is changed, the rate of chemical reaction changes, and in particular, if the current is interrupted, the chemical reactions may partially reverse, returning some of the chemical energy as current which decays in time. The process can be considered to be roughly analogous to the charging and discharging of a capacitor. This leads to a time-varying behavior of the electric field in the earth, but when the frequencies are low enough that we can still say $-\partial\mathbf{B}/\partial t \approx 0$, the behavior can still be described adequately with what we call DC theory. The IP method has been found to be extraordinarily effective for use in exploration for mineral deposits since its introduction in the 1940s. A sectioning approach is often used with IP surveys, that is, an electrode array is both expanded in size and moved laterally along a traverse in the course of a survey. The product is a pseudosection resembling a cross section of the earth along the traverse.

The basic premise in development of time-varying DC methods is that the term $-\partial\mathbf{B}/\partial t$ in Maxwell's equations can be considered to equal zero, and therefore, no magnetic induction effect exists. However, we need not assume that all magnetic effects are absent. In fact, the equation

$$\nabla \times \mathbf{H} = \mathbf{J}$$

holds independently of the size of the term $-\partial\mathbf{B}/\partial t$. This equation states that we can measure a magnetic field as a means for characterizing the behavior of a time-varying direct current field. Jakosky [31, 32] suggested that magnetic field measurements be used in place of electric field measurements in determinations of earth resistivity, while Seigal has developed the approach of using magnetic field sensors in induced polarization surveys (Seigal [51], Seigel and Howland-Rose [52]). The use of magnetic field measurements in resistivity determinations has been termed the magnetometric resistivity method, or MMR (Edwards [15], Edwards and Howell [16], Nabighian et al. [43]). The MMR method differs from the traditional resistivity method in that the potential electrodes are replaced by a highly sensitive coil or magnetometer and one or more components of the magnetic field are recorded. This method has been used successfully to explore for massive sulfides and for geothermal resources, to map regional geology, to study hard rock sites for nuclear waste disposal, to locate reef structures in sedimentary basins, and to obtain conductivity profiles of the sea floor with depth, both in shallow and deep water.

1.2 Outline of the Thesis

This thesis deals with development and application of new electrical techniques for enhanced investigation in geophysical explorations. A horizontally stratified structure of the earth is studied in this research work.

Chapter 2 presents an electrical method used for investigation of a multilayered earth structure. The method proposed here is based on the measurement of low-level, low-frequency static magnetic fields associated with noninductive current flow between two current electrodes on the earth's surface. Analytical solutions of the steady state magnetic field due to a direct current source are derived in this study. Two types of multilayered earth structures are considered, including layers having constant and exponentially varying conductivities. The Hankel transform is introduced to our problems and analytical results are obtained. Our solutions are achieved by solving a boundary value problem in the wave number domain and then transforming the solution back to the spatial domain. The propagator matrix technique is used to formulate recurrence relations for solving the problems. The curves of magnetic fields obtained from the DC and MMR methods are plotted and compared to show the behavior in response to different ground structures while some parameters are approximately given. The ground structures of rice paddy field and marine shrimp aquaculture farm are used to investigate the magnetic field responses.

In Chapter 3, analytical solutions of the steady state magnetic field are developed for the problem of a transitional medium in which the ground layers have linearly and binomially varying conductivities. An inverse problem via the use of the Newton-Raphson optimization technique is introduced for finding a conductivity parameter of the ground.

Chapter 4 describes a study of interpretation of electrical surveys using buried current electrodes. The area of investigated study is situated in a transitional zone. We derive analytical solutions of the electric potential resulting from a direct current point source located anywhere within multilayered earth structures. The propagator matrix technique is also applied to make upward and downward recurrences for solving the problems. The inversion processes, using the Newton-Raphson and quasi-Newton methods, are conducted to estimate the conductivity variation parameters.

Chapter 5 presents an inversion scheme for nonlinear ill-posed problems arising in geoelectrical resistivity sounding. The proposed method is the regularized conjugate gradient method which is used to interpret magnetic field data gathered from a horizontally stratified layered earth. The L-curve criterion is applied to determine a suitable value of the regularization parameter. A comparison of this scheme with conventional conjugate gradient and Levenberg-Marquardt methods on a test model is also presented.

Finally, in Chapter 6, we summarize the results and contributions of this thesis, and indicate future research directions.

Chapter 2

Magnetic Field of a DC Source on a Multilayered Earth

2.1 Introduction

Usually interpretations of traditional resistivity soundings are conducted by assuming that the earth's structure consists of horizontally stratified layers having constant conductivities. In many practical cases, the assumption may be valid. A layered earth model is used to simulate the stratigraphic target. The numerical evaluation of apparent resistivities for a horizontally stratified earth is done by integrating the Bessel integral of a recurrence relation, usually by digital filtering. However, in the real earth situation, there are cases where the subsurface conductivity varies continuously rather than discontinuously with depth. Although stratified earth models with a large number of layers may satisfactorily represent the geoelectric structure of continuously varying conductivity, numerical computation is not efficient. Many authors have investigated the case where the subsurface has a monotonic continuous variation of conductivity with depth. A particularly interesting case is a multilayered earth with one or more layers having exponentially varying conductivities. Stoyer and Wait [58] studied the problem of computing apparent resistivity for a structure with a homogeneous overburden overlying a medium whose resistivity varies exponentially with depth. Banerjee et al. [7] gave expressions for apparent resistivity of a multilayered earth with a layer having exponentially varying conductivity. Kim and Lee [34] derived a new resistivity kernel function for calculating apparent resistivity of a multilayered earth with layers having exponentially varying resistivities.

The mathematical and analytical aspects of the magnetometric resistivity (MMR) method are summarized in a review paper by Edwards et al. [17]. The characteristic anomalies for an anisotropic earth, vertical and dipping contacts, thin and thick dykes, semicylindrical and hemispherical depressions as well as alpha media are described. Edwards [15] concentrated upon estimating the ratio of the magnetic fields below and above a known conductive layer to infer the basement resistivity. Inayat-Hussain [26] gave a new proof that the magnetic field outside the one-dimensional medium is independent of the electrical conductivity. Veitch et al. [62] indirectly derived the magnetic field within a layered earth excited from a point source by applying Stoke's theorem and Ampère's law to the electric potential, which was presented by Daniels [13]. Unfortunately, these works are not sufficiently general about the magnetic field to be used for many current applications. Chen and Oldenburg [11] derived the magnetic field directly by solving a boundary value problem of a horizontally stratified layered earth with homogeneous layers, similar to the approach used by Edwards [15]. Yooyuanyong and Sripanya [70, 71] developed analytical solutions for the problems of heterogeneous layers in which the conductivities vary exponentially, linearly and binomially with depth.

In this study, the electrical exploration method based on the measurement of static magnetic fields associated with noninductive current flow between two current electrodes on the earth's surface is introduced. We derive analytical solutions of the steady state magnetic field due to a direct current source on two types of multilayered earth structures including layers having constant conductivities and layers having exponentially varying conductivities. The Hankel transform is introduced to our problems and analytical results are obtained. Our solutions are achieved by solving a boundary value problem in the wave number domain and then transforming the solution back to the spatial domain. The propagator matrix technique is used to formulate recurrence relations for solving the problems. The curves of magnetic fields obtained from the DC and MMR methods are plotted and compared to show the behavior in response to different ground structures while some parameters are approximately given. The ground structures of rice paddy field and marine shrimp aquaculture farm are used to investigate the magnetic field responses. An inverse problem via the use of the Newton-Raphson optimization technique is introduced for finding a conductivity parameter of the ground.

2.2 Model and Basic Equations

In our geometric model, a point source of direct current I is located at the interface between two half-spaces (see Figure 2.1). The half-space above the interface ($z < 0$) is the region of air with conductivity approximately equal to zero, whereas the half-space below the interface ($z > 0$) is an n-layered horizontally stratified earth with depths to the layers $h_1, h_2, \ldots, h_{n-1}$ (the lowermost layer extending to infinity) measured from the ground surface, where $n \geq 2$ is an integer. Each layer has conductivity as a function of depth, i.e., $\sigma_k(z)$ for layer $1 \leq k \leq n$. The general steady state Maxwell's equations in the frequency domain (Chen and Oldenburg [11, 12]) can be used to determine the magnetic field for this problem, namely

$$\nabla \times \mathbf{E} = \mathbf{0} \tag{2.1}$$

and

$$\nabla \times \mathbf{H} = \sigma \mathbf{E}, \tag{2.2}$$

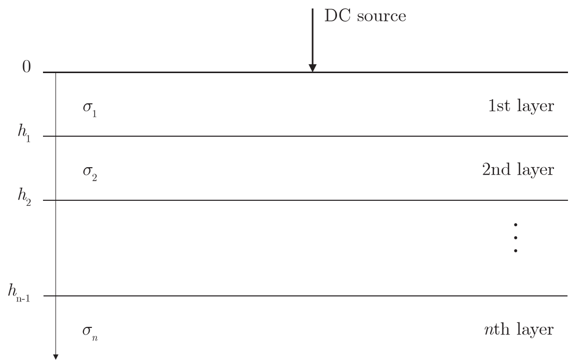

Figure 2.1: Geometric model of the earth's structure.

where $\mathbf{E}$ is the vector electric field, $\mathbf{H}$ is the vector magnetic field, σ is the conductivity of the medium and ∇ is the del operator. Eliminating $\mathbf{E}$ from equations (2.1) and (2.2), we obtain

$$\nabla \times \frac{1}{\sigma} \nabla \times \mathbf{H} = \mathbf{0}.$$

This can be expressed in cylindrical coordinates (r, ϕ, z) as

$$\begin{aligned} \mathbf{0} = &\left(\frac{1}{r}\frac{\partial}{\partial \phi}\frac{1}{\sigma}\left(\frac{1}{r}\frac{\partial}{\partial r}(rH_\phi) - \frac{1}{r}\frac{\partial H_r}{\partial \phi}\right) - \frac{\partial}{\partial z}\frac{1}{\sigma}\left(\frac{\partial H_r}{\partial z} - \frac{\partial H_z}{\partial r}\right)\right)\mathbf{e}_r \\ &+ \left(\frac{\partial}{\partial z}\frac{1}{\sigma}\left(\frac{1}{r}\frac{\partial H_z}{\partial \phi} - \frac{\partial H_\phi}{\partial z}\right) - \frac{\partial}{\partial r}\frac{1}{\sigma}\left(\frac{1}{r}\frac{\partial}{\partial r}(rH_\phi) - \frac{1}{r}\frac{\partial H_r}{\partial \phi}\right)\right)\mathbf{e}_\phi \\ &+ \left(\frac{1}{r}\frac{\partial}{\partial r}\left(\frac{r}{\sigma}\left(\frac{\partial H_r}{\partial z} - \frac{\partial H_z}{\partial r}\right)\right) - \frac{1}{r}\frac{\partial}{\partial \phi}\frac{1}{\sigma}\left(\frac{1}{r}\frac{\partial H_z}{\partial \phi} - \frac{\partial H_\phi}{\partial z}\right)\right)\mathbf{e}_z, \end{aligned} \quad (2.3)$$

where H_r, H_ϕ and H_z are the components of $\mathbf{H}$ in $\mathbf{e}_r$, $\mathbf{e}_\phi$ and $\mathbf{e}_z$ directions, respectively. Since the problem is axisymmetric and $\mathbf{H}$ has only the azimuthal component in cylindrical coordinates, for simplicity, we use H to represent the azimuthal component in the following derivations. Simplifying equation (2.3) yields

$$-\frac{\partial}{\partial z}\frac{1}{\sigma}\frac{\partial H}{\partial z} - \frac{\partial}{\partial r}\frac{1}{\sigma r}\frac{\partial}{\partial r}(rH) = 0,$$

or

$$\begin{aligned} \frac{1}{\sigma}\frac{\partial^2 H}{\partial z^2} + \frac{\partial}{\partial z}\left(\frac{1}{\sigma}\right)\frac{\partial H}{\partial z} + \frac{1}{\sigma}\left(\frac{1}{r}\frac{\partial^2}{\partial r^2}(rH) + \frac{\partial}{\partial r}\left(\frac{1}{r}\right)\frac{\partial}{\partial r}(rH)\right) \\ + \frac{\partial}{\partial r}\left(\frac{1}{\sigma}\right)\frac{1}{r}\frac{\partial}{\partial r}(rH) = 0. \end{aligned}$$

In our study, we denote σ as a function of only depth z, and we now have

$$\frac{\partial^2 H}{\partial z^2} + \sigma\frac{\partial}{\partial z}\left(\frac{1}{\sigma}\right)\frac{\partial H}{\partial z} + \frac{\partial^2 H}{\partial r^2} + \frac{1}{r}\frac{\partial H}{\partial r} - \frac{1}{r^2}H = 0. \quad (2.4)$$

The Hankel transform (Ali and Kalla [2]) is introduced and defined by

$$\tilde{H}(\lambda, z) = \int_0^\infty \lambda r H(r, z) J_1(\lambda r)\, dr$$

and

$$H(r, z) = \int_0^\infty \tilde{H}(\lambda, z) J_1(\lambda r)\, d\lambda,$$

where J_1 is the Bessel function of the first kind of order one and λ is the scaling factor. Taking the transformation on both sides of equation (2.4), we obtain

$$\int_0^\infty \lambda r \left(\frac{\partial^2 H}{\partial z^2} + \sigma \frac{\partial}{\partial z}\left(\frac{1}{\sigma}\right)\frac{\partial H}{\partial z} + \frac{\partial^2 H}{\partial r^2} + \frac{1}{r}\frac{\partial H}{\partial r} - \frac{1}{r^2} H \right) J_1(\lambda r)\, dr$$
$$= \int_0^\infty \lambda r \cdot 0 \cdot J_1(\lambda r)\, dr,$$

or

$$\int_0^\infty \lambda r \frac{\partial^2 H}{\partial z^2} J_1(\lambda r)\, dr + \sigma \frac{\partial}{\partial z}\left(\frac{1}{\sigma}\right) \int_0^\infty \lambda r \frac{\partial H}{\partial z} J_1(\lambda r)\, dr$$
$$+ \int_0^\infty \lambda \left(r \frac{\partial^2 H}{\partial r^2} + \frac{\partial H}{\partial r} \right) J_1(\lambda r)\, dr - \int_0^\infty \frac{\lambda}{r} H J_1(\lambda r)\, dr = 0,$$

or

$$\int_0^\infty \lambda r \frac{\partial^2 H}{\partial z^2} J_1(\lambda r)\, dr + \sigma \frac{\partial}{\partial z}\left(\frac{1}{\sigma}\right) \int_0^\infty \lambda r \frac{\partial H}{\partial z} J_1(\lambda r)\, dr$$
$$+ \int_0^\infty \lambda \frac{\partial}{\partial r}\left(r \frac{\partial H}{\partial r} \right) J_1(\lambda r)\, dr - \int_0^\infty \frac{\lambda}{r} H J_1(\lambda r)\, dr = 0,$$

or

$$\int_0^\infty \lambda r \frac{\partial^2 H}{\partial z^2} J_1(\lambda r)\, dr + \sigma \frac{\partial}{\partial z}\left(\frac{1}{\sigma}\right) \int_0^\infty \lambda r \frac{\partial H}{\partial z} J_1(\lambda r)\, dr$$
$$+ \lim_{a \to 0^+} \int_a^1 \lambda \frac{\partial}{\partial r}\left(r \frac{\partial H}{\partial r} \right) J_1(\lambda r)\, dr + \lim_{b \to \infty} \int_1^b \lambda \frac{\partial}{\partial r}\left(r \frac{\partial H}{\partial r} \right) J_1(\lambda r)\, dr$$
$$- \int_0^\infty \frac{\lambda}{r} H J_1(\lambda r)\, dr = 0.$$

Integrating by parts on the third and fourth terms of the above equation yields

$$\int_0^\infty \lambda r \frac{\partial^2 H}{\partial z^2} J_1(\lambda r)\, dr + \sigma \frac{\partial}{\partial z}\left(\frac{1}{\sigma}\right) \int_0^\infty \lambda r \frac{\partial H}{\partial z} J_1(\lambda r)\, dr$$
$$+ \lim_{a \to 0^+} \left(\lambda r \frac{\partial H}{\partial r} J_1(\lambda r) \right)\Bigg|_a^1 - \lim_{a \to 0^+} \int_a^1 \lambda r \frac{\partial H}{\partial r} \frac{d}{dr} J_1(\lambda r)\, dr$$
$$+ \lim_{b \to \infty} \left(\lambda r \frac{\partial H}{\partial r} J_1(\lambda r) \right)\Bigg|_1^b - \lim_{b \to \infty} \int_1^b \lambda r \frac{\partial H}{\partial r} \frac{d}{dr} J_1(\lambda r)\, dr$$
$$- \int_0^\infty \frac{\lambda}{r} H J_1(\lambda r)\, dr = 0,$$

or

$$\int_0^\infty \lambda r \frac{\partial^2 H}{\partial z^2} J_1(\lambda r)\,dr + \sigma \frac{\partial}{\partial z}\left(\frac{1}{\sigma}\right) \int_0^\infty \lambda r \frac{\partial H}{\partial z} J_1(\lambda r)\,dr - \lim_{a\to 0^+} \int_a^1 \lambda r \frac{\partial H}{\partial r} \frac{d}{dr} J_1(\lambda r)\,dr - \lim_{b\to\infty} \int_1^b \lambda r \frac{\partial H}{\partial r} \frac{d}{dr} J_1(\lambda r)\,dr - \int_0^\infty \frac{\lambda}{r} H J_1(\lambda r)\,dr = 0.$$

Integrating by parts again on the third and fourth terms of the above equation, we obtain

$$\int_0^\infty \lambda r \frac{\partial^2 H}{\partial z^2} J_1(\lambda r)\,dr + \sigma \frac{\partial}{\partial z}\left(\frac{1}{\sigma}\right) \int_0^\infty \lambda r \frac{\partial H}{\partial z} J_1(\lambda r)\,dr - \lim_{a\to 0^+} \left(\lambda r H \frac{d}{dr} J_1(\lambda r)\right)\Bigg|_a^1 + \lim_{a\to 0^+} \int_a^1 \lambda H \frac{d}{dr}\left(r \frac{d}{dr} J_1(\lambda r)\right) dr - \lim_{b\to\infty} \left(\lambda r H \frac{d}{dr} J_1(\lambda r)\right)\Bigg|_1^b + \lim_{b\to\infty} \int_1^b \lambda H \frac{d}{dr}\left(r \frac{d}{dr} J_1(\lambda r)\right) dr - \int_0^\infty \frac{\lambda}{r} H J_1(\lambda r)\,dr = 0,$$

or

$$\int_0^\infty \lambda r \frac{\partial^2 H}{\partial z^2} J_1(\lambda r)\,dr + \sigma \frac{\partial}{\partial z}\left(\frac{1}{\sigma}\right) \int_0^\infty \lambda r \frac{\partial H}{\partial z} J_1(\lambda r)\,dr + \lim_{a\to 0^+} \int_a^1 \lambda H \frac{d}{dr}\left(r \frac{d}{dr} J_1(\lambda r)\right) dr + \lim_{b\to\infty} \int_1^b \lambda H \frac{d}{dr}\left(r \frac{d}{dr} J_1(\lambda r)\right) dr - \int_0^\infty \frac{\lambda}{r} H J_1(\lambda r)\,dr = 0,$$

or

$$\int_0^\infty \lambda r \frac{\partial^2 H}{\partial z^2} J_1(\lambda r)\,dr + \sigma \frac{\partial}{\partial z}\left(\frac{1}{\sigma}\right) \int_0^\infty \lambda r \frac{\partial H}{\partial z} J_1(\lambda r)\,dr + \int_0^\infty \lambda H \frac{d}{dr}\left(r \frac{d}{dr} J_1(\lambda r)\right) dr - \int_0^\infty \frac{\lambda}{r} H J_1(\lambda r)\,dr = 0,$$

or

$$\int_0^\infty \lambda r \frac{\partial^2 H}{\partial z^2} J_1(\lambda r)\,dr + \sigma \frac{\partial}{\partial z}\left(\frac{1}{\sigma}\right) \int_0^\infty \lambda r \frac{\partial H}{\partial z} J_1(\lambda r)\,dr + \int_0^\infty \lambda H \left(r \frac{d^2}{dr^2} J_1(\lambda r) + \frac{d}{dr} J_1(\lambda r)\right) dr - \int_0^\infty \frac{\lambda}{r} H J_1(\lambda r)\,dr = 0,$$

or

$$\int_0^\infty \lambda r \frac{\partial^2 H}{\partial z^2} J_1(\lambda r)\,dr + \sigma \frac{\partial}{\partial z}\left(\frac{1}{\sigma}\right) \int_0^\infty \lambda r \frac{\partial H}{\partial z} J_1(\lambda r)\,dr + \int_0^\infty \lambda H \left(\lambda^2 r J_1''(\lambda r) + \lambda J_1'(\lambda r)\right) dr - \int_0^\infty \frac{\lambda}{r} H J_1(\lambda r)\,dr = 0,$$

or

$$\int_0^\infty \lambda r \frac{\partial^2 H}{\partial z^2} J_1(\lambda r)\, dr + \sigma \frac{\partial}{\partial z}\left(\frac{1}{\sigma}\right) \int_0^\infty \lambda r \frac{\partial H}{\partial z} J_1(\lambda r)\, dr$$
$$+ \int_0^\infty \lambda r H \left(\lambda^2 J_1''(\lambda r) + \frac{\lambda}{r} J_1'(\lambda r) - \frac{1}{r^2} J_1(\lambda r)\right) dr = 0.$$

Since J_1 is the solution of Bessel's differential equation, we now have

$$\lambda^2 J_1''(\lambda r) + \frac{\lambda}{r} J_1'(\lambda r) - \frac{1}{r^2} J_1(\lambda r) = -\lambda^2 J_1(\lambda r).$$

This yields

$$\int_0^\infty \lambda r \frac{\partial^2 H}{\partial z^2} J_1(\lambda r)\, dr + \sigma \frac{\partial}{\partial z}\left(\frac{1}{\sigma}\right) \int_0^\infty \lambda r \frac{\partial H}{\partial z} J_1(\lambda r)\, dr$$
$$- \lambda^2 \int_0^\infty \lambda r H J_1(\lambda r)\, dr = 0.$$

Hence, the Hankel transform of equation (2.4) results in

$$\frac{\partial^2 \tilde{H}}{\partial z^2} + \sigma \frac{\partial}{\partial z}\left(\frac{1}{\sigma}\right) \frac{\partial \tilde{H}}{\partial z} - \lambda^2 \tilde{H} = 0. \tag{2.5}$$

Therefore, the magnetic field in each layer can be obtained by taking the inverse Hankel transform to the solution of equation (2.5), which satisfies the following boundary conditions:

1. The azimuthal component of the magnetic field tends to zero as z tends to infinity, i.e.,
$$\lim_{z \to \infty} \tilde{H}_n = 0. \tag{2.6}$$

2. The vertical component of the current density must be zero at the free surface ($z = 0$) except in an infinitesimal neighborhood around a current source (Kim and Lee [34]), i.e.,
$$\sigma_1 E_1^z\big|_{z=0} = \frac{I}{2\pi} \frac{\delta(r)}{r}, \tag{2.7}$$
where E^z is the vertical component of the electric field.

3. The azimuthal component of the magnetic field needs to be continuous on each of the boundary planes in the earth, i.e., for each $1 \le k \le n-1$,
$$\lim_{z \to h_k^-} \tilde{H}_k = \lim_{z \to h_k^+} \tilde{H}_{k+1}. \tag{2.8}$$

4. The radial component of the electric field, denoted by E^r, needs to be continuous on each of the boundary planes in the earth, i.e., for each $1 \le k \le n-1$,
$$\lim_{z \to h_k^-} \tilde{E}_k^r = \lim_{z \to h_k^+} \tilde{E}_{k+1}^r. \tag{2.9}$$

To determine the radial and vertical components of the electric field related to the azimuthal component of the magnetic field, we expand equation (2.2) and obtain

$$\mathbf{E} = \left(\frac{1}{\sigma r}\frac{\partial H_z}{\partial \phi} - \frac{1}{\sigma}\frac{\partial H_\phi}{\partial z}\right)\mathbf{e}_r + \left(\frac{1}{\sigma}\frac{\partial H_r}{\partial z} - \frac{1}{\sigma}\frac{\partial H_z}{\partial r}\right)\mathbf{e}_\phi + \left(\frac{1}{\sigma r}\frac{\partial}{\partial r}\left(rH_\phi\right) - \frac{1}{\sigma r}\frac{\partial H_r}{\partial \phi}\right)\mathbf{e}_z.$$

This yields

$$E^r = -\frac{1}{\sigma}\frac{\partial H}{\partial z}, \qquad E^z = \frac{1}{\sigma r}\frac{\partial}{\partial r}\left(rH\right).$$

2.3 Response of a Layer Having Constant Conductivity

For each layer k, where $1 \leq k \leq n$ and $n \geq 2$, having constant conductivity, equation (2.5) reduces to

$$\frac{\partial^2 \tilde{H}_k}{\partial z^2} - \lambda^2 \tilde{H}_k = 0$$

and the solution is

$$\tilde{H}_k\left(\lambda, z\right) = A_k e^{-\lambda z} + B_k e^{\lambda z},$$

where A_k and B_k are arbitrary constants, which can be determined by using the boundary conditions. Thus, the magnetic field in layer k is

$$H_k\left(r, z\right) = \int_0^\infty \left(A_k e^{-\lambda z} + B_k e^{\lambda z}\right) J_1\left(\lambda r\right) d\lambda. \tag{2.10}$$

2.3.1 Solution for a 2-layered Earth

We firstly consider a 2-layered earth model. An overburden has a constant conductivity σ_1 with thickness h over a host medium having constant conductivity σ_2. The magnetic fields in an overburden, denoted by $\tilde{H}_1$, and in a host, denoted by $\tilde{H}_2$, can be written as

$$\tilde{H}_1\left(\lambda, z\right) = A_1 e^{-\lambda z} + B_1 e^{\lambda z}$$

and

$$\tilde{H}_2\left(\lambda, z\right) = A_2 e^{-\lambda z} + B_2 e^{\lambda z},$$

where A_1, B_1, A_2 and B_2 are arbitrary constants, which can be determined by using the boundary conditions. To satisfy (2.6), we require

$$B_2 = 0.$$

The boundary condition (2.7) can be applied to obtain

$$\left.\frac{1}{r}\frac{\partial}{\partial r}\left(rH_1\right)\right|_{z=0} = \frac{I}{2\pi}\frac{\delta\left(r\right)}{r}. \tag{2.11}$$

Replacing k by 1 in (2.10), equation (2.11) then becomes

$$\begin{aligned}\frac{I}{2\pi}\frac{\delta(r)}{r} &= \int_0^\infty (A_1+B_1)\left(\frac{1}{r}\frac{\partial}{\partial r}(rJ_1(\lambda r))\right)d\lambda \\ &= \int_0^\infty (A_1+B_1)\left(\frac{\partial}{\partial r}J_1(\lambda r)+\frac{J_1(\lambda r)}{r}\right)d\lambda \\ &= \int_0^\infty (A_1+B_1)\left(\lambda J_1'(\lambda r)+\frac{J_1(\lambda r)}{r}\right)d\lambda.\end{aligned}$$

Using the recurrence relation for Bessel functions (Watson [67])

$$\lambda r J_1'(\lambda r) + J_1(\lambda r) = \lambda r J_0(\lambda r)$$

and the integral

$$\int_0^\infty \lambda J_0(\lambda r)\,d\lambda = \frac{\delta(r)}{r},$$

we obtain

$$\int_0^\infty (A_1+B_1)\,\lambda J_0(\lambda r)\,d\lambda = \int_0^\infty \frac{I}{2\pi}\lambda J_0(\lambda r)\,d\lambda.$$

Inverting the above equation yields

$$A_1 = \frac{I}{2\pi} - B_1.$$

Hence, the magnetic fields $\tilde{H}_1$ and $\tilde{H}_2$ can be rewritten as

$$\tilde{H}_1(\lambda, z) = \frac{I}{2\pi}e^{-\lambda z} + B_1\left(e^{\lambda z} - e^{-\lambda z}\right)$$

and

$$\tilde{H}_2(\lambda, z) = A_2 e^{-\lambda z}.$$

Thus, the boundary conditions (2.8) and (2.9) lead to

$$\frac{I}{2\pi}e^{-\lambda h} + B_1\left(e^{\lambda h} - e^{-\lambda h}\right) = A_2 e^{-\lambda h}$$

and

$$\frac{1}{\sigma_1}\left(\frac{I}{2\pi}e^{-\lambda h} - B_1\left(e^{\lambda h} + e^{-\lambda h}\right)\right) = \frac{1}{\sigma_2}A_2 e^{-\lambda h}.$$

Solving these equations for the unknowns B_1 and A_2, we obtain

$$B_1 = \frac{I}{2\pi}\frac{(\sigma_2/\sigma_1) - 1}{(e^{2\lambda h} - 1) + (\sigma_2/\sigma_1)(e^{2\lambda h} + 1)}$$

and

$$A_2 = \frac{I}{\pi}\frac{\sigma_2}{\sigma_1}\frac{e^{2\lambda h}}{(e^{2\lambda h} - 1) + (\sigma_2/\sigma_1)(e^{2\lambda h} + 1)}.$$

In the case of a uniform half-space, the magnetic field in a homogeneous medium can be determined by setting $\sigma_1 = \sigma_2$ and we then have

$$\tilde{H}(\lambda, z) = \frac{I}{2\pi} e^{-\lambda z}. \tag{2.12}$$

Using the Lipschitz-Hankel integral (Watson [67])

$$\int_0^\infty e^{-\lambda z} J_1(\lambda r)\, d\lambda = \frac{1}{r}\left(1 - \frac{z}{\sqrt{r^2 + z^2}}\right),$$

we can transform equation (2.12) back to the spatial domain and obtain

$$H(r, z) = \frac{I}{2\pi r}\left(1 - \frac{z}{\sqrt{r^2 + z^2}}\right). \tag{2.13}$$

2.3.2 Solution for an n-layered Earth

We now consider an n-layered earth model. Each layer k, where $1 \le k \le n$ and $n \ge 2$, has a constant conductivity σ_k. For $1 \le k \le n-1$, the magnetic fields in layers k and $k+1$ can be written as

$$\tilde{H}_k(\lambda, z) = A_k e^{-\lambda z} + B_k e^{\lambda z}$$

and

$$\tilde{H}_{k+1}(\lambda, z) = A_{k+1} e^{-\lambda z} + B_{k+1} e^{\lambda z}.$$

Using the boundary conditions (2.8) and (2.9), we obtain

$$A_k e^{-\lambda h_k} + B_k e^{\lambda h_k} = A_{k+1} e^{-\lambda h_k} + B_{k+1} e^{\lambda h_k}$$

and

$$\frac{1}{\sigma_k}\left(A_k e^{-\lambda h_k} - B_k e^{\lambda h_k}\right) = \frac{1}{\sigma_{k+1}}\left(A_{k+1} e^{-\lambda h_k} - B_{k+1} e^{\lambda h_k}\right).$$

Hence, A_k and B_k can be written in terms of A_{k+1} and B_{k+1} as

$$A_k = \frac{1}{2}\left(\left(1 + \frac{\sigma_k}{\sigma_{k+1}}\right) A_{k+1} + \left(1 - \frac{\sigma_k}{\sigma_{k+1}}\right) B_{k+1} e^{2\lambda z_k}\right)$$

and

$$B_k = \frac{1}{2}\left(\left(1 - \frac{\sigma_k}{\sigma_{k+1}}\right) A_{k+1} e^{-2\lambda z_k} + \left(1 + \frac{\sigma_k}{\sigma_{k+1}}\right) B_{k+1}\right),$$

or, in matrix form,

$$\begin{bmatrix} A_k \\ B_k \end{bmatrix} = \Gamma_{k+1} \begin{bmatrix} A_{k+1} \\ B_{k+1} \end{bmatrix}, \tag{2.14}$$

where the propagator matrix is

$$\Gamma_{k+1} = \frac{1}{2}\begin{bmatrix} (1 + (\sigma_k/\sigma_{k+1})) & (1 - (\sigma_k/\sigma_{k+1}))\, e^{2\lambda h_k} \\ (1 - (\sigma_k/\sigma_{k+1}))\, e^{-2\lambda h_k} & (1 + (\sigma_k/\sigma_{k+1})) \end{bmatrix}.$$

Thus, equation (2.14) can be applied to obtain

$$\begin{bmatrix} A_1 \\ B_1 \end{bmatrix} = \prod_{j=1}^{n} \Gamma_j \begin{bmatrix} A_n \\ B_n \end{bmatrix}, \tag{2.15}$$

where Γ_1 is the 2×2 identity matrix. Similarly, the boundary conditions (2.6) and (2.7) lead to

$$A_1 = \frac{I}{2\pi} - B_1, \qquad B_n = 0.$$

Substituting A_1 and B_n into equation (2.15), we obtain

$$\begin{bmatrix} (I/\,2\pi) - B_1 \\ B_1 \end{bmatrix} = \prod_{j=1}^{n} \Gamma_j \begin{bmatrix} A_n \\ 0 \end{bmatrix}.$$

This can be rewritten as a system of two linear equations in terms of the unknowns B_1 and A_n as

$$\begin{bmatrix} F_n^{(11)} & 1 \\ -F_n^{(21)} & 1 \end{bmatrix} \begin{bmatrix} A_n \\ B_1 \end{bmatrix} = \begin{bmatrix} I/\,2\pi \\ 0 \end{bmatrix}, \tag{2.16}$$

where $F_k^{(ij)}$ is determined by

$$\prod_{j=1}^{k} \Gamma_j = \begin{bmatrix} F_k^{(11)} & F_k^{(12)} \\ F_k^{(21)} & F_k^{(22)} \end{bmatrix}.$$

Since the coefficient matrix of the above system is nonsingular (see Section 2.5), by Cramer's rule, the system has a unique solution

$$B_1 = \frac{I}{2\pi} \frac{F_n^{(21)}}{F_n^{(11)} + F_n^{(21)}}, \qquad A_n = \frac{I}{2\pi} \frac{1}{F_n^{(11)} + F_n^{(21)}}.$$

As A_1, B_1, A_n and B_n are determined, so A_k and B_k, where $k \neq 1$ and n, can be obtained from the recurrence relation (2.14).

2.4 Response of a Layer Having Exponentially Varying Conductivity

For each layer k, where $1 \leq k \leq n$ and $n \geq 2$, the variation of conductivity is denoted by

$$\sigma_k(z) = a_k e^{b_k z}, \tag{2.17}$$

where $a_k > 0$ and $b_k \in \mathbb{R}$. Hence, the equation for the magnetic field in each layer can be simplified by substituting equation (2.17) into (2.5) and we obtain

$$\frac{\partial^2 \tilde{H}_k}{\partial z^2} - b_k \frac{\partial \tilde{H}_k}{\partial z} - \lambda^2 \tilde{H}_k = 0.$$

The solution to the above equation is

$$\tilde{H}_k(\lambda, z) = C_k e^{z\alpha_k^-} + D_k e^{z\alpha_k^+},$$

where

$$\alpha_k^- = \frac{b_k - \sqrt{b_k^2 + 4\lambda^2}}{2}, \qquad \alpha_k^+ = \frac{b_k + \sqrt{b_k^2 + 4\lambda^2}}{2},$$

C_k and D_k are arbitrary constants, which can be determined by using the boundary conditions. Thus, the magnetic field in layer k is

$$H_k(r, z) = \int_0^\infty \left(C_k e^{z\alpha_k^-} + D_k e^{z\alpha_k^+} \right) J_1(\lambda r)\, d\lambda. \tag{2.18}$$

Consider an n-layered earth model, for $1 \leq k \leq n-1$, the magnetic fields in layers k and $k+1$ can be written as

$$\tilde{H}_k(\lambda, z) = C_k e^{z\alpha_k^-} + D_k e^{z\alpha_k^+}$$

and

$$\tilde{H}_{k+1}(\lambda, z) = C_{k+1} e^{z\alpha_{k+1}^-} + D_{k+1} e^{z\alpha_{k+1}^+}.$$

Using the boundary conditions (2.8) and (2.9), we obtain

$$C_k e^{h_k\alpha_k^-} + D_k e^{h_k\alpha_k^+} = C_{k+1} e^{h_k\alpha_{k+1}^-} + D_{k+1} e^{h_k\alpha_{k+1}^+}$$

and

$$-\frac{1}{\sigma_k^\circ}\left(C_k\alpha_k^- e^{h_k\alpha_k^-} + D_k\alpha_k^+ e^{h_k\alpha_k^+} \right) = -\frac{1}{\sigma_{k+1}^\bullet}\left(C_{k+1}\alpha_{k+1}^- e^{h_k\alpha_{k+1}^-} + D_{k+1}\alpha_{k+1}^+ e^{h_k\alpha_{k+1}^+} \right),$$

where

$$\lim_{z\to h_k^-} \sigma_k(z) = \sigma_k^\circ, \qquad \lim_{z\to h_k^+} \sigma_{k+1}(z) = \sigma_{k+1}^\bullet.$$

Hence, C_k and D_k can be written in terms of C_{k+1} and D_{k+1} as

$$C_k = \frac{1}{\alpha_k^+ - \alpha_k^-}\left(\left(\alpha_k^+ - \frac{\sigma_k^\circ \alpha_{k+1}^-}{\sigma_{k+1}^\bullet} \right) C_{k+1} e^{h_k\left(\alpha_{k+1}^- - \alpha_k^-\right)} + \left(\alpha_k^+ - \frac{\sigma_k^\circ \alpha_{k+1}^+}{\sigma_{k+1}^\bullet} \right) D_{k+1} e^{h_k\left(\alpha_{k+1}^+ - \alpha_k^-\right)} \right)$$

and

$$D_k = \frac{1}{\alpha_k^+ - \alpha_k^-}\left(\left(\frac{\sigma_k^\circ \alpha_{k+1}^-}{\sigma_{k+1}^\bullet} - \alpha_k^- \right) C_{k+1} e^{h_k\left(\alpha_{k+1}^- - \alpha_k^+\right)} + \left(\frac{\sigma_k^\circ \alpha_{k+1}^+}{\sigma_{k+1}^\bullet} - \alpha_k^- \right) D_{k+1} e^{h_k\left(\alpha_{k+1}^+ - \alpha_k^+\right)} \right),$$

or, in matrix form,

$$\begin{bmatrix} C_k \\ D_k \end{bmatrix} = \Theta_{k+1} \begin{bmatrix} C_{k+1} \\ D_{k+1} \end{bmatrix}, \tag{2.19}$$

where the propagator matrix is

$$\Theta_{k+1} = \frac{1}{\alpha_k^+ - \alpha_k^-} \begin{bmatrix} \left(\alpha_k^+ - \frac{\sigma_k^\circ \alpha_{k+1}^-}{\sigma_{k+1}^\bullet}\right) e^{h_k\left(\alpha_{k+1}^- - \alpha_k^-\right)} & \left(\alpha_k^+ - \frac{\sigma_k^\circ \alpha_{k+1}^+}{\sigma_{k+1}^\bullet}\right) e^{h_k\left(\alpha_{k+1}^+ - \alpha_k^-\right)} \\ \left(\frac{\sigma_k^\circ \alpha_{k+1}^-}{\sigma_{k+1}^\bullet} - \alpha_k^-\right) e^{h_k\left(\alpha_{k+1}^- - \alpha_k^+\right)} & \left(\frac{\sigma_k^\circ \alpha_{k+1}^+}{\sigma_{k+1}^\bullet} - \alpha_k^-\right) e^{h_k\left(\alpha_{k+1}^+ - \alpha_k^+\right)} \end{bmatrix}.$$

Thus, equation (2.19) can be applied to obtain

$$\begin{bmatrix} C_1 \\ D_1 \end{bmatrix} = \prod_{j=1}^{n} \Theta_j \begin{bmatrix} C_n \\ D_n \end{bmatrix}, \tag{2.20}$$

where Θ_1 is the 2×2 identity matrix. To satisfy (2.6), we require

$$D_n = 0.$$

The boundary condition as given in (2.7) leads to

$$\frac{1}{r}\frac{\partial}{\partial r}\left(rH_1\right)\bigg|_{z=0} = \frac{I}{2\pi}\frac{\delta\left(r\right)}{r}. \tag{2.21}$$

Replacing k by 1 in (2.18), equation (2.21) then becomes

$$\int_0^\infty \left(C_1 + D_1\right)\left(\lambda J_1'\left(\lambda r\right) + \frac{J_1\left(\lambda r\right)}{r}\right) d\lambda = \frac{I}{2\pi}\frac{\delta\left(r\right)}{r}.$$

Using the recurrence relation for Bessel functions

$$\lambda r J_1'\left(\lambda r\right) + J_1\left(\lambda r\right) = \lambda r J_0\left(\lambda r\right)$$

and the integral

$$\int_0^\infty \lambda J_0\left(\lambda r\right) d\lambda = \frac{\delta\left(r\right)}{r},$$

we obtain

$$\int_0^\infty \left(C_1 + D_1\right) \lambda J_0\left(\lambda r\right) d\lambda = \int_0^\infty \frac{I}{2\pi} \lambda J_0\left(\lambda r\right) d\lambda.$$

Inverting the above equation yields

$$C_1 = \frac{I}{2\pi} - D_1.$$

Substituting C_1 and D_n into equation (2.20), we obtain

$$\begin{bmatrix} \left(I/2\pi\right) - D_1 \\ D_1 \end{bmatrix} = \prod_{j=1}^{n} \Theta_j \begin{bmatrix} C_n \\ 0 \end{bmatrix}.$$

This can be rewritten as a system of two linear equations in terms of the unknowns D_1 and C_n as

$$\begin{bmatrix} G_n^{(11)} & 1 \\ -G_n^{(21)} & 1 \end{bmatrix} \begin{bmatrix} C_n \\ D_1 \end{bmatrix} = \begin{bmatrix} I/\,2\pi \\ 0 \end{bmatrix}, \tag{2.22}$$

where $G_k^{(ij)}$ is determined by

$$\prod_{j=1}^{k} \Theta_j = \begin{bmatrix} G_k^{(11)} & G_k^{(12)} \\ G_k^{(21)} & G_k^{(22)} \end{bmatrix}.$$

Since the coefficient matrix of the above system is nonsingular (see Section 2.5), by Cramer's rule, the system has a unique solution

$$D_1 = \frac{I}{2\pi} \frac{G_n^{(21)}}{G_n^{(11)} + G_n^{(21)}}, \qquad C_n = \frac{I}{2\pi} \frac{1}{G_n^{(11)} + G_n^{(21)}}.$$

As C_1, D_1, C_n and D_n are determined, so C_k and D_k, where $k \neq 1$ and n, can be obtained from the recurrence relation (2.19).

2.5 Analysis of Nonsingular Matrices

The coefficient matrices of the linear systems of equations (2.16) and (2.22) are discussed in this section. We are going to show that both of the coefficient matrices are nonsingular. The main idea of the proof is to use a well established result that if A is an $n \times n$ matrix, then A is a singular matrix if and only if the determinant of A is zero.

We start off by proving a few simple properties of the entries $F_k^{(ij)}$ and $G_k^{(ij)}$.

Lemma 2.1. *The statement*

$$\left| F_k^{(12)} + F_k^{(22)} \right| e^{-2\lambda h_k} < F_k^{(11)} + F_k^{(21)}$$

is true for all $k \geq 1$.

Proof. We prove the above statement by using the principle of mathematical induction on k. If $k = 1$, then $F_k^{(ij)}$ is an entry of the 2×2 identity matrix, and so

$$\left| F_k^{(12)} + F_k^{(22)} \right| e^{-2\lambda h_k} = e^{-2\lambda h_k} < 1 = F_k^{(11)} + F_k^{(21)}.$$

Suppose that $k > 1$ and that the statement is true for $k-1$, i.e.,

$$\left| F_{k-1}^{(12)} + F_{k-1}^{(22)} \right| e^{-2\lambda h_{k-1}} < F_{k-1}^{(11)} + F_{k-1}^{(21)}.$$

This yields

$$\left(F_{k-1}^{(11)} + F_{k-1}^{(21)} \right) + \left(F_{k-1}^{(12)} + F_{k-1}^{(22)} \right) e^{-2\lambda h_{k-1}} > 0 \tag{2.23}$$

and

$$\left(F_{k-1}^{(11)}+F_{k-1}^{(21)}\right)-\left(F_{k-1}^{(12)}+F_{k-1}^{(22)}\right)e^{-2\lambda h_{k-1}}>0. \tag{2.24}$$

Since we have

$$\begin{aligned}\begin{bmatrix}F_k^{(11)} & F_k^{(12)}\\ F_k^{(21)} & F_k^{(22)}\end{bmatrix} &= \prod_{j=1}^{k}\Gamma_j=\left(\prod_{j=1}^{k-1}\Gamma_j\right)\Gamma_k\\ &= \begin{bmatrix}F_{k-1}^{(11)} & F_{k-1}^{(12)}\\ F_{k-1}^{(21)} & F_{k-1}^{(22)}\end{bmatrix}\begin{bmatrix}\frac{1}{2}\left(1+\frac{\sigma_{k-1}}{\sigma_k}\right) & \frac{1}{2}\left(1-\frac{\sigma_{k-1}}{\sigma_k}\right)e^{2\lambda h_{k-1}}\\ \frac{1}{2}\left(1-\frac{\sigma_{k-1}}{\sigma_k}\right)e^{-2\lambda h_{k-1}} & \frac{1}{2}\left(1+\frac{\sigma_{k-1}}{\sigma_k}\right)\end{bmatrix},\end{aligned}$$

it follows from (2.23) and (2.24) that

$$\begin{aligned}\left|F_k^{(12)}+F_k^{(22)}\right|e^{-2\lambda h_k} &= \frac{1}{2}\left|\left(1-\frac{\sigma_{k-1}}{\sigma_k}\right)F_{k-1}^{(11)}e^{2\lambda h_{k-1}}+\left(1+\frac{\sigma_{k-1}}{\sigma_k}\right)F_{k-1}^{(12)}\right.\\ &\quad\left.+\left(1-\frac{\sigma_{k-1}}{\sigma_k}\right)F_{k-1}^{(21)}e^{2\lambda h_{k-1}}+\left(1+\frac{\sigma_{k-1}}{\sigma_k}\right)F_{k-1}^{(22)}\right|e^{-2\lambda h_k}\\ &< \frac{1}{2}\left|\left(1-\frac{\sigma_{k-1}}{\sigma_k}\right)F_{k-1}^{(11)}e^{2\lambda h_{k-1}}+\left(1+\frac{\sigma_{k-1}}{\sigma_k}\right)F_{k-1}^{(12)}\right.\\ &\quad\left.+\left(1-\frac{\sigma_{k-1}}{\sigma_k}\right)F_{k-1}^{(21)}e^{2\lambda h_{k-1}}+\left(1+\frac{\sigma_{k-1}}{\sigma_k}\right)F_{k-1}^{(22)}\right|e^{-2\lambda h_{k-1}}\\ &= \frac{1}{2}\left|\left(1-\frac{\sigma_{k-1}}{\sigma_k}\right)\left(F_{k-1}^{(11)}+F_{k-1}^{(21)}\right)\right.\\ &\quad\left.+\left(1+\frac{\sigma_{k-1}}{\sigma_k}\right)\left(F_{k-1}^{(12)}+F_{k-1}^{(22)}\right)e^{-2\lambda h_{k-1}}\right|\\ &= \frac{1}{2}\left|\left(\left(F_{k-1}^{(11)}+F_{k-1}^{(21)}\right)+\left(F_{k-1}^{(12)}+F_{k-1}^{(22)}\right)e^{-2\lambda h_{k-1}}\right)\right.\\ &\quad\left.-\frac{\sigma_{k-1}}{\sigma_k}\left(\left(F_{k-1}^{(11)}+F_{k-1}^{(21)}\right)-\left(F_{k-1}^{(12)}+F_{k-1}^{(22)}\right)e^{-2\lambda h_{k-1}}\right)\right|\\ &< \frac{1}{2}\left(\left(\left(F_{k-1}^{(11)}+F_{k-1}^{(21)}\right)+\left(F_{k-1}^{(12)}+F_{k-1}^{(22)}\right)e^{-2\lambda h_{k-1}}\right)\right.\\ &\quad\left.+\frac{\sigma_{k-1}}{\sigma_k}\left(\left(F_{k-1}^{(11)}+F_{k-1}^{(21)}\right)-\left(F_{k-1}^{(12)}+F_{k-1}^{(22)}\right)e^{-2\lambda h_{k-1}}\right)\right)\\ &= \frac{1}{2}\left(\left(1+\frac{\sigma_{k-1}}{\sigma_k}\right)\left(F_{k-1}^{(11)}+F_{k-1}^{(21)}\right)\right.\\ &\quad\left.+\left(1-\frac{\sigma_{k-1}}{\sigma_k}\right)\left(F_{k-1}^{(12)}+F_{k-1}^{(22)}\right)e^{-2\lambda h_{k-1}}\right)\\ &= \frac{1}{2}\left(1+\frac{\sigma_{k-1}}{\sigma_k}\right)F_{k-1}^{(11)}+\frac{1}{2}\left(1-\frac{\sigma_{k-1}}{\sigma_k}\right)F_{k-1}^{(12)}e^{-2\lambda h_{k-1}}\\ &\quad+\frac{1}{2}\left(1+\frac{\sigma_{k-1}}{\sigma_k}\right)F_{k-1}^{(21)}+\frac{1}{2}\left(1-\frac{\sigma_{k-1}}{\sigma_k}\right)F_{k-1}^{(22)}e^{-2\lambda h_{k-1}}\\ &= F_k^{(11)}+F_k^{(21)}.\end{aligned}$$

Therefore, the principle of mathematical induction yields the assertion. □

Lemma 2.2. *The statements*

$$\left(G_k^{(12)} + G_k^{(22)}\right)\alpha_k^- e^{-h_k\alpha_k^+} < \left(G_k^{(11)} + G_k^{(21)}\right)\alpha_k^+ e^{-h_k\alpha_k^-}$$

and

$$\left(G_k^{(12)} + G_k^{(22)}\right) e^{-h_k\alpha_k^+} < \left(G_k^{(11)} + G_k^{(21)}\right) e^{-h_k\alpha_k^-}$$

are true for all $k \geq 1$.

Proof. We also prove the above statements by using the principle of mathematical induction on k. If $k = 1$, then the entry $G_k^{(ij)}$ is in the 2×2 identity matrix. Thus, we obtain

$$\left(G_k^{(12)} + G_k^{(22)}\right)\alpha_k^- e^{-h_k\alpha_k^+} = \alpha_k^- e^{-h_k\alpha_k^+} < \alpha_k^+ e^{-h_k\alpha_k^-} = \left(G_k^{(11)} + G_k^{(21)}\right)\alpha_k^+ e^{-h_k\alpha_k^-}$$

and

$$\left(G_k^{(12)} + G_k^{(22)}\right) e^{-h_k\alpha_k^+} = e^{-h_k\alpha_k^+} < e^{-h_k\alpha_k^-} = \left(G_k^{(11)} + G_k^{(21)}\right) e^{-h_k\alpha_k^-}.$$

Next, we suppose that $k > 1$ and that the statements are true for $k - 1$, i.e.,

$$\left(G_{k-1}^{(12)} + G_{k-1}^{(22)}\right)\alpha_{k-1}^- e^{-h_{k-1}\alpha_{k-1}^+} < \left(G_{k-1}^{(11)} + G_{k-1}^{(21)}\right)\alpha_{k-1}^+ e^{-h_{k-1}\alpha_{k-1}^-} \tag{2.25}$$

and

$$\left(G_{k-1}^{(12)} + G_{k-1}^{(22)}\right) e^{-h_{k-1}\alpha_{k-1}^+} < \left(G_{k-1}^{(11)} + G_{k-1}^{(21)}\right) e^{-h_{k-1}\alpha_{k-1}^-}. \tag{2.26}$$

Since we have

$$\begin{aligned}
\begin{bmatrix} G_k^{(11)} & G_k^{(12)} \\ G_k^{(21)} & G_k^{(22)} \end{bmatrix} &= \prod_{j=1}^{k} \Theta_j = \left(\prod_{j=1}^{k-1} \Theta_j\right)\Theta_k \\
&= \begin{bmatrix} G_{k-1}^{(11)} & G_{k-1}^{(12)} \\ G_{k-1}^{(21)} & G_{k-1}^{(22)} \end{bmatrix} \left(\frac{1}{\alpha_{k-1}^+ - \alpha_{k-1}^-}\right) \\
&\times \begin{bmatrix} \left(\alpha_{k-1}^+ - \frac{\sigma_{k-1}^\circ \alpha_k^-}{\sigma_k^\bullet}\right) e^{h_{k-1}\left(\alpha_k^- - \alpha_{k-1}^-\right)} & \left(\alpha_{k-1}^+ - \frac{\sigma_{k-1}^\circ \alpha_k^+}{\sigma_k^\bullet}\right) e^{h_{k-1}\left(\alpha_k^+ - \alpha_{k-1}^-\right)} \\ \left(\frac{\sigma_{k-1}^\circ \alpha_k^-}{\sigma_k^\bullet} - \alpha_{k-1}^-\right) e^{h_{k-1}\left(\alpha_k^- - \alpha_{k-1}^+\right)} & \left(\frac{\sigma_{k-1}^\circ \alpha_k^+}{\sigma_k^\bullet} - \alpha_{k-1}^-\right) e^{h_{k-1}\left(\alpha_k^+ - \alpha_{k-1}^+\right)} \end{bmatrix},
\end{aligned}$$

it follows from (2.25) and (2.26) that

$$\begin{aligned}
\left(G_k^{(12)} + G_k^{(22)}\right)\alpha_k^- e^{-h_k\alpha_k^+} &= \frac{1}{\alpha_{k-1}^+ - \alpha_{k-1}^-}\Bigg(\left(\alpha_{k-1}^+ - \frac{\sigma_{k-1}^\circ \alpha_k^+}{\sigma_k^\bullet}\right) G_{k-1}^{(11)} e^{h_{k-1}\left(\alpha_k^+ - \alpha_{k-1}^-\right)} \\
&\quad + \left(\frac{\sigma_{k-1}^\circ \alpha_k^+}{\sigma_k^\bullet} - \alpha_{k-1}^-\right) G_{k-1}^{(12)} e^{h_{k-1}\left(\alpha_k^+ - \alpha_{k-1}^+\right)} \\
&\quad + \left(\alpha_{k-1}^+ - \frac{\sigma_{k-1}^\circ \alpha_k^+}{\sigma_k^\bullet}\right) G_{k-1}^{(21)} e^{h_{k-1}\left(\alpha_k^+ - \alpha_{k-1}^-\right)} \\
&\quad + \left(\frac{\sigma_{k-1}^\circ \alpha_k^+}{\sigma_k^\bullet} - \alpha_{k-1}^-\right) G_{k-1}^{(22)} e^{h_{k-1}\left(\alpha_k^+ - \alpha_{k-1}^+\right)}\Bigg)\alpha_k^- e^{-h_k\alpha_k^+} \\
&= \frac{1}{\alpha_{k-1}^+ - \alpha_{k-1}^-}\Bigg(\left(\alpha_{k-1}^+ - \frac{\sigma_{k-1}^\circ \alpha_k^+}{\sigma_k^\bullet}\right)\left(G_{k-1}^{(11)} + G_{k-1}^{(21)}\right) e^{-h_{k-1}\alpha_{k-1}^-} \\
&\quad + \left(\frac{\sigma_{k-1}^\circ \alpha_k^+}{\sigma_k^\bullet} - \alpha_{k-1}^-\right)\left(G_{k-1}^{(12)} + G_{k-1}^{(22)}\right) e^{-h_{k-1}\alpha_{k-1}^+}\Bigg)\alpha_k^- e^{(h_{k-1} - h_k)\alpha_k^+},
\end{aligned}$$

or

$$
\begin{aligned}
\left(G_k^{(12)}+G_k^{(22)}\right)\alpha_k^- e^{-h_k\alpha_k^+} &= \frac{1}{\alpha_{k-1}^+-\alpha_{k-1}^-}\left(\left(\left(G_{k-1}^{(11)}+G_{k-1}^{(21)}\right)\alpha_{k-1}^+ e^{-h_{k-1}\alpha_{k-1}^-}\right.\right.\\
&\quad\left.-\left(G_{k-1}^{(12)}+G_{k-1}^{(22)}\right)\alpha_{k-1}^- e^{-h_{k-1}\alpha_{k-1}^+}\right)\alpha_k^-\\
&\quad-\frac{\sigma_{k-1}^\circ\alpha_k^-\alpha_k^+}{\sigma_k^\bullet}\left(\left(G_{k-1}^{(11)}+G_{k-1}^{(21)}\right)e^{-h_{k-1}\alpha_{k-1}^-}\right.\\
&\quad\left.\left.-\left(G_{k-1}^{(12)}+G_{k-1}^{(22)}\right)e^{-h_{k-1}\alpha_{k-1}^+}\right)\right)e^{(h_{k-1}-h_k)\alpha_k^+}\\
&< \frac{1}{\alpha_{k-1}^+-\alpha_{k-1}^-}\left(\left(\left(G_{k-1}^{(11)}+G_{k-1}^{(21)}\right)\alpha_{k-1}^+ e^{-h_{k-1}\alpha_{k-1}^-}\right.\right.\\
&\quad\left.-\left(G_{k-1}^{(12)}+G_{k-1}^{(22)}\right)\alpha_{k-1}^- e^{-h_{k-1}\alpha_{k-1}^+}\right)\alpha_k^+\\
&\quad-\frac{\sigma_{k-1}^\circ\alpha_k^-\alpha_k^+}{\sigma_k^\bullet}\left(\left(G_{k-1}^{(11)}+G_{k-1}^{(21)}\right)e^{-h_{k-1}\alpha_{k-1}^-}\right.\\
&\quad\left.\left.-\left(G_{k-1}^{(12)}+G_{k-1}^{(22)}\right)e^{-h_{k-1}\alpha_{k-1}^+}\right)\right)e^{(h_{k-1}-h_k)\alpha_k^+}\\
&< \frac{1}{\alpha_{k-1}^+-\alpha_{k-1}^-}\left(\left(\left(G_{k-1}^{(11)}+G_{k-1}^{(21)}\right)\alpha_{k-1}^+ e^{-h_{k-1}\alpha_{k-1}^-}\right.\right.\\
&\quad\left.-\left(G_{k-1}^{(12)}+G_{k-1}^{(22)}\right)\alpha_{k-1}^- e^{-h_{k-1}\alpha_{k-1}^+}\right)\alpha_k^+\\
&\quad-\frac{\sigma_{k-1}^\circ\alpha_k^-\alpha_k^+}{\sigma_k^\bullet}\left(\left(G_{k-1}^{(11)}+G_{k-1}^{(21)}\right)e^{-h_{k-1}\alpha_{k-1}^-}\right.\\
&\quad\left.\left.-\left(G_{k-1}^{(12)}+G_{k-1}^{(22)}\right)e^{-h_{k-1}\alpha_{k-1}^+}\right)\right)e^{(h_{k-1}-h_k)\alpha_k^-}\\
&= \frac{1}{\alpha_{k-1}^+-\alpha_{k-1}^-}\left(\left(\alpha_{k-1}^+-\frac{\sigma_{k-1}^\circ\alpha_k^-}{\sigma_k^\bullet}\right)\left(G_{k-1}^{(11)}+G_{k-1}^{(21)}\right)e^{-h_{k-1}\alpha_{k-1}^-}\right.\\
&\quad\left.+\left(\frac{\sigma_{k-1}^\circ\alpha_k^-}{\sigma_k^\bullet}-\alpha_{k-1}^-\right)\left(G_{k-1}^{(12)}+G_{k-1}^{(22)}\right)e^{-h_{k-1}\alpha_{k-1}^+}\right)\alpha_k^+ e^{(h_{k-1}-h_k)\alpha_k^-}\\
&= \frac{1}{\alpha_{k-1}^+-\alpha_{k-1}^-}\left(\left(\alpha_{k-1}^+-\frac{\sigma_{k-1}^\circ\alpha_k^-}{\sigma_k^\bullet}\right)G_{k-1}^{(11)}e^{h_{k-1}\left(\alpha_k^--\alpha_{k-1}^-\right)}\right.\\
&\quad+\left(\frac{\sigma_{k-1}^\circ\alpha_k^-}{\sigma_k^\bullet}-\alpha_{k-1}^-\right)G_{k-1}^{(12)}e^{h_{k-1}\left(\alpha_k^--\alpha_{k-1}^+\right)}\\
&\quad+\left(\alpha_{k-1}^+-\frac{\sigma_{k-1}^\circ\alpha_k^-}{\sigma_k^\bullet}\right)G_{k-1}^{(21)}e^{h_{k-1}\left(\alpha_k^--\alpha_{k-1}^-\right)}\\
&\quad\left.+\left(\frac{\sigma_{k-1}^\circ\alpha_k^-}{\sigma_k^\bullet}-\alpha_{k-1}^-\right)G_{k-1}^{(22)}e^{h_{k-1}\left(\alpha_k^--\alpha_{k-1}^+\right)}\right)\alpha_k^+ e^{-h_k\alpha_k^-}\\
&= \left(G_k^{(11)}+G_k^{(21)}\right)\alpha_k^+ e^{-h_k\alpha_k^-}.
\end{aligned}
$$

By a similar argument, we also have

$$
\begin{aligned}
\left(G_k^{(12)}+G_k^{(22)}\right)e^{-h_k\alpha_k^+} &= \frac{1}{\alpha_{k-1}^+-\alpha_{k-1}^-}\left(\left(\alpha_{k-1}^+-\frac{\sigma_{k-1}^\circ\alpha_k^+}{\sigma_k^\bullet}\right)G_{k-1}^{(11)}e^{h_{k-1}\left(\alpha_k^+-\alpha_{k-1}^-\right)}\right.\\
&\quad+\left(\frac{\sigma_{k-1}^\circ\alpha_k^+}{\sigma_k^\bullet}-\alpha_{k-1}^-\right)G_{k-1}^{(12)}e^{h_{k-1}\left(\alpha_k^+-\alpha_{k-1}^+\right)}\\
&\quad+\left(\alpha_{k-1}^+-\frac{\sigma_{k-1}^\circ\alpha_k^+}{\sigma_k^\bullet}\right)G_{k-1}^{(21)}e^{h_{k-1}\left(\alpha_k^+-\alpha_{k-1}^-\right)}\\
&\quad\left.+\left(\frac{\sigma_{k-1}^\circ\alpha_k^+}{\sigma_k^\bullet}-\alpha_{k-1}^-\right)G_{k-1}^{(22)}e^{h_{k-1}\left(\alpha_k^+-\alpha_{k-1}^+\right)}\right)e^{-h_k\alpha_k^+}\\
&= \frac{1}{\alpha_{k-1}^+-\alpha_{k-1}^-}\left(\left(\alpha_{k-1}^+-\frac{\sigma_{k-1}^\circ\alpha_k^+}{\sigma_k^\bullet}\right)\left(G_{k-1}^{(11)}+G_{k-1}^{(21)}\right)e^{-h_{k-1}\alpha_{k-1}^-}\right.\\
&\quad\left.+\left(\frac{\sigma_{k-1}^\circ\alpha_k^+}{\sigma_k^\bullet}-\alpha_{k-1}^-\right)\left(G_{k-1}^{(12)}+G_{k-1}^{(22)}\right)e^{-h_{k-1}\alpha_{k-1}^+}\right)e^{(h_{k-1}-h_k)\alpha_k^+}\\
&= \frac{1}{\alpha_{k-1}^+-\alpha_{k-1}^-}\left(\left(\left(G_{k-1}^{(11)}+G_{k-1}^{(21)}\right)\alpha_{k-1}^+e^{-h_{k-1}\alpha_{k-1}^-}\right.\right.\\
&\quad\left.-\left(G_{k-1}^{(12)}+G_{k-1}^{(22)}\right)\alpha_{k-1}^-e^{-h_{k-1}\alpha_{k-1}^+}\right)\\
&\quad-\frac{\sigma_{k-1}^\circ\alpha_k^+}{\sigma_k^\bullet}\left(\left(G_{k-1}^{(11)}+G_{k-1}^{(21)}\right)e^{-h_{k-1}\alpha_{k-1}^-}\right.\\
&\quad\left.\left.-\left(G_{k-1}^{(12)}+G_{k-1}^{(22)}\right)e^{-h_{k-1}\alpha_{k-1}^+}\right)\right)e^{(h_{k-1}-h_k)\alpha_k^+}\\
&< \frac{1}{\alpha_{k-1}^+-\alpha_{k-1}^-}\left(\left(\left(G_{k-1}^{(11)}+G_{k-1}^{(21)}\right)\alpha_{k-1}^+e^{-h_{k-1}\alpha_{k-1}^-}\right.\right.\\
&\quad\left.-\left(G_{k-1}^{(12)}+G_{k-1}^{(22)}\right)\alpha_{k-1}^-e^{-h_{k-1}\alpha_{k-1}^+}\right)\\
&\quad-\frac{\sigma_{k-1}^\circ\alpha_k^-}{\sigma_k^\bullet}\left(\left(G_{k-1}^{(11)}+G_{k-1}^{(21)}\right)e^{-h_{k-1}\alpha_{k-1}^-}\right.\\
&\quad\left.\left.-\left(G_{k-1}^{(12)}+G_{k-1}^{(22)}\right)e^{-h_{k-1}\alpha_{k-1}^+}\right)\right)e^{(h_{k-1}-h_k)\alpha_k^+}\\
&< \frac{1}{\alpha_{k-1}^+-\alpha_{k-1}^-}\left(\left(\left(G_{k-1}^{(11)}+G_{k-1}^{(21)}\right)\alpha_{k-1}^+e^{-h_{k-1}\alpha_{k-1}^-}\right.\right.\\
&\quad\left.-\left(G_{k-1}^{(12)}+G_{k-1}^{(22)}\right)\alpha_{k-1}^-e^{-h_{k-1}\alpha_{k-1}^+}\right)\\
&\quad-\frac{\sigma_{k-1}^\circ\alpha_k^-}{\sigma_k^\bullet}\left(\left(G_{k-1}^{(11)}+G_{k-1}^{(21)}\right)e^{-h_{k-1}\alpha_{k-1}^-}\right.\\
&\quad\left.\left.-\left(G_{k-1}^{(12)}+G_{k-1}^{(22)}\right)e^{-h_{k-1}\alpha_{k-1}^+}\right)\right)e^{(h_{k-1}-h_k)\alpha_k^-}\\
&= \frac{1}{\alpha_{k-1}^+-\alpha_{k-1}^-}\left(\left(\alpha_{k-1}^+-\frac{\sigma_{k-1}^\circ\alpha_k^-}{\sigma_k^\bullet}\right)\left(G_{k-1}^{(11)}+G_{k-1}^{(21)}\right)e^{-h_{k-1}\alpha_{k-1}^-}\right.\\
&\quad\left.+\left(\frac{\sigma_{k-1}^\circ\alpha_k^-}{\sigma_k^\bullet}-\alpha_{k-1}^-\right)\left(G_{k-1}^{(12)}+G_{k-1}^{(22)}\right)e^{-h_{k-1}\alpha_{k-1}^+}\right)e^{(h_{k-1}-h_k)\alpha_k^-},
\end{aligned}
$$

or

$$\begin{aligned}\left(G_k^{(12)}+G_k^{(22)}\right)e^{-h_k\alpha_k^+} &= \frac{1}{\alpha_{k-1}^+-\alpha_{k-1}^-}\Bigg(\left(\alpha_{k-1}^+-\frac{\sigma_{k-1}^\circ\alpha_k^-}{\sigma_k^\bullet}\right)G_{k-1}^{(11)}e^{h_{k-1}\left(\alpha_k^--\alpha_{k-1}^-\right)}\\ &\quad+\left(\frac{\sigma_{k-1}^\circ\alpha_k^-}{\sigma_k^\bullet}-\alpha_{k-1}^-\right)G_{k-1}^{(12)}e^{h_{k-1}\left(\alpha_k^--\alpha_{k-1}^+\right)}\\ &\quad+\left(\alpha_{k-1}^+-\frac{\sigma_{k-1}^\circ\alpha_k^-}{\sigma_k^\bullet}\right)G_{k-1}^{(21)}e^{h_{k-1}\left(\alpha_k^--\alpha_{k-1}^-\right)}\\ &\quad+\left(\frac{\sigma_{k-1}^\circ\alpha_k^-}{\sigma_k^\bullet}-\alpha_{k-1}^-\right)G_{k-1}^{(22)}e^{h_{k-1}\left(\alpha_k^--\alpha_{k-1}^+\right)}\Bigg)e^{-h_k\alpha_k^-}\\ &= \left(G_k^{(11)}+G_k^{(21)}\right)e^{-h_k\alpha_k^-}.\end{aligned}$$

Therefore, the principle of mathematical induction yields the assertion. □

We are now in the position to prove the nonsingularity of the coefficient matrices, which can be used to solve the linear systems of equations (2.16) and (2.22), valid in these cases where there is a unique solution.

Proposition 2.3. *The coefficient matrix of equation* (2.16) *is nonsingular.*

Proof. We are going to show that the determinant of the coefficient matrix of system (2.16) is nonzero, i.e.,

$$\begin{vmatrix} F_n^{(11)} & 1 \\ -F_n^{(21)} & 1 \end{vmatrix} = F_n^{(11)} + F_n^{(21)} \neq 0.$$

To prove this, we note that

$$\begin{aligned}\begin{bmatrix} F_n^{(11)} & F_n^{(12)} \\ F_n^{(21)} & F_n^{(22)} \end{bmatrix} &= \prod_{j=1}^{n}\Gamma_j = \left(\prod_{j=1}^{n-1}\Gamma_j\right)\Gamma_n\\ &= \begin{bmatrix} F_{n-1}^{(11)} & F_{n-1}^{(12)} \\ F_{n-1}^{(21)} & F_{n-1}^{(22)} \end{bmatrix}\begin{bmatrix} \frac{1}{2}\left(1+\frac{\sigma_{n-1}}{\sigma_n}\right) & \frac{1}{2}\left(1-\frac{\sigma_{n-1}}{\sigma_n}\right)e^{2\lambda h_{n-1}} \\ \frac{1}{2}\left(1-\frac{\sigma_{n-1}}{\sigma_n}\right)e^{-2\lambda h_{n-1}} & \frac{1}{2}\left(1+\frac{\sigma_{n-1}}{\sigma_n}\right) \end{bmatrix}.\end{aligned}$$

Since $n-1\geq 1$, by Lemma 2.1, we have

$$\left|F_{n-1}^{(12)}+F_{n-1}^{(22)}\right|e^{-2\lambda h_{n-1}} < F_{n-1}^{(11)}+F_{n-1}^{(21)}.$$

This yields

$$\left(F_{n-1}^{(11)}+F_{n-1}^{(21)}\right)+\left(F_{n-1}^{(12)}+F_{n-1}^{(22)}\right)e^{-2\lambda h_{n-1}}>0$$

and

$$\left(F_{n-1}^{(11)}+F_{n-1}^{(21)}\right)-\left(F_{n-1}^{(12)}+F_{n-1}^{(22)}\right)e^{-2\lambda h_{n-1}}>0.$$

Hence, we obtain

$$
\begin{aligned}
F_n^{(11)} + F_n^{(21)} &= \frac{1}{2}\left(1+\frac{\sigma_{n-1}}{\sigma_n}\right) F_{n-1}^{(11)} + \frac{1}{2}\left(1-\frac{\sigma_{n-1}}{\sigma_n}\right) F_{n-1}^{(12)} e^{-2\lambda h_{n-1}} \\
&\quad + \frac{1}{2}\left(1+\frac{\sigma_{n-1}}{\sigma_n}\right) F_{n-1}^{(21)} + \frac{1}{2}\left(1-\frac{\sigma_{n-1}}{\sigma_n}\right) F_{n-1}^{(22)} e^{-2\lambda h_{n-1}} \\
&= \frac{1}{2}\left(\left(1+\frac{\sigma_{n-1}}{\sigma_n}\right)\left(F_{n-1}^{(11)} + F_{n-1}^{(21)}\right)\right. \\
&\quad \left. + \left(1-\frac{\sigma_{n-1}}{\sigma_n}\right)\left(F_{n-1}^{(12)} + F_{n-1}^{(22)}\right) e^{-2\lambda h_{n-1}}\right) \\
&= \frac{1}{2}\left(\left(\left(F_{n-1}^{(11)} + F_{n-1}^{(21)}\right) + \left(F_{n-1}^{(12)} + F_{n-1}^{(22)}\right) e^{-2\lambda h_{n-1}}\right)\right. \\
&\quad \left. + \frac{\sigma_{n-1}}{\sigma_n}\left(\left(F_{n-1}^{(11)} + F_{n-1}^{(21)}\right) - \left(F_{n-1}^{(12)} + F_{n-1}^{(22)}\right) e^{-2\lambda h_{n-1}}\right)\right) > 0.
\end{aligned}
$$

Therefore, the determinant of the coefficient matrix is nonzero. This implies that the coefficient matrix of system (2.16) is nonsingular. □

Proposition 2.4. *The coefficient matrix of equation* (2.22) *is nonsingular.*

Proof. We also want to show that the determinant of the coefficient matrix of system (2.22) is nonzero, i.e.,

$$
\begin{vmatrix} G_n^{(11)} & 1 \\ -G_n^{(21)} & 1 \end{vmatrix} = G_n^{(11)} + G_n^{(21)} \neq 0.
$$

To prove this, we note that

$$
\begin{aligned}
\begin{bmatrix} G_n^{(11)} & G_n^{(12)} \\ G_n^{(21)} & G_n^{(22)} \end{bmatrix} &= \prod_{j=1}^{n} \Theta_j = \left(\prod_{j=1}^{n-1} \Theta_j\right) \Theta_n \\
&= \begin{bmatrix} G_{n-1}^{(11)} & G_{n-1}^{(12)} \\ G_{n-1}^{(21)} & G_{n-1}^{(22)} \end{bmatrix} \left(\frac{1}{\alpha_{n-1}^{+} - \alpha_{n-1}^{-}}\right) \\
&\times \begin{bmatrix} \left(\alpha_{n-1}^{+} - \frac{\sigma_{n-1}^{\circ}\alpha_n^{-}}{\sigma_n^{\bullet}}\right) e^{h_{n-1}\left(\alpha_n^{-} - \alpha_{n-1}^{-}\right)} & \left(\alpha_{n-1}^{+} - \frac{\sigma_{n-1}^{\circ}\alpha_n^{+}}{\sigma_n^{\bullet}}\right) e^{h_{n-1}\left(\alpha_n^{+} - \alpha_{n-1}^{-}\right)} \\ \left(\frac{\sigma_{n-1}^{\circ}\alpha_n^{-}}{\sigma_n^{\bullet}} - \alpha_{n-1}^{-}\right) e^{h_{n-1}\left(\alpha_n^{-} - \alpha_{n-1}^{+}\right)} & \left(\frac{\sigma_{n-1}^{\circ}\alpha_n^{+}}{\sigma_n^{\bullet}} - \alpha_{n-1}^{-}\right) e^{h_{n-1}\left(\alpha_n^{+} - \alpha_{n-1}^{+}\right)} \end{bmatrix}.
\end{aligned}
$$

Because $n-1 \geq 1$, Lemma 2.2 asserts that

$$
\left(G_{n-1}^{(12)} + G_{n-1}^{(22)}\right) \alpha_{n-1}^{-} e^{-h_{n-1}\alpha_{n-1}^{+}} < \left(G_{n-1}^{(11)} + G_{n-1}^{(21)}\right) \alpha_{n-1}^{+} e^{-h_{n-1}\alpha_{n-1}^{-}}
$$

and

$$
\left(G_{n-1}^{(12)} + G_{n-1}^{(22)}\right) e^{-h_{n-1}\alpha_{n-1}^{+}} < \left(G_{n-1}^{(11)} + G_{n-1}^{(21)}\right) e^{-h_{n-1}\alpha_{n-1}^{-}},
$$

it follows that

$$
\begin{aligned}
G_n^{(11)} + G_n^{(21)} &= \frac{1}{\alpha_{n-1}^{+} - \alpha_{n-1}^{-}} \Bigg(\left(\alpha_{n-1}^{+} - \frac{\sigma_{n-1}^{\circ}\alpha_n^{-}}{\sigma_n^{\bullet}} \right) G_{n-1}^{(11)} e^{h_{n-1}\left(\alpha_n^{-} - \alpha_{n-1}^{-}\right)} \\
&\quad + \left(\frac{\sigma_{n-1}^{\circ}\alpha_n^{-}}{\sigma_n^{\bullet}} - \alpha_{n-1}^{-} \right) G_{n-1}^{(12)} e^{h_{n-1}\left(\alpha_n^{-} - \alpha_{n-1}^{+}\right)} \\
&\quad + \left(\alpha_{n-1}^{+} - \frac{\sigma_{n-1}^{\circ}\alpha_n^{-}}{\sigma_n^{\bullet}} \right) G_{n-1}^{(21)} e^{h_{n-1}\left(\alpha_n^{-} - \alpha_{n-1}^{-}\right)} \\
&\quad + \left(\frac{\sigma_{n-1}^{\circ}\alpha_n^{-}}{\sigma_n^{\bullet}} - \alpha_{n-1}^{-} \right) G_{n-1}^{(22)} e^{h_{n-1}\left(\alpha_n^{-} - \alpha_{n-1}^{+}\right)} \Bigg) \\
&= \frac{1}{\alpha_{n-1}^{+} - \alpha_{n-1}^{-}} \Bigg(\left(\alpha_{n-1}^{+} - \frac{\sigma_{n-1}^{\circ}\alpha_n^{-}}{\sigma_n^{\bullet}} \right) \left(G_{n-1}^{(11)} + G_{n-1}^{(21)} \right) e^{-h_{n-1}\alpha_{n-1}^{-}} \\
&\quad + \left(\frac{\sigma_{n-1}^{\circ}\alpha_n^{-}}{\sigma_n^{\bullet}} - \alpha_{n-1}^{-} \right) \left(G_{n-1}^{(12)} + G_{n-1}^{(22)} \right) e^{-h_{n-1}\alpha_{n-1}^{+}} \Bigg) e^{h_{n-1}\alpha_n^{-}} \\
&= \frac{1}{\alpha_{n-1}^{+} - \alpha_{n-1}^{-}} \Bigg(\bigg(\left(G_{n-1}^{(11)} + G_{n-1}^{(21)} \right) \alpha_{n-1}^{+} e^{-h_{n-1}\alpha_{n-1}^{-}} \\
&\quad - \left(G_{n-1}^{(12)} + G_{n-1}^{(22)} \right) \alpha_{n-1}^{-} e^{-h_{n-1}\alpha_{n-1}^{+}} \bigg) \\
&\quad - \frac{\sigma_{n-1}^{\circ}\alpha_n^{-}}{\sigma_n^{\bullet}} \bigg(\left(G_{n-1}^{(11)} + G_{n-1}^{(21)} \right) e^{-h_{n-1}\alpha_{n-1}^{-}} \\
&\quad - \left(G_{n-1}^{(12)} + G_{n-1}^{(22)} \right) e^{-h_{n-1}\alpha_{n-1}^{+}} \bigg) \Bigg) e^{h_{n-1}\alpha_n^{-}} > 0.
\end{aligned}
$$

Therefore, the determinant of the coefficient matrix is nonzero. This shows that the coefficient matrix of system (2.22) is nonsingular. □

2.6 Numerical Experiments

In our numerical experiments, we calculate the magnetic fields due to a direct current source on multilayered earth structures of six models. Chave's algorithm [10] is used for numerically calculating the inverse Hankel transform of the magnetic field solutions. Our example models are compared to the models using the MMR method obtained by Chen and Oldenburg [11], Yooyuanyong and Sripanya [70, 71]. The electric current of 1 ampere is used in our computations. The magnetic fields from many kinds of ground structures are ploted to show the behavior of fields against source-receiver spacing at different depths.

2.6.1 Synthesis Models

We firstly consider the synthesis models of 2-layered earth. Our models are grouped into two categories. The models denoted by Models A-1, A-2, B-1 and B-2 of the first category have conductivity discontinuity at the interface of layers. The models A-1 and B-1 are obtained from the DC method, whereas the models A-2 and B-2 are gotten from the MMR method. The conductivities of the first and second layers for this category are constant. The magnetic fields can be described by the model in Section 2.3.1. The values of the model parameters are given in Table 2.1. The models of the second category are referred to as Models C-1, C-2, D-1 and D-2. The conductivities for these models have continuity at the interface of layers. The models C-1 and D-1 are obtained from the DC method, whereas the models C-2 and D-2 are gotten from the MMR method. The overburden of these models has an exponentially varying conductivity denoted by $\sigma(z) = ae^{bz}$ with thickness h, and the host has a constant conductivity $\sigma(h)$ with infinite depth. The values of the model parameters for this category are given in Table 2.2. The results of all models are plotted to show the behavior of magnetic fields against source-receiver spacing r at different depths $z = 0, 0.5, 1, \ldots, 10$ metres as shown in Figures 2.2 and 2.3.

Table 2.1: Methods and model parameters used in the first category.

Methods		Model Parameters		
DC	MMR	σ_1 $(\text{S}\cdot\text{m}^{-1})$	σ_2 $(\text{S}\cdot\text{m}^{-1})$	h (m)
A-1	A-2	0.05	0.5	5
B-1	B-2	0.5	0.05	5

Table 2.2: Methods and model parameters used in the second category.

Methods		Model Parameters		
DC	MMR	a $(\text{S}\cdot\text{m}^{-1})$	b (m^{-1})	h (m)
C-1	C-2	0.05	$0.2\ln 10$	5
D-1	D-2	0.5	$-0.2\ln 10$	5

2.6.2 Real Earth Models

We now consider the conductivity data of the real earth structures of rice paddy field and marine shrimp aquaculture farm, Banglen, Nakhon Pathom, Thailand (Yooyuanyong et al. [69]). Soil salinity profiles frequently display monotonically increasing or decreasing salt concentrations with depth z. This salt concentration is strongly correlated with the conductivity σ of the ground and can be frequently denoted by an equation $\sigma(z) = ae^{bz}$, where a and b are the parameters that define the conductivity profile (Lee and Ignetik [37]). The models of rice paddy field are denoted by Models E-1 and E-2, and for marine shrimp aquaculture farm, the models are referred to as Models F-1 and F-2. The models E-1 and F-1 are obtained from the DC method, whereas the models E-2 and F-2

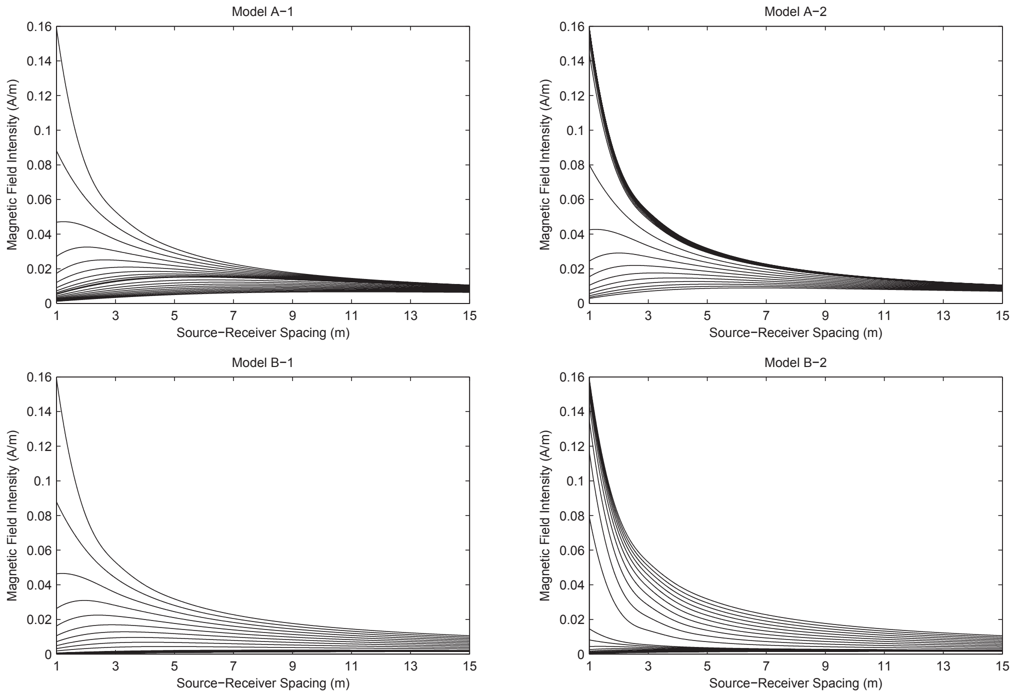

Figure 2.2: Behavior of magnetic fields from our models in the first category.

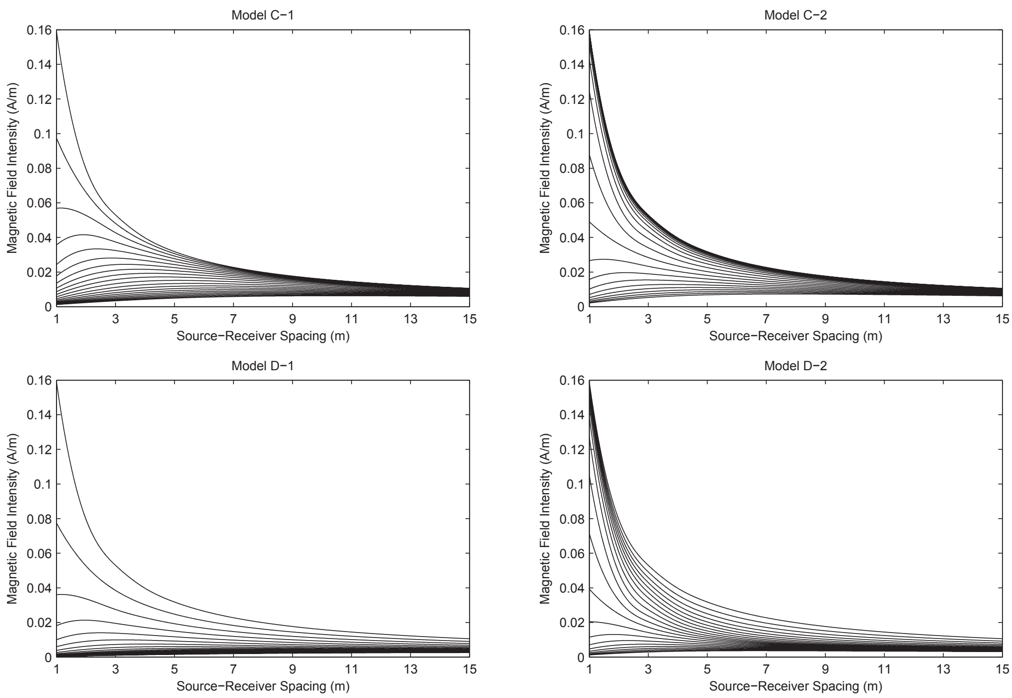

Figure 2.3: Behavior of magnetic fields from our models in the second category.

are gotten from the MMR method. All the models are the heterogeneous conductive half-spaces and have exponentially varying conductivities as given above. The values of the model parameters for the real earth structures are given in Table 2.3. The results of these models are also plotted to show the behavior of magnetic fields against source-receiver spacing r at different depths $z = 0, 0.5, 1, \ldots, 10$ metres as shown in Figure 2.4.

Table 2.3: Methods and model parameters used in real earth models.

	Methods		Model Parameters	
Structure	DC	MMR	a $(\mathrm{S{\cdot}m^{-1}})$	b $(\mathrm{m^{-1}})$
Rice paddy field	E-1	E-2	0.0780032423	0.1399913356
Marine shrimp aquaculture farm	F-1	F-2	0.1743262126	0.1006195806

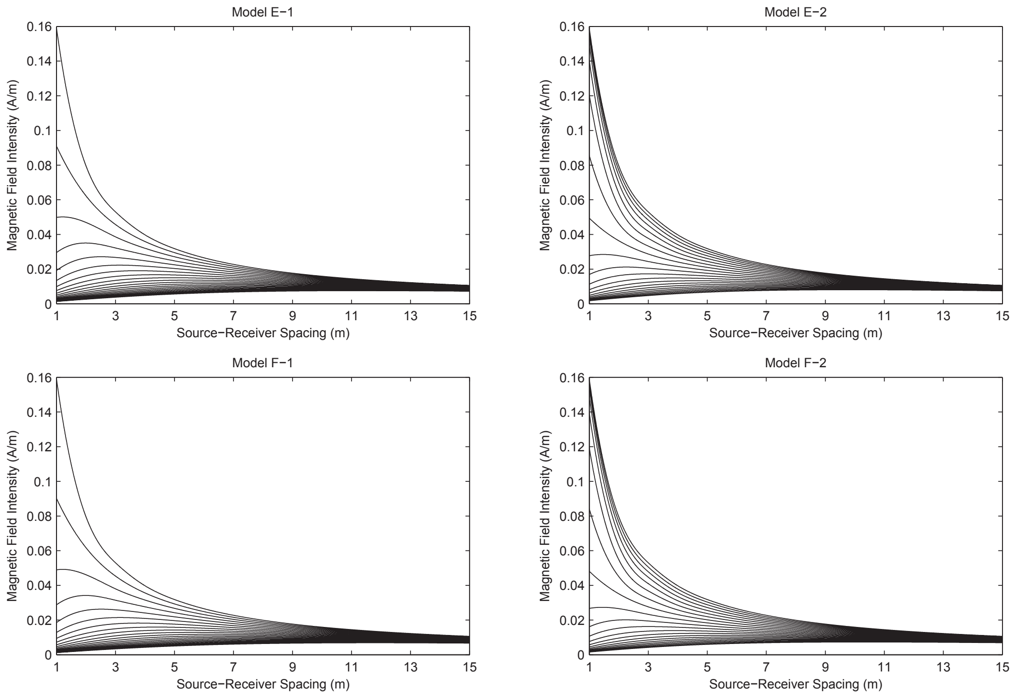

Figure 2.4: Behavior of magnetic fields from real earth models.

2.7 Inversion Process

In our inverse model examples, we simulate the reflection of magnetic radiation data from our forward models of practical interest. Two types of ground structures are used to investigate the conductivity profiles. Newton's method in optimization is applied to find a conductivity parameter of the ground.

2.7.1 Sample Tests

We firstly consider the magnetic field data obtained from the models of two simple cases. Both of the test models are the heterogeneous conductive half-spaces. The first model has exponentially increasing conductivity with depth, whereas the second model has exponentially decreasing conductivity. The values of the model parameters are given in Table 2.4. The parameter a is a conductivity of the earth's surface, which can be assumed to be known from the measurement. The iterative procedure using the Newton-Raphson method (Press et al. [48]) is applied to estimate the model parameter b of conductivity variation. We start the iterative process to find the values of the conductivity parameter with an initial guess $b = 0$ m^{-1}. The optimal results are close to the true values with misfits less than 10^{-15} A·m^{-1} after using only 4 iterations (see Tables 2.5 and 2.6).

Table 2.4: Model parameters used in our sample tests.

	Parameters	
Model	a (S·m^{-1})	b (m^{-1})
1	0.0780032423	0.1399913356
2	0.1743262126	-0.1006195806

Table 2.5: Successive iterations for finding a conductivity parameter of the first model in our sample tests.

Iteration	Parameter b (S·m^{-1})	Misfit (A·m^{-1})
0	0.000000000000000	$1.214058494446720 \times 10^{-3}$
1	$1.307946426785820 \times 10^{-1}$	$7.517654261963835 \times 10^{-5}$
2	$1.399565344760604 \times 10^{-1}$	$2.834058869836987 \times 10^{-7}$
3	$1.399913351184671 \times 10^{-1}$	$3.920654203089532 \times 10^{-12}$
4	$1.399913355999150 \times 10^{-1}$	$3.680364159319444 \times 10^{-16}$

2.7.2 Interpretation of Simulated Real Data

We now consider the real data of magnetic radiation obtained from the simulation model. The magnetic fields are generated by the forward problem of the first model in our sample tests. Random errors up to 3% are superimposed on the scaled magnetic fields to simulate the set of real data. The iterative procedure using the Newton-Raphson method is also applied to estimate the model parameter of conductivity variation. The optimal result is close to the true value

Table 2.6: Successive iterations for finding a conductivity parameter of the second model in our sample tests.

Iteration	Parameter b $\left(\mathrm{S{\cdot}m^{-1}}\right)$	Misfit $\left(\mathrm{A{\cdot}m^{-1}}\right)$
0	0.000000000000000	$9.884545374948975 \times 10^{-4}$
1	$-1.062912668426295 \times 10^{-1}$	$5.856702123732604 \times 10^{-5}$
2	$-1.006326489408686 \times 10^{-1}$	$1.346242571305827 \times 10^{-7}$
3	$-1.006195806657319 \times 10^{-1}$	$6.769917897069811 \times 10^{-13}$
4	$-1.006195806000140 \times 10^{-1}$	$1.562021926317163 \times 10^{-16}$

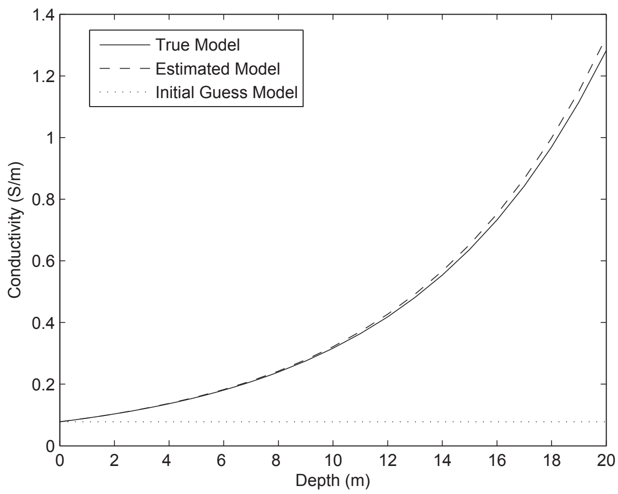

Figure 2.5: Graphs of conductivity σ against depth z for our model example.

with percentage error less than only 1.2% after using 15 iterations. The graphs of the true and estimated conductivity models are plotted as shown in Figure 2.5.

2.8 Discussions

Analytical solutions of the steady state magnetic field due to a direct current source are derived by using the recurrence relations (2.14) and (2.19). The recurrence relation (2.19) is applicable to general cases in which the layers have either constant or exponentially varying conductivities. In the case of a uniform half-space, we can obtain the magnetic field as shown in equation (2.13), which is the same result obtained by Chen and Oldenburg [11].

The effects of magnetic fields obtained from the DC and MMR methods are plotted and compared to show the behavior in response to different ground structures at many depths. The magnetic curves of the models using the DC method are quite different from the models using the MMR method. The length of the probe source gives effect to the magnitude of magnetic field. It can be seen that the magnitude of magnetic field from the MMR method is much higher than the magnetic field from the DC method at the same depth. As well as the different ground structures, even the same method, the curves of magnetic fields are also different at the same depth and source-receiver spacing. We observe that if the ratio of the conductivities between two connected layers is high, it will lead to the large sized magnitude of magnetic field. Moreover, in the case of an exponential conductivity profile, if the exponent of the conductivity function is high, it will also lead to the large size of magnitude. This means that the differences of curves for our entire models are depended on the variation of conductivity. We also observe that the responses of magnetic fields drop very fast as the source-receiver spacing increases to 5 metres.

An inverse problem via the use of an optimization technique is introduced for finding a conductivity parameter of the ground. Two types of ground structures are used to investigate the conductivity profiles. The iterative procedure using the Newton-Raphson method is applied to estimate the model parameter of conductivity variation. The optimal results of our sample tests converge very fast to the true values with misfits less than 10^{-15} A·m^{-1} after using only 4 iterations. These illustrate the advantage in using Newton-Raphson method which gives the convergence much faster than using another method of inversion (e.g., Oldenburg [44], Vozoff and Jupp [65]). Moreover, the optimal result for the simulated real data also converges to the true value with percentage error less than only 1.2% after using 15 iterations. The graphs of the true and estimated conductivity models are plotted as shown in Figure 2.5. We see that the graph of the estimated model is close to the true model. The inversion method leads to very good results and has high speed of convergence. This shows the robustness of our models and procedure.

2.9 Summary and Conclusions

A new electrical method used for investigation of a multilayered earth structure is presented in this study. The method proposed here is based on the measurement of low-level, low-frequency static magnetic fields associated with noninductive current flow between two current electrodes on the earth's surface. We derive analytical solutions of the steady state magnetic field due to a direct current source on two types of multilayered earth structures including layers having constant conductivities and layers having exponentially varying conductivities. The Hankel transform is introduced to our problems and analytical results are obtained. Our solutions are achieved by solving a boundary value problem in the wave number domain and then transforming the solution back to the spatial domain. The propagator matrix technique is used to formulate recurrence relations for solving the problems. One of these relations is generalized in all cases where the layers have either constant or exponentially varying conductivities. The effects of magnetic fields obtained from the DC and MMR methods are plotted and compared to show the behavior in response to different ground structures at many depths while some parameters are approximately given. The ground structures of rice paddy field and marine shrimp aquaculture farm are used to investigate the magnetic field responses. The magnetic fields obtained from different ground structures and methods of investigation are very much different, especially for the first 5 metres of source-receiver spacing. The curves of magnetic fields show some significance to the depth of overburden layer. The inversion process, using the Newton-Raphson method, is conducted to estimate a conductivity parameter of the ground. The method leads to very good results and has high speed of convergence.

Chapter 3

Magnetic Field of a DC Source on a Transitional Multilayered Earth

3.1 Introduction

In many instances where the geological section can be approximated by horizontal layers, the boundaries between the layers are not sharp but are transitional in nature. The concept of transition is enlarged to the cases where at least in one geological formation, the electrical conductivity is not constant. For simplicity, the electrical conductivity is assumed to be linearly dependent upon depth. In practice, the transitional layer can stand for the weathered zone in hard rock areas where the degree of weathering diminishes with depth. This problem was first treated by Mallick and Roy [40] who obtained a theoretical solution for the problem of a two-layered earth with transitional boundary. Lal [36] presented a theory of resistivity sounding on a three-layered earth comprising an inhomogeneous interstratum. The electrical conductivity in the intermediate layer, embedded between two layers of uniform conductivity, is assumed to follow either binomial or exponential variation. Jain [30] derived expressions for apparent resistivity of a horizontal three-layered earth where the conductivity in the second layer varies linearly with depth and changes abruptly at the boundaries. Patella [45, 46] considered a horizontally stratified earth where the layers with even numbers have linear conductivities varying with depth and the layers with odd numbers have uniform conductivities. Koefoed [35] solved the problem of a transitional layer with linear change of the resistivity with depth, a type of change that seems to be more common in nature than the type considered by Mallick and Roy. A solution is extended to layered stratifications involving an arbitrary number of homogeneous layers and of transitional layers. Banerjee et al. [8] obtained expressions for apparent resistivity of a multilayered earth where one or more of the layers has a binomial variation of conductivity with depth. Raghuwanshi and Singh [49] studied the problem of a multilayered earth consisting of homogeneous overburden of constant conductivity over a stack of transitional layers where the conductivity varies with depth according to binomial and exponential laws in even and odd layers, respectively.

In this chapter, we study the problem of a multilayered earth in which the layers have transitional ground profiles. Two types of transitional zones are considered, including layers having linearly and binomially varying conductivities. We develop analytical solutions of the steady state magnetic field for this problem. The governing equations in Section 2.2 are reused to determine our solutions. The propagator matrix technique is also used to formulate recurrence relations for solving the problems. An inverse problem via the use of the Newton-Raphson optimization technique is introduced for finding a conductivity parameter of the ground.

3.2 Response of a Layer Having Linearly Varying Conductivity

For each layer k, where $1 \leq k \leq n$ and $n \geq 2$, the variation of conductivity is denoted by

$$\sigma_k(z) = m_k z + c_k, \tag{3.1}$$

where c_k and $m_k \neq 0$ are constants, which preserve $\sigma_k(z) > 0$. Hence, the equation for the magnetic field in each layer can be simplified by substituting equation (3.1) into (2.5) and we obtain

$$\frac{\partial^2 \tilde{H}_k}{\partial z^2} - \frac{m_k}{m_k z + c_k} \frac{\partial \tilde{H}_k}{\partial z} - \lambda^2 \tilde{H}_k = 0.$$

The solution to the above equation has been found by Lal [36] and given as

$$\tilde{H}_k(\lambda, z) = \psi_k(z) \left(A_k I_1 \left(\frac{\lambda}{\varrho_k} \psi_k(z) \right) + B_k K_1 \left(\frac{\lambda}{\varrho_k} \psi_k(z) \right) \right),$$

where

$$\varrho_k = \frac{m_k}{c_k}, \qquad \psi_k(z) = 1 + \varrho_k z,$$

I_ν and K_ν are the modified Bessel functions of the first and second kinds of order ν. The unknown coefficients A_k and B_k are arbitrary constants, which can be determined by using the boundary conditions. Thus, the magnetic field in layer k is

$$H_k(r, z) = \int_0^\infty \left(\psi_k(z) \left(A_k I_1 \left(\frac{\lambda}{\varrho_k} \psi_k(z) \right) + B_k K_1 \left(\frac{\lambda}{\varrho_k} \psi_k(z) \right) \right) \right) J_1(\lambda r)\, d\lambda. \tag{3.2}$$

Consider an n-layered earth model, for $1 \leq k \leq n-1$, the magnetic fields in layers k and $k+1$ can be written as

$$\tilde{H}_k(\lambda, z) = \psi_k(z) \left(A_k I_1 \left(\frac{\lambda}{\varrho_k} \psi_k(z) \right) + B_k K_1 \left(\frac{\lambda}{\varrho_k} \psi_k(z) \right) \right)$$

and

$$\tilde{H}_{k+1}(\lambda, z) = \psi_{k+1}(z)\left(A_{k+1}I_1\left(\frac{\lambda}{\varrho_{k+1}}\psi_{k+1}(z)\right) + B_{k+1}K_1\left(\frac{\lambda}{\varrho_{k+1}}\psi_{k+1}(z)\right)\right).$$

Using the boundary conditions (2.8) and (2.9), we obtain

$$\psi_k(h_k)\left(A_kI_1\left(\frac{\lambda}{\varrho_k}\psi_k(h_k)\right) + B_kK_1\left(\frac{\lambda}{\varrho_k}\psi_k(h_k)\right)\right)$$
$$= \psi_{k+1}(h_k)\left(A_{k+1}I_1\left(\frac{\lambda}{\varrho_{k+1}}\psi_{k+1}(h_k)\right) + B_{k+1}K_1\left(\frac{\lambda}{\varrho_{k+1}}\psi_{k+1}(h_k)\right)\right)$$

and

$$\frac{\lambda}{c_k}\left(B_kK_0\left(\frac{\lambda}{\varrho_k}\psi_k(h_k)\right) - A_kI_0\left(\frac{\lambda}{\varrho_k}\psi_k(h_k)\right)\right)$$
$$= \frac{\lambda}{c_{k+1}}\left(B_{k+1}K_0\left(\frac{\lambda}{\varrho_{k+1}}\psi_{k+1}(h_k)\right) - A_{k+1}I_0\left(\frac{\lambda}{\varrho_{k+1}}\psi_{k+1}(h_k)\right)\right).$$

Hence, A_k and B_k can be written in terms of A_{k+1} and B_{k+1} as

$$A_k = M_{k+1}^{(11)}A_{k+1} + M_{k+1}^{(12)}B_{k+1}$$

and

$$B_k = M_{k+1}^{(21)}A_{k+1} + M_{k+1}^{(22)}B_{k+1},$$

where all the coefficients $M_{k+1}^{(ij)}$ are given by

$$M_{k+1}^{(11)} = \frac{\lambda}{\varrho_k c_{k+1}}\left(\sigma_k^{\circ}K_1\left(\frac{\lambda}{\varrho_k}\psi_k(h_k)\right)I_0\left(\frac{\lambda}{\varrho_{k+1}}\psi_{k+1}(h_k)\right)\right.$$
$$\left. + \sigma_{k+1}^{\bullet}K_0\left(\frac{\lambda}{\varrho_k}\psi_k(h_k)\right)I_1\left(\frac{\lambda}{\varrho_{k+1}}\psi_{k+1}(h_k)\right)\right),$$

$$M_{k+1}^{(12)} = \frac{\lambda}{\varrho_k c_{k+1}}\left(\sigma_{k+1}^{\bullet}K_0\left(\frac{\lambda}{\varrho_k}\psi_k(h_k)\right)K_1\left(\frac{\lambda}{\varrho_{k+1}}\psi_{k+1}(h_k)\right)\right.$$
$$\left. - \sigma_k^{\circ}K_1\left(\frac{\lambda}{\varrho_k}\psi_k(h_k)\right)K_0\left(\frac{\lambda}{\varrho_{k+1}}\psi_{k+1}(h_k)\right)\right),$$

$$M_{k+1}^{(21)} = \frac{\lambda}{\varrho_k c_{k+1}}\left(\sigma_{k+1}^{\bullet}I_0\left(\frac{\lambda}{\varrho_k}\psi_k(h_k)\right)I_1\left(\frac{\lambda}{\varrho_{k+1}}\psi_{k+1}(h_k)\right)\right.$$
$$\left. - \sigma_k^{\circ}I_1\left(\frac{\lambda}{\varrho_k}\psi_k(h_k)\right)I_0\left(\frac{\lambda}{\varrho_{k+1}}\psi_{k+1}(h_k)\right)\right),$$

$$M_{k+1}^{(22)} = \frac{\lambda}{\varrho_k c_{k+1}}\left(\sigma_k^{\circ}I_1\left(\frac{\lambda}{\varrho_k}\psi_k(h_k)\right)K_0\left(\frac{\lambda}{\varrho_{k+1}}\psi_{k+1}(h_k)\right)\right.$$
$$\left. + \sigma_{k+1}^{\bullet}I_0\left(\frac{\lambda}{\varrho_k}\psi_k(h_k)\right)K_1\left(\frac{\lambda}{\varrho_{k+1}}\psi_{k+1}(h_k)\right)\right)$$

and

$$\lim_{z \to h_k^-} \sigma_k(z) = \sigma_k^{\circ}, \qquad \lim_{z \to h_k^+} \sigma_{k+1}(z) = \sigma_{k+1}^{\bullet}.$$

These can be rewritten in matrix form as

$$\begin{bmatrix} A_k \\ B_k \end{bmatrix} = \Gamma_{k+1} \begin{bmatrix} A_{k+1} \\ B_{k+1} \end{bmatrix}, \tag{3.3}$$

where the propagator matrix is

$$\Gamma_{k+1} = \begin{bmatrix} M_{k+1}^{(11)} & M_{k+1}^{(12)} \\ M_{k+1}^{(21)} & M_{k+1}^{(22)} \end{bmatrix}.$$

Thus, equation (3.3) can be applied to obtain

$$\begin{bmatrix} A_1 \\ B_1 \end{bmatrix} = \prod_{j=1}^{n} \Gamma_j \begin{bmatrix} A_n \\ B_n \end{bmatrix}, \tag{3.4}$$

where Γ_1 is the 2×2 identity matrix. To satisfy (2.6), we require

$$A_n = 0.$$

The boundary condition as given in (2.7) leads to

$$\left. \frac{1}{r} \frac{\partial}{\partial r} (r H_1) \right|_{z=0} = \frac{I}{2\pi} \frac{\delta(r)}{r}. \tag{3.5}$$

Replacing k by 1 in (3.2), equation (3.5) then becomes

$$\int_0^{\infty} \left(A_1 I_1 \left(\frac{\lambda}{\varrho_1} \right) + B_1 K_1 \left(\frac{\lambda}{\varrho_1} \right) \right) \left(\lambda J_1' (\lambda r) + \frac{J_1(\lambda r)}{r} \right) d\lambda = \frac{I}{2\pi} \frac{\delta(r)}{r}.$$

Using the recurrence relation for Bessel functions

$$\lambda r J_1'(\lambda r) + J_1(\lambda r) = \lambda r J_0(\lambda r)$$

and the integral

$$\int_0^{\infty} \lambda J_0(\lambda r)\, d\lambda = \frac{\delta(r)}{r},$$

we obtain

$$\int_0^{\infty} \left(A_1 I_1 \left(\frac{\lambda}{\varrho_1} \right) + B_1 K_1 \left(\frac{\lambda}{\varrho_1} \right) \right) \lambda J_0(\lambda r)\, d\lambda = \int_0^{\infty} \frac{I}{2\pi} \lambda J_0(\lambda r)\, d\lambda.$$

Inverting the above equation yields

$$B_1 = \frac{I}{2\pi\xi} - A_1 \zeta,$$

where

$$\xi = K_1\left(\frac{\lambda}{\varrho_1}\right), \qquad \zeta = I_1\left(\frac{\lambda}{\varrho_1}\right)/\xi.$$

Substituting B_1 and A_n into equation (3.4), we obtain

$$\begin{bmatrix} A_1 \\ (I/2\pi\xi) - A_1\zeta \end{bmatrix} = \prod_{j=1}^{n} \Gamma_j \begin{bmatrix} 0 \\ B_n \end{bmatrix}.$$

This can be rewritten as a system of two linear equations in terms of the unknowns A_1 and B_n as

$$\begin{bmatrix} 1 & -F_n^{(12)} \\ \zeta & F_n^{(22)} \end{bmatrix} \begin{bmatrix} A_1 \\ B_n \end{bmatrix} = \begin{bmatrix} 0 \\ I/2\pi\xi \end{bmatrix},$$

where $F_k^{(ij)}$ is determined by

$$\prod_{j=1}^{k} \Gamma_j = \begin{bmatrix} F_k^{(11)} & F_k^{(12)} \\ F_k^{(21)} & F_k^{(22)} \end{bmatrix}.$$

Similar to Section 2.5, we can prove that the coefficient matrix of the above system is nonsingular. By virtue of Cramer's rule, the system has a unique solution

$$A_1 = \frac{I}{2\pi\xi}\frac{F_n^{(12)}}{F_n^{(22)} + \zeta F_n^{(12)}}, \qquad B_n = \frac{I}{2\pi\xi}\frac{1}{F_n^{(22)} + \zeta F_n^{(12)}}.$$

As A_1, B_1, A_n and B_n are determined, so A_k and B_k, where $k \neq 1$ and n, can be obtained from the recurrence relation (3.3).

3.3 Response of a Layer Having Binomially Varying Conductivity

For each layer k, where $1 \leq k \leq n$ and $n \geq 2$, the variation of conductivity is denoted by

$$\sigma_k(z) = c_k(1 + d_k z)^{p_k}, \tag{3.6}$$

where c_k, p_k and $d_k \neq 0$ are constants, which preserve $\sigma_k(z) > 0$. Hence, the equation for the magnetic field in each layer can be simplified by substituting equation (3.6) into (2.5) and we obtain

$$\frac{\partial^2 \tilde{H}_k}{\partial z^2} - \frac{d_k p_k}{1 + d_k z}\frac{\partial \tilde{H}_k}{\partial z} - \lambda^2 \tilde{H}_k = 0.$$

The solution to the above equation has been found by Lal [36] and given as

$$\tilde{H}_k(\lambda, z) = \tilde{\psi}_k^{\gamma_k}(z)\left(C_k I_{-\gamma_k}\left(\frac{\lambda}{\tilde{\varrho}_k}\tilde{\psi}_k(z)\right) + D_k K_{-\gamma_k}\left(\frac{\lambda}{\tilde{\varrho}_k}\tilde{\psi}_k(z)\right)\right),$$

where

$$\tilde{\varrho}_k = d_k, \qquad \tilde{\psi}_k(z) = 1 + \tilde{\varrho}_k z, \qquad \gamma_k = \frac{1+p_k}{2},$$

C_k and D_k are arbitrary constants, which can be determined by using the boundary conditions. Thus, the magnetic field in layer k is

$$H_k(r,z) = \int_0^\infty \left(\tilde{\psi}_k^{\gamma_k}(z) \left(C_k I_{-\gamma_k}\left(\frac{\lambda}{\tilde{\varrho}_k} \tilde{\psi}_k(z) \right) + D_k K_{-\gamma_k}\left(\frac{\lambda}{\tilde{\varrho}_k} \tilde{\psi}_k(z) \right) \right) \right) J_1(\lambda r)\, d\lambda. \quad (3.7)$$

3.3.1 Solution for a 2-layered Earth

In this section, we firstly consider a 2-layered earth model with an overburden depth h. Both of the ground layers have binomially varying conductivities as given in (3.6). The magnetic fields in an overburden, denoted by $\tilde{H}_1$, and in a host, denoted by $\tilde{H}_2$, can be written as

$$\tilde{H}_1(\lambda,z) = \tilde{\psi}_1^{\gamma_1}(z) \left(C_1 I_{-\gamma_1}\left(\frac{\lambda}{\tilde{\varrho}_1} \tilde{\psi}_1(z) \right) + D_1 K_{-\gamma_1}\left(\frac{\lambda}{\tilde{\varrho}_1} \tilde{\psi}_1(z) \right) \right)$$

and

$$\tilde{H}_2(\lambda,z) = \tilde{\psi}_2^{\gamma_2}(z) \left(C_2 I_{-\gamma_2}\left(\frac{\lambda}{\tilde{\varrho}_2} \tilde{\psi}_2(z) \right) + D_2 K_{-\gamma_2}\left(\frac{\lambda}{\tilde{\varrho}_2} \tilde{\psi}_2(z) \right) \right),$$

where C_1, D_1, C_2 and D_2 are arbitrary constants, which can be determined by using the boundary conditions. To satisfy (2.6), we require

$$C_2 = 0.$$

The boundary condition (2.7) can be applied to obtain

$$\left. \frac{1}{r}\frac{\partial}{\partial r}(rH_1) \right|_{z=0} = \frac{I}{2\pi}\frac{\delta(r)}{r}. \quad (3.8)$$

Replacing k by 1 in (3.7), equation (3.8) then becomes

$$\int_0^\infty \left(C_1 I_{-\gamma_1}\left(\frac{\lambda}{\tilde{\varrho}_1} \right) + D_1 K_{-\gamma_1}\left(\frac{\lambda}{\tilde{\varrho}_1} \right) \right) \left(\lambda J_1'(\lambda r) + \frac{J_1(\lambda r)}{r} \right) d\lambda = \frac{I}{2\pi}\frac{\delta(r)}{r}.$$

Using the recurrence relation for Bessel functions

$$\lambda r J_1'(\lambda r) + J_1(\lambda r) = \lambda r J_0(\lambda r)$$

and the integral

$$\int_0^\infty \lambda J_0(\lambda r)\, d\lambda = \frac{\delta(r)}{r},$$

we obtain

$$\int_0^\infty \left(C_1 I_{-\gamma_1}\left(\frac{\lambda}{\tilde{\varrho}_1}\right) + D_1 K_{-\gamma_1}\left(\frac{\lambda}{\tilde{\varrho}_1}\right)\right) \lambda J_0\left(\lambda r\right) d\lambda = \int_0^\infty \frac{I}{2\pi} \lambda J_0\left(\lambda r\right) d\lambda.$$

Inverting the above equation yields

$$D_1 = \frac{I}{2\pi\tilde{\xi}} - C_1 \tilde{\zeta},$$

where

$$\tilde{\xi} = K_{-\gamma_1}\left(\frac{\lambda}{\tilde{\varrho}_1}\right), \qquad \tilde{\zeta} = I_{-\gamma_1}\left(\frac{\lambda}{\tilde{\varrho}_1}\right)/\tilde{\xi}.$$

Hence, the magnetic fields $\tilde{H}_1$ and $\tilde{H}_2$ can be rewritten as

$$\begin{aligned}\tilde{H}_1\left(\lambda, z\right) = \tilde{\psi}_1^{\gamma_1}\left(z\right) \Bigg(& \frac{I}{2\pi\tilde{\xi}} K_{-\gamma_1}\left(\frac{\lambda}{\tilde{\varrho}_1}\tilde{\psi}_1\left(z\right)\right) \\ & + C_1 \left(I_{-\gamma_1}\left(\frac{\lambda}{\tilde{\varrho}_1}\tilde{\psi}_1\left(z\right)\right) - \tilde{\zeta} K_{-\gamma_1}\left(\frac{\lambda}{\tilde{\varrho}_1}\tilde{\psi}_1\left(z\right)\right)\right)\Bigg)\end{aligned}$$

and

$$\tilde{H}_2\left(\lambda, z\right) = \tilde{\psi}_2^{\gamma_2}\left(z\right) D_2 K_{-\gamma_2}\left(\frac{\lambda}{\tilde{\varrho}_2}\tilde{\psi}_2\left(z\right)\right).$$

Thus, the boundary conditions (2.8) and (2.9) lead to

$$\begin{aligned}\tilde{\psi}_1^{\gamma_1}\left(h\right) \Bigg(& \frac{I}{2\pi\tilde{\xi}} K_{-\gamma_1}\left(\frac{\lambda}{\tilde{\varrho}_1}\tilde{\psi}_1\left(h\right)\right) \\ & + C_1 \left(I_{-\gamma_1}\left(\frac{\lambda}{\tilde{\varrho}_1}\tilde{\psi}_1\left(h\right)\right) - \tilde{\zeta} K_{-\gamma_1}\left(\frac{\lambda}{\tilde{\varrho}_1}\tilde{\psi}_1\left(h\right)\right)\right)\Bigg) \\ & = \tilde{\psi}_2^{\gamma_2}\left(h\right) D_2 K_{-\gamma_2}\left(\frac{\lambda}{\tilde{\varrho}_2}\tilde{\psi}_2\left(h\right)\right)\end{aligned}$$

and

$$\begin{aligned}\frac{\lambda}{c_1}\tilde{\psi}_1^{\upsilon_1}\left(h\right) \Bigg(& \frac{I}{2\pi\tilde{\xi}} K_{\upsilon_1}\left(\frac{\lambda}{\tilde{\varrho}_1}\tilde{\psi}_1\left(h\right)\right) \\ & - C_1 \left(I_{\upsilon_1}\left(\frac{\lambda}{\tilde{\varrho}_1}\tilde{\psi}_1\left(h\right)\right) + \tilde{\zeta} K_{\upsilon_1}\left(\frac{\lambda}{\tilde{\varrho}_1}\tilde{\psi}_1\left(h\right)\right)\right)\Bigg) \\ & = \frac{\lambda}{c_2}\tilde{\psi}_2^{\upsilon_2}\left(h\right) D_2 K_{\upsilon_2}\left(\frac{\lambda}{\tilde{\varrho}_2}\tilde{\psi}_2\left(h\right)\right),\end{aligned}$$

where

$$\upsilon_k = \frac{1 - p_k}{2}.$$

Solving these equations for the unknowns C_1 and D_2, we obtain

$$C_1 = \frac{I}{2\pi\tilde{\xi}} \frac{U}{V + \tilde{\zeta} U}, \qquad D_2 = \frac{I}{2\pi\tilde{\xi}} \frac{1}{V + \tilde{\zeta} U},$$

where

$$U = \frac{\lambda}{\tilde{\varrho}_1 c_2} \tilde{\psi}_1^{\upsilon_1}(h)\, \tilde{\psi}_2^{\upsilon_2}(h) \left(\sigma_2^{\bullet} K_{\upsilon_1} \left(\frac{\lambda}{\tilde{\varrho}_1} \tilde{\psi}_1(h) \right) K_{-\gamma_2} \left(\frac{\lambda}{\tilde{\varrho}_2} \tilde{\psi}_2(h) \right) \right.$$
$$\left. - \sigma_1^{\circ} K_{-\gamma_1} \left(\frac{\lambda}{\tilde{\varrho}_1} \tilde{\psi}_1(h) \right) K_{\upsilon_2} \left(\frac{\lambda}{\tilde{\varrho}_2} \tilde{\psi}_2(h) \right) \right)$$

and

$$V = \frac{\lambda}{\tilde{\varrho}_1 c_2} \tilde{\psi}_1^{\upsilon_1}(h)\, \tilde{\psi}_2^{\upsilon_2}(h) \left(\sigma_1^{\circ} I_{-\gamma_1} \left(\frac{\lambda}{\tilde{\varrho}_1} \tilde{\psi}_1(h) \right) K_{\upsilon_2} \left(\frac{\lambda}{\tilde{\varrho}_2} \tilde{\psi}_2(h) \right) \right.$$
$$\left. + \sigma_2^{\bullet} I_{\upsilon_1} \left(\frac{\lambda}{\tilde{\varrho}_1} \tilde{\psi}_1(h) \right) K_{-\gamma_2} \left(\frac{\lambda}{\tilde{\varrho}_2} \tilde{\psi}_2(h) \right) \right).$$

In the case of a uniform half-space, the magnetic field in a homogeneous medium can be written as

$$\tilde{H}(\lambda, z) = \frac{I}{2\pi} e^{-\lambda z}. \tag{3.9}$$

Using the Lipschitz-Hankel integral

$$\int_0^{\infty} e^{-\lambda z} J_1(\lambda r)\, d\lambda = \frac{1}{r} \left(1 - \frac{z}{\sqrt{r^2 + z^2}} \right),$$

we can transform equation (3.9) back to the spatial domain and obtain

$$H(r, z) = \frac{I}{2\pi r} \left(1 - \frac{z}{\sqrt{r^2 + z^2}} \right). \tag{3.10}$$

3.3.2 Solution for an n-layered Earth

We now consider an n-layered earth model. Each layer k, where $1 \leq k \leq n$ and $n \geq 2$, has a binomially varying conductivity as given in (3.6). For $1 \leq k \leq n-1$, the magnetic fields in layers k and $k+1$ can be written as

$$\tilde{H}_k(\lambda, z) = \tilde{\psi}_k^{\gamma_k}(z) \left(C_k I_{-\gamma_k} \left(\frac{\lambda}{\tilde{\varrho}_k} \tilde{\psi}_k(z) \right) + D_k K_{-\gamma_k} \left(\frac{\lambda}{\tilde{\varrho}_k} \tilde{\psi}_k(z) \right) \right)$$

and

$$\tilde{H}_{k+1}(\lambda, z) = \tilde{\psi}_{k+1}^{\gamma_{k+1}}(z) \left(C_{k+1} I_{-\gamma_{k+1}} \left(\frac{\lambda}{\tilde{\varrho}_{k+1}} \tilde{\psi}_{k+1}(z) \right) \right.$$
$$\left. + D_{k+1} K_{-\gamma_{k+1}} \left(\frac{\lambda}{\tilde{\varrho}_{k+1}} \tilde{\psi}_{k+1}(z) \right) \right).$$

Using the boundary conditions (2.8) and (2.9), we obtain

$$\tilde{\psi}_k^{\gamma_k}(h_k) \left(C_k I_{-\gamma_k} \left(\frac{\lambda}{\tilde{\varrho}_k} \tilde{\psi}_k(h_k) \right) + D_k K_{-\gamma_k} \left(\frac{\lambda}{\tilde{\varrho}_k} \tilde{\psi}_k(h_k) \right) \right)$$
$$= \tilde{\psi}_{k+1}^{\gamma_{k+1}}(h_k) \left(C_{k+1} I_{-\gamma_{k+1}} \left(\frac{\lambda}{\tilde{\varrho}_{k+1}} \tilde{\psi}_{k+1}(h_k) \right) \right.$$
$$\left. + D_{k+1} K_{-\gamma_{k+1}} \left(\frac{\lambda}{\tilde{\varrho}_{k+1}} \tilde{\psi}_{k+1}(h_k) \right) \right)$$

and

$$\frac{\lambda}{c_k}\tilde{\psi}_k^{\upsilon_k}(h_k)\left(D_k K_{\upsilon_k}\left(\frac{\lambda}{\tilde{\varrho}_k}\tilde{\psi}_k(h_k)\right) - C_k I_{\upsilon_k}\left(\frac{\lambda}{\tilde{\varrho}_k}\tilde{\psi}_k(h_k)\right)\right)$$
$$= \frac{\lambda}{c_{k+1}}\tilde{\psi}_{k+1}^{\upsilon_{k+1}}(h_k)\left(D_{k+1} K_{\upsilon_{k+1}}\left(\frac{\lambda}{\tilde{\varrho}_{k+1}}\tilde{\psi}_{k+1}(h_k)\right)\right.$$
$$\left. - C_{k+1} I_{\upsilon_{k+1}}\left(\frac{\lambda}{\tilde{\varrho}_{k+1}}\tilde{\psi}_{k+1}(h_k)\right)\right).$$

Hence, C_k and D_k can be written in terms of C_{k+1} and D_{k+1} as

$$C_k = N_{k+1}^{(11)} C_{k+1} + N_{k+1}^{(12)} D_{k+1}$$

and

$$D_k = N_{k+1}^{(21)} C_{k+1} + N_{k+1}^{(22)} D_{k+1},$$

where all the coefficients $N_{k+1}^{(ij)}$ are given by

$$N_{k+1}^{(11)} = \frac{\lambda}{\tilde{\varrho}_k c_{k+1}}\tilde{\psi}_k^{\upsilon_k}(h_k)\,\tilde{\psi}_{k+1}^{\upsilon_{k+1}}(h_k)$$
$$\times\left(\sigma_k^{\circ} K_{-\gamma_k}\left(\frac{\lambda}{\tilde{\varrho}_k}\tilde{\psi}_k(h_k)\right) I_{\upsilon_{k+1}}\left(\frac{\lambda}{\tilde{\varrho}_{k+1}}\tilde{\psi}_{k+1}(h_k)\right)\right.$$
$$\left. + \sigma_{k+1}^{\bullet} K_{\upsilon_k}\left(\frac{\lambda}{\tilde{\varrho}_k}\tilde{\psi}_k(h_k)\right) I_{-\gamma_{k+1}}\left(\frac{\lambda}{\tilde{\varrho}_{k+1}}\tilde{\psi}_{k+1}(h_k)\right)\right),$$

$$N_{k+1}^{(12)} = \frac{\lambda}{\tilde{\varrho}_k c_{k+1}}\tilde{\psi}_k^{\upsilon_k}(h_k)\,\tilde{\psi}_{k+1}^{\upsilon_{k+1}}(h_k)$$
$$\times\left(\sigma_{k+1}^{\bullet} K_{\upsilon_k}\left(\frac{\lambda}{\tilde{\varrho}_k}\tilde{\psi}_k(h_k)\right) K_{-\gamma_{k+1}}\left(\frac{\lambda}{\tilde{\varrho}_{k+1}}\tilde{\psi}_{k+1}(h_k)\right)\right.$$
$$\left. - \sigma_k^{\circ} K_{-\gamma_k}\left(\frac{\lambda}{\tilde{\varrho}_k}\tilde{\psi}_k(h_k)\right) K_{\upsilon_{k+1}}\left(\frac{\lambda}{\tilde{\varrho}_{k+1}}\tilde{\psi}_{k+1}(h_k)\right)\right),$$

$$N_{k+1}^{(21)} = \frac{\lambda}{\tilde{\varrho}_k c_{k+1}}\tilde{\psi}_k^{\upsilon_k}(h_k)\,\tilde{\psi}_{k+1}^{\upsilon_{k+1}}(h_k)$$
$$\times\left(\sigma_{k+1}^{\bullet} I_{\upsilon_k}\left(\frac{\lambda}{\tilde{\varrho}_k}\tilde{\psi}_k(h_k)\right) I_{-\gamma_{k+1}}\left(\frac{\lambda}{\tilde{\varrho}_{k+1}}\tilde{\psi}_{k+1}(h_k)\right)\right.$$
$$\left. - \sigma_k^{\circ} I_{-\gamma_k}\left(\frac{\lambda}{\tilde{\varrho}_k}\tilde{\psi}_k(h_k)\right) I_{\upsilon_{k+1}}\left(\frac{\lambda}{\tilde{\varrho}_{k+1}}\tilde{\psi}_{k+1}(h_k)\right)\right),$$

$$N_{k+1}^{(22)} = \frac{\lambda}{\tilde{\varrho}_k c_{k+1}}\tilde{\psi}_k^{\upsilon_k}(h_k)\,\tilde{\psi}_{k+1}^{\upsilon_{k+1}}(h_k)$$
$$\times\left(\sigma_k^{\circ} I_{-\gamma_k}\left(\frac{\lambda}{\tilde{\varrho}_k}\tilde{\psi}_k(h_k)\right) K_{\upsilon_{k+1}}\left(\frac{\lambda}{\tilde{\varrho}_{k+1}}\tilde{\psi}_{k+1}(h_k)\right)\right.$$
$$\left. + \sigma_{k+1}^{\bullet} I_{\upsilon_k}\left(\frac{\lambda}{\tilde{\varrho}_k}\tilde{\psi}_k(h_k)\right) K_{-\gamma_{k+1}}\left(\frac{\lambda}{\tilde{\varrho}_{k+1}}\tilde{\psi}_{k+1}(h_k)\right)\right).$$

These can be rewritten in matrix form as

$$\begin{bmatrix} C_k \\ D_k \end{bmatrix} = \Theta_{k+1} \begin{bmatrix} C_{k+1} \\ D_{k+1} \end{bmatrix}, \tag{3.11}$$

where the propagator matrix is

$$\Theta_{k+1} = \begin{bmatrix} N_{k+1}^{(11)} & N_{k+1}^{(12)} \\ N_{k+1}^{(21)} & N_{k+1}^{(22)} \end{bmatrix}.$$

Thus, equation (3.11) can be applied to obtain

$$\begin{bmatrix} C_1 \\ D_1 \end{bmatrix} = \prod_{j=1}^{n} \Theta_j \begin{bmatrix} C_n \\ D_n \end{bmatrix}, \tag{3.12}$$

where Θ_1 is the 2×2 identity matrix. Similarly, the boundary conditions (2.6) and (2.7) lead to

$$D_1 = \frac{I}{2\pi\tilde{\xi}} - C_1\tilde{\zeta}, \qquad C_n = 0,$$

where

$$\tilde{\xi} = K_{-\gamma_1}\left(\frac{\lambda}{\tilde{\varrho}_1}\right), \qquad \tilde{\zeta} = I_{-\gamma_1}\left(\frac{\lambda}{\tilde{\varrho}_1}\right)/\tilde{\xi}.$$

Substituting D_1 and C_n into equation (3.12), we obtain

$$\begin{bmatrix} C_1 \\ \left(I/\,2\pi\tilde{\xi}\right) - C_1\tilde{\zeta} \end{bmatrix} = \prod_{j=1}^{n} \Theta_j \begin{bmatrix} 0 \\ D_n \end{bmatrix}.$$

This can be rewritten as a system of two linear equations in terms of the unknowns C_1 and D_n as

$$\begin{bmatrix} 1 & -G_n^{(12)} \\ \tilde{\zeta} & G_n^{(22)} \end{bmatrix} \begin{bmatrix} C_1 \\ D_n \end{bmatrix} = \begin{bmatrix} 0 \\ I/\,2\pi\tilde{\xi} \end{bmatrix},$$

where $G_k^{(ij)}$ is determined by

$$\prod_{j=1}^{k} \Theta_j = \begin{bmatrix} G_k^{(11)} & G_k^{(12)} \\ G_k^{(21)} & G_k^{(22)} \end{bmatrix}.$$

Similar to Section 2.5, we can prove that the coefficient matrix of the above system is nonsingular. By virtue of Cramer's rule, the system has a unique solution

$$C_1 = \frac{I}{2\pi\tilde{\xi}} \frac{G_n^{(12)}}{G_n^{(22)} + \tilde{\zeta} G_n^{(12)}}, \qquad D_n = \frac{I}{2\pi\tilde{\xi}} \frac{1}{G_n^{(22)} + \tilde{\zeta} G_n^{(12)}}.$$

As C_1, D_1, C_n and D_n are determined, so C_k and D_k, where $k \neq 1$ and n, can be obtained from the recurrence relation (3.11).

3.4 Numerical Experiments and Inversion Process

In our inverse model example, we simulate the reflection of magnetic radiation data from our forward model of practical interest. The model of a simple case for the ground structure is used to investigate the conductivity profile. Chave's algorithm is used for numerically calculating the inverse Hankel transform of the magnetic field solutions. The special functions are computed by using the Numerical Recipes source codes (Press et al. [48]). The electric current of 1 ampere is used in our computations. Newton's method in optimization is applied to find a conductivity parameter of the ground.

3.4.1 Sample Test

We firstly consider the magnetic field data obtained from the model of a simple case. The test model is a heterogeneous conductive half-space having linearly varying conductivity. The values of the model parameters are given in Table 3.1. The parameter c is a conductivity of the earth's surface, which can be assumed to be known from the measurement. The iterative procedure using the Newton-Raphson method is applied to estimate the model parameter m of conductivity variation. We start the iterative process to find the value of the conductivity parameter with an initial guess $m = 0.01$ $\mathrm{S{\cdot}m^{-2}}$. The optimal result is close to the true value with misfit less than 10^{-15} $\mathrm{A \cdot m^{-1}}$ after using only 4 iterations (see Table 3.2).

Table 3.1: Model parameters used in our sample test.

Model Parameters	
c ($\mathrm{S{\cdot}m^{-1}}$)	m ($\mathrm{S{\cdot}m^{-2}}$)
0.0732142857	0.0192857142

3.4.2 Interpretation of Simulated Real Data

We now consider the real data of magnetic radiation obtained from the simulation model. The magnetic fields are generated by the forward problem of the example model in our sample test. Random errors up to 3% are superimposed on the scaled magnetic fields to simulate the set of real data. The iterative procedure using the Newton-Raphson method is also applied to estimate the model parameter of conductivity variation. The optimal result is close to the true value with percentage error less than only 2.5% after using 10 iterations. The graphs of the true and estimated conductivity models are plotted as shown in Figure 3.1.

Table 3.2: Successive iterations for finding a conductivity parameter of example model in our sample test.

Iteration	Parameter m $\left(\text{S}\cdot\text{m}^{-2}\right)$	Misfit $\left(\text{A}\cdot\text{m}^{-1}\right)$
0	$1.000000000000000 \times 10^{-2}$	$8.180001750383465 \times 10^{-4}$
1	$1.852032793499813 \times 10^{-2}$	$6.250561100953308 \times 10^{-5}$
2	$1.928092324273490 \times 10^{-2}$	$3.888282783978445 \times 10^{-7}$
3	$1.928571404354892 \times 10^{-2}$	$1.269670704489176 \times 10^{-11}$
4	$1.928571419999880 \times 10^{-2}$	$2.203713394566984 \times 10^{-16}$

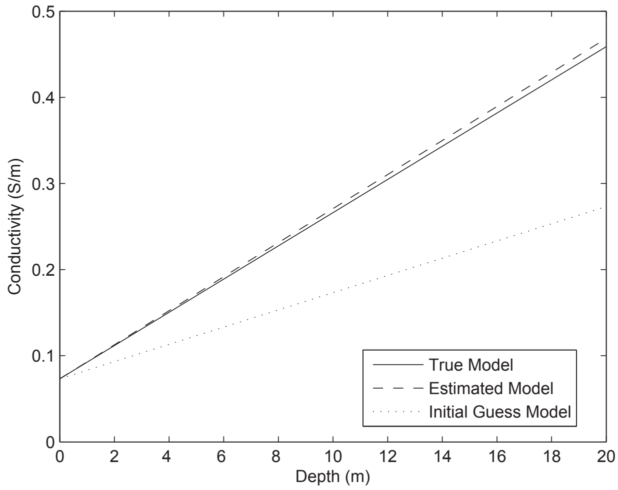

Figure 3.1: Graphs of conductivity σ against depth z for our model example.

3.5 Discussions

Analytical solutions of the steady state magnetic field for transitional ground profiles are derived by using the recurrence relations (3.3) and (3.11). The recurrence relation (3.11) is applicable to general cases in which the layers have constant, linearly or binomially varying conductivities. In the case of a uniform half-space, we can obtain the magnetic field as shown in equation (3.10), which is the same result obtained by Chen and Oldenburg [11].

An inverse problem via the use of an optimization technique is introduced for finding a conductivity parameter of the ground. The model of a simple case for the ground structure is used to investigate the conductivity profile. The iterative procedure using the Newton-Raphson method is applied to estimate the model parameter of conductivity variation. The optimal result of our sample test converges very fast to the true value with misfit less than 10^{-15} A$\cdot$m^{-1} after using only 4 iterations. This illustrates the advantage in using Newton-Raphson method which gives the convergence much faster than using another method of inversion (e.g., Oldenburg [44], Vozoff and Jupp [65]). Moreover, the optimal result for the simulated real data also converges to the true value with percentage error less than only 2.5% after using 10 iterations. The graphs of the true and estimated conductivity models are plotted as shown in Figure 3.1. We see that the graph of the estimated model is close to the true model. The inversion method leads to very good results and has high speed of convergence. This shows the robustness of our model and procedure.

3.6 Summary and Conclusions

The problem of determining resistivity kernel function for a transitional medium is studied in this chapter. Two types of transitional zones are considered, including ground layers having linearly and binomially varying conductivities. We develop analytical solutions of the steady state magnetic field for this problem. The governing equations in Section 2.2 are reused to determine our solutions. The propagator matrix technique is also used to formulate recurrence relations for solving the problems. One of these relations is generalized in all cases where the layers have constant, linearly or binomially varying conductivities. The inversion process, using the Newton-Raphson method, is conducted to estimate a conductivity parameter of the ground. The method leads to very good results and has high speed of convergence.

Chapter 4

Electric Potential in a Transitional Multilayered Earth Containing Buried Electrodes

4.1 Introduction

Conventional resistivity surveys over deeply buried targets are often performed for the purpose of outlining mineralization. Frequently, however, these surveys are of limited value due to poor resolution resulting from the depth of the target and a very small amplitude response due to conductive overburden. Yet, as the target depth increases, it becomes even more important to outline mineralization in some manner so as to reduce a number of deep and costly exploratory drill holes necessary to evaluate a prospect.

The use of current electrodes down a drill hole, which has presumably intersected some portion of the target zone or in any case is at least a near miss, improves the response and provides valuable data concerning the direction and offset of the target with respect to the drill hole. An electrical survey on the surface around the drill hole containing a buried current electrode is often more effective in outlining mineralization in the immediate vicinity of the drill hole than conventional electrical surveys employing surface current electrodes, and therefore, should be considered as a part of any borehole geophysics program in which surface electrical surveys have insufficient penetration.

Investigations using buried electrodes were reported for layers having constant and exponentially varying conductivities. Alfano [1] considered a three-layered earth model with homogeneous layers and demonstrated that the uncertainty in the interpretation of resistivity soundings can be reduced by using buried electrodes. Daniels [13] presented a solution for the layered earth problem of a buried current source and a buried receiver. The model is developed for source and receiver electrodes buried anywhere within a horizontally stratified layered earth containing an arbitrary number of homogeneous layers. Baumgartner [9] studied underwater formulations which show that apparent resistivity data can be enhanced by using submerged electrodes in the water layer. Sato [50] developed a theoretical solution for the potential field due to a direct current source buried in a horizontally layered space with all layers possessing exponentially varying resistivities.

In this study, we consider the problem of a multilayered earth in which the layers have transitional ground profiles. We derive analytical solutions of the electric potential resulting from a direct current point source located anywhere within two types of multilayered earth structures including layers having linearly varying conductivities and layers having binomially varying conductivities. The Hankel transform is introduced to our problems and analytical results are obtained. Our solutions are achieved by solving a boundary value problem in the wave number domain and then transforming the solution back to the spatial domain. The propagator matrix technique is used to formulate upward and downward recurrences for solving the problems. Inverse problems via the use of the Newton-Raphson and quasi-Newton optimization techniques are introduced for finding the conductivity parameters of the ground.

4.2 Model and Basic Equations

A geometric model of the earth's structure consists of two conductive half-spaces (see Figure 4.1). The half-space above the ground surface ($z < 0$) is a region of air, whereas the half-space below the ground surface ($z > 0$) is an n-layered horizontally stratified earth with depths to the layers $h_1, h_2, \ldots, h_{n-1}$ (the lowermost layer extending to infinity) measured from the ground surface, where $n \geq 2$ is an integer. A point source of direct current I is deliberately located at the interface $z = h_s$ of layer s and layer $s+1$ ($1 \leq s \leq n-1$) for simplifying the mathematics. Each layer has conductivity as a function of depth, i.e., $\sigma_k(z)$ for layer $0 \leq k \leq n$. The electric potential V in direct current conditions satisfies the equation

$$\mathbf{E} = -\nabla V, \tag{4.1}$$

where $\mathbf{E}$ is the vector electric field and ∇ is the del operator. The vector current density $\mathbf{J}$ and the vector electric field are related through Ohm's law as

$$\mathbf{J} = \sigma \mathbf{E}, \tag{4.2}$$

where σ is the conductivity of the medium. The vector current density satisfies the equation

$$\nabla \cdot \mathbf{J} = 0, \tag{4.3}$$

except at current sources or sinks. Eliminating $\mathbf{E}$ and $\mathbf{J}$ from equations (4.1), (4.2) and (4.3), we obtain

$$\nabla \cdot (\sigma \nabla V) = 0.$$

This can be expressed in cylindrical coordinates (r, ϕ, z) as

$$\frac{1}{r}\left(\frac{\partial}{\partial r}\left(\sigma r \frac{\partial V}{\partial r}\right) + \frac{\partial}{\partial \phi}\left(\frac{\sigma}{r}\frac{\partial V}{\partial \phi}\right) + r\frac{\partial}{\partial z}\left(\sigma \frac{\partial V}{\partial z}\right)\right) = 0. \tag{4.4}$$

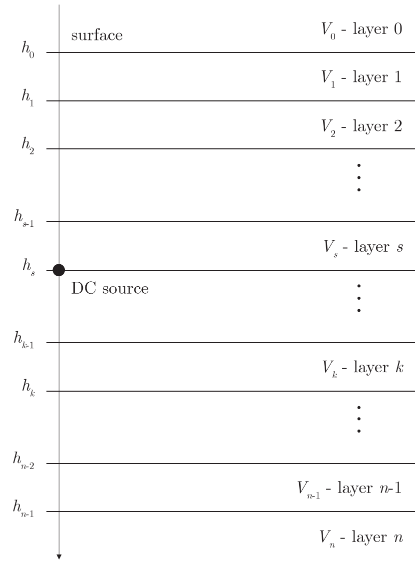

Figure 4.1: Geometric model of the earth's structure.

Since the problem is axisymmetric in cylindrical coordinates, it follows that V depends only on r and z. Simplifying equation (4.4) yields

$$\frac{1}{r}\frac{\partial}{\partial r}\left(\sigma r\,\frac{\partial V}{\partial r}\right)+\frac{\partial}{\partial z}\left(\sigma\,\frac{\partial V}{\partial z}\right)=0,$$

or

$$\frac{1}{r}\left(\sigma\,\frac{\partial}{\partial r}\left(r\,\frac{\partial V}{\partial r}\right)+r\,\frac{\partial \sigma}{\partial r}\frac{\partial V}{\partial r}\right)+\frac{\sigma}{r}\frac{\partial V}{\partial r}+\sigma\,\frac{\partial^2 V}{\partial z^2}+\frac{\partial \sigma}{\partial z}\frac{\partial V}{\partial z}=0.$$

In our study, we denote σ as a function of only depth z, and we now have

$$\frac{\partial^2 V}{\partial r^2}+\frac{1}{r}\frac{\partial V}{\partial r}+\frac{\partial^2 V}{\partial z^2}+\frac{1}{\sigma}\frac{\partial \sigma}{\partial z}\frac{\partial V}{\partial z}=0. \tag{4.5}$$

The Hankel transform (Ali and Kalla [2]) is introduced and defined by

$$\tilde{V}(\lambda,z)=\int_0^\infty \lambda r V(r,z)\,J_0(\lambda r)\,dr$$

and

$$V(r,z)=\int_0^\infty \tilde{V}(\lambda,z)\,J_0(\lambda r)\,d\lambda,$$

where J_0 is the Bessel function of the first kind of order zero and λ is the scaling factor. Taking the transformation on both sides of equation (4.5), we obtain

$$\int_0^\infty \lambda r\left(\frac{\partial^2 V}{\partial r^2}+\frac{1}{r}\frac{\partial V}{\partial r}+\frac{\partial^2 V}{\partial z^2}+\frac{1}{\sigma}\frac{\partial \sigma}{\partial z}\frac{\partial V}{\partial z}\right)J_0(\lambda r)\,dr=\int_0^\infty \lambda r\cdot 0\cdot J_0(\lambda r)\,dr,$$

or

$$\int_0^\infty \lambda \left(r \frac{\partial^2 V}{\partial r^2} + \frac{\partial V}{\partial r} \right) J_0(\lambda r)\, dr + \int_0^\infty \lambda r \frac{\partial^2 V}{\partial z^2} J_0(\lambda r)\, dr + \frac{1}{\sigma}\frac{\partial \sigma}{\partial z} \int_0^\infty \lambda r \frac{\partial V}{\partial z} J_0(\lambda r)\, dr = 0,$$

or

$$\int_0^\infty \lambda \frac{\partial}{\partial r} \left(r \frac{\partial V}{\partial r} \right) J_0(\lambda r)\, dr + \int_0^\infty \lambda r \frac{\partial^2 V}{\partial z^2} J_0(\lambda r)\, dr + \frac{1}{\sigma}\frac{\partial \sigma}{\partial z} \int_0^\infty \lambda r \frac{\partial V}{\partial z} J_0(\lambda r)\, dr = 0,$$

or

$$\lim_{a\to 0^+} \int_a^1 \lambda \frac{\partial}{\partial r} \left(r \frac{\partial V}{\partial r} \right) J_0(\lambda r)\, dr + \lim_{b\to\infty} \int_1^b \lambda \frac{\partial}{\partial r} \left(r \frac{\partial V}{\partial r} \right) J_0(\lambda r)\, dr + \int_0^\infty \lambda r \frac{\partial^2 V}{\partial z^2} J_0(\lambda r)\, dr + \frac{1}{\sigma}\frac{\partial \sigma}{\partial z} \int_0^\infty \lambda r \frac{\partial V}{\partial z} J_0(\lambda r)\, dr = 0.$$

Integrating by parts on the first and second terms of the above equation yields

$$\lim_{a\to 0^+} \left(\lambda r \frac{\partial V}{\partial r} J_0(\lambda r) \right)\Bigg|_a^1 - \lim_{a\to 0^+} \int_a^1 \lambda r \frac{\partial V}{\partial r} \frac{d}{dr} J_0(\lambda r)\, dr + \lim_{b\to\infty} \left(\lambda r \frac{\partial V}{\partial r} J_0(\lambda r) \right)\Bigg|_1^b - \lim_{b\to\infty} \int_1^b \lambda r \frac{\partial V}{\partial r} \frac{d}{dr} J_0(\lambda r)\, dr + \int_0^\infty \lambda r \frac{\partial^2 V}{\partial z^2} J_0(\lambda r)\, dr + \frac{1}{\sigma}\frac{\partial \sigma}{\partial z} \int_0^\infty \lambda r \frac{\partial V}{\partial z} J_0(\lambda r)\, dr = 0,$$

or

$$\int_0^\infty \lambda r \frac{\partial^2 V}{\partial z^2} J_0(\lambda r)\, dr + \frac{1}{\sigma}\frac{\partial \sigma}{\partial z} \int_0^\infty \lambda r \frac{\partial V}{\partial z} J_0(\lambda r)\, dr - \lim_{a\to 0^+} \int_a^1 \lambda r \frac{\partial V}{\partial r} \frac{d}{dr} J_0(\lambda r)\, dr - \lim_{b\to\infty} \int_1^b \lambda r \frac{\partial V}{\partial r} \frac{d}{dr} J_0(\lambda r)\, dr = 0.$$

Integrating by parts again on the third and fourth terms of the above equation, we obtain

$$\int_0^\infty \lambda r \frac{\partial^2 V}{\partial z^2} J_0(\lambda r)\, dr + \frac{1}{\sigma}\frac{\partial \sigma}{\partial z} \int_0^\infty \lambda r \frac{\partial V}{\partial z} J_0(\lambda r)\, dr - \lim_{a\to 0^+} \left(\lambda r V \frac{d}{dr} J_0(\lambda r) \right)\Bigg|_a^1 + \lim_{a\to 0^+} \int_a^1 \lambda V \frac{d}{dr} \left(r \frac{d}{dr} J_0(\lambda r) \right) dr - \lim_{b\to\infty} \left(\lambda r V \frac{d}{dr} J_0(\lambda r) \right)\Bigg|_1^b + \lim_{b\to\infty} \int_1^b \lambda V \frac{d}{dr} \left(r \frac{d}{dr} J_0(\lambda r) \right) dr = 0,$$

or

$$\int_0^\infty \lambda r \frac{\partial^2 V}{\partial z^2} J_0(\lambda r)\, dr + \frac{1}{\sigma}\frac{\partial \sigma}{\partial z}\int_0^\infty \lambda r \frac{\partial V}{\partial z} J_0(\lambda r)\, dr$$
$$+ \lim_{a\to 0^+}\int_a^1 \lambda V \frac{d}{dr}\left(r\frac{d}{dr}J_0(\lambda r)\right) dr + \lim_{b\to\infty}\int_1^b \lambda V \frac{d}{dr}\left(r\frac{d}{dr}J_0(\lambda r)\right) dr = 0,$$

or

$$\int_0^\infty \lambda r \frac{\partial^2 V}{\partial z^2} J_0(\lambda r)\, dr + \frac{1}{\sigma}\frac{\partial \sigma}{\partial z}\int_0^\infty \lambda r \frac{\partial V}{\partial z} J_0(\lambda r)\, dr$$
$$+ \int_0^\infty \lambda V \frac{d}{dr}\left(r\frac{d}{dr}J_0(\lambda r)\right) dr = 0,$$

or

$$\int_0^\infty \lambda r \frac{\partial^2 V}{\partial z^2} J_0(\lambda r)\, dr + \frac{1}{\sigma}\frac{\partial \sigma}{\partial z}\int_0^\infty \lambda r \frac{\partial V}{\partial z} J_0(\lambda r)\, dr$$
$$+ \int_0^\infty \lambda V \left(r\frac{d^2}{dr^2}J_0(\lambda r) + \frac{d}{dr}J_0(\lambda r)\right) dr = 0,$$

or

$$\int_0^\infty \lambda r \frac{\partial^2 V}{\partial z^2} J_0(\lambda r)\, dr + \frac{1}{\sigma}\frac{\partial \sigma}{\partial z}\int_0^\infty \lambda r \frac{\partial V}{\partial z} J_0(\lambda r)\, dr$$
$$+ \int_0^\infty \lambda V \left(\lambda^2 r J_0''(\lambda r) + \lambda J_0'(\lambda r)\right) dr = 0,$$

or

$$\int_0^\infty \lambda r \frac{\partial^2 V}{\partial z^2} J_0(\lambda r)\, dr + \frac{1}{\sigma}\frac{\partial \sigma}{\partial z}\int_0^\infty \lambda r \frac{\partial V}{\partial z} J_0(\lambda r)\, dr$$
$$+ \int_0^\infty \lambda r V \left(\lambda^2 J_0''(\lambda r) + \frac{\lambda}{r} J_0'(\lambda r)\right) dr = 0.$$

Since J_0 is the solution of Bessel's differential equation, we now have

$$\lambda^2 J_0''(\lambda r) + \frac{\lambda}{r} J_0'(\lambda r) = -\lambda^2 J_0(\lambda r).$$

This yields

$$\int_0^\infty \lambda r \frac{\partial^2 V}{\partial z^2} J_0(\lambda r)\, dr + \frac{1}{\sigma}\frac{\partial \sigma}{\partial z}\int_0^\infty \lambda r \frac{\partial V}{\partial z} J_0(\lambda r)\, dr - \lambda^2 \int_0^\infty \lambda r V J_0(\lambda r)\, dr = 0.$$

Hence, the Hankel transform of equation (4.5) results in

$$\frac{\partial^2 \tilde{V}}{\partial z^2} + \frac{1}{\sigma}\frac{\partial \sigma}{\partial z}\frac{\partial \tilde{V}}{\partial z} - \lambda^2 \tilde{V} = 0. \tag{4.6}$$

Therefore, the electric potential in each layer can be obtained by taking the inverse Hankel transform to the solution of equation (4.6), which satisfies the following boundary conditions (Sato [50]):

1. The electric potential V_0 actually converges as z tends to minus infinity.

2. The electric potential V_n also converges as z tends to infinity.

3. The electric potential needs to be continuous on each of the boundary planes, i.e., for each $0 \leq k \leq n-1$,

$$\lim_{z \to h_k^-} \tilde{V}_k = \lim_{z \to h_k^+} \tilde{V}_{k+1}. \tag{4.7}$$

4. The vertical component of the current density needs to be continuous on each of the boundary planes except on $z = h_s$, i.e., for each $0 \leq k \leq n-1$ and $k \neq s$,

$$\lim_{z \to h_k^-} \sigma_k \frac{\partial \tilde{V}_k}{\partial z} = \lim_{z \to h_k^+} \sigma_{k+1} \frac{\partial \tilde{V}_{k+1}}{\partial z}. \tag{4.8}$$

5. The total current flowing out of any cylindrical surface around a current source must be equal to the current intensity, i.e., for any radius ξ,

$$\lim_{h \to 0} \left(\int_{\phi=0}^{2\pi} \int_{r=0}^{\xi} \mathbf{J}_s|_{z=h_s-h} \cdot (-\hat{z} r dr d\phi) + \int_{\phi=0}^{2\pi} \int_{r=0}^{\xi} \mathbf{J}_{s+1}|_{z=h_s+h} \cdot (\hat{z} r dr d\phi) \right) = I. \tag{4.9}$$

4.3 Response of an Air Region

The equation for the electric potential in an air region, denoted by $\tilde{V}_0$, can be determined by simplifying equation (4.6) with constant σ_0 as

$$\frac{\partial^2 \tilde{V}_0}{\partial z^2} - \lambda^2 \tilde{V}_0 = 0$$

and the solution is

$$\tilde{V}_0(\lambda, z) = A_0 e^{\lambda z} + B_0 e^{-\lambda z},$$

where A_0 and B_0 are arbitrary constants, which can be determined by using the boundary conditions. Thus, the electric potential in an air region is

$$V_0(r, z) = \int_0^{\infty} \left(A_0 e^{\lambda z} + B_0 e^{-\lambda z} \right) J_0(\lambda r)\, d\lambda.$$

4.4 Response of a Ground Layer Having Linearly Varying Conductivity

For each layer k, where $1 \leq k \leq n$ and $n \geq 2$, the variation of conductivity is denoted by

$$\sigma_k(z) = m_k z + c_k, \tag{4.10}$$

where c_k and $m_k \neq 0$ are constants, which preserve $\sigma_k(z) > 0$. Hence, the equation for the electric potential in layer k can be simplified by substituting equation (4.10) into (4.6) and we obtain

$$\frac{\partial^2 \tilde{V}_k}{\partial z^2} + \frac{m_k}{m_k z + c_k}\frac{\partial \tilde{V}_k}{\partial z} - \lambda^2 \tilde{V}_k = 0.$$

The solution to the above equation has been found by Lal [36] and given as

$$\tilde{V}_k(\lambda, z) = A_k I_0\left(\frac{\lambda}{\varrho_k}\psi_k(z)\right) + B_k K_0\left(\frac{\lambda}{\varrho_k}\psi_k(z)\right),$$

where

$$\varrho_k = \frac{m_k}{c_k}, \qquad \psi_k(z) = 1 + \varrho_k z,$$

A_k and B_k are arbitrary constants, which can be determined by using the boundary conditions. Thus, the electric potential in layer k is

$$V_k(r, z) = \int_0^\infty \left(A_k I_0\left(\frac{\lambda}{\varrho_k}\psi_k(z)\right) + B_k K_0\left(\frac{\lambda}{\varrho_k}\psi_k(z)\right)\right) J_0(\lambda r)\, d\lambda. \tag{4.11}$$

4.4.1 Downward Recurrence

The objective is to establish a linear equation with arbitrary constants A_k and B_k, incorporating the physical and geometric parameters of the layers and interfaces above layer k. This section involves only equations with arbitrary constants A_k and B_k for $k = 0, 1, \ldots, s$. If $1 \leq k \leq s-1$, then the electric potentials in layers k and $k+1$ can be written as

$$\tilde{V}_k(\lambda, z) = A_k I_0\left(\frac{\lambda}{\varrho_k}\psi_k(z)\right) + B_k K_0\left(\frac{\lambda}{\varrho_k}\psi_k(z)\right)$$

and

$$\tilde{V}_{k+1}(\lambda, z) = A_{k+1} I_0\left(\frac{\lambda}{\varrho_{k+1}}\psi_{k+1}(z)\right) + B_{k+1} K_0\left(\frac{\lambda}{\varrho_{k+1}}\psi_{k+1}(z)\right).$$

Using the boundary conditions (4.7) and (4.8), we obtain

$$\begin{aligned} A_k I_0\left(\frac{\lambda}{\varrho_k}\psi_k(h_k)\right) &+ B_k K_0\left(\frac{\lambda}{\varrho_k}\psi_k(h_k)\right) \\ &= A_{k+1} I_0\left(\frac{\lambda}{\varrho_{k+1}}\psi_{k+1}(h_k)\right) + B_{k+1} K_0\left(\frac{\lambda}{\varrho_{k+1}}\psi_{k+1}(h_k)\right) \end{aligned}$$

and

$$\begin{aligned} \lambda\sigma_k^{\circ} &\left(A_k I_1\left(\frac{\lambda}{\varrho_k}\psi_k(h_k)\right) - B_k K_1\left(\frac{\lambda}{\varrho_k}\psi_k(h_k)\right)\right) \\ &= \lambda\sigma_{k+1}^{\bullet}\left(A_{k+1} I_1\left(\frac{\lambda}{\varrho_{k+1}}\psi_{k+1}(h_k)\right) - B_{k+1} K_1\left(\frac{\lambda}{\varrho_{k+1}}\psi_{k+1}(h_k)\right)\right), \end{aligned}$$

where

$$\lim_{z\to h_k^-}\sigma_k(z)=\sigma_k^{\circ},\qquad \lim_{z\to h_k^+}\sigma_{k+1}(z)=\sigma_{k+1}^{\bullet}.$$

Hence, A_{k+1} and B_{k+1} can be written in terms of A_k and B_k as

$$A_{k+1}=M_{k+1}^{(11)}A_k+M_{k+1}^{(12)}B_k$$

and

$$B_{k+1}=M_{k+1}^{(21)}A_k+M_{k+1}^{(22)}B_k,$$

where all the coefficients $M_{k+1}^{(ij)}$ are given by

$$M_{k+1}^{(11)}=\frac{\lambda}{m_{k+1}}\left(\sigma_k^{\circ}I_1\left(\frac{\lambda}{\varrho_k}\psi_k(h_k)\right)K_0\left(\frac{\lambda}{\varrho_{k+1}}\psi_{k+1}(h_k)\right)\right.$$
$$\left.+\,\sigma_{k+1}^{\bullet}I_0\left(\frac{\lambda}{\varrho_k}\psi_k(h_k)\right)K_1\left(\frac{\lambda}{\varrho_{k+1}}\psi_{k+1}(h_k)\right)\right),$$

$$M_{k+1}^{(12)}=\frac{\lambda}{m_{k+1}}\left(\sigma_{k+1}^{\bullet}K_0\left(\frac{\lambda}{\varrho_k}\psi_k(h_k)\right)K_1\left(\frac{\lambda}{\varrho_{k+1}}\psi_{k+1}(h_k)\right)\right.$$
$$\left.-\,\sigma_k^{\circ}K_1\left(\frac{\lambda}{\varrho_k}\psi_k(h_k)\right)K_0\left(\frac{\lambda}{\varrho_{k+1}}\psi_{k+1}(h_k)\right)\right),$$

$$M_{k+1}^{(21)}=\frac{\lambda}{m_{k+1}}\left(\sigma_{k+1}^{\bullet}I_0\left(\frac{\lambda}{\varrho_k}\psi_k(h_k)\right)I_1\left(\frac{\lambda}{\varrho_{k+1}}\psi_{k+1}(h_k)\right)\right.$$
$$\left.-\,\sigma_k^{\circ}I_1\left(\frac{\lambda}{\varrho_k}\psi_k(h_k)\right)I_0\left(\frac{\lambda}{\varrho_{k+1}}\psi_{k+1}(h_k)\right)\right),$$

$$M_{k+1}^{(22)}=\frac{\lambda}{m_{k+1}}\left(\sigma_k^{\circ}K_1\left(\frac{\lambda}{\varrho_k}\psi_k(h_k)\right)I_0\left(\frac{\lambda}{\varrho_{k+1}}\psi_{k+1}(h_k)\right)\right.$$
$$\left.+\,\sigma_{k+1}^{\bullet}K_0\left(\frac{\lambda}{\varrho_k}\psi_k(h_k)\right)I_1\left(\frac{\lambda}{\varrho_{k+1}}\psi_{k+1}(h_k)\right)\right).$$

Similarly, if $k=0$, then we have

$$\tilde{V}_k(\lambda,z)=A_ke^{\lambda z}+B_ke^{-\lambda z}$$

and

$$\tilde{V}_{k+1}(\lambda,z)=A_{k+1}I_0\left(\frac{\lambda}{\varrho_{k+1}}\psi_{k+1}(z)\right)+B_{k+1}K_0\left(\frac{\lambda}{\varrho_{k+1}}\psi_{k+1}(z)\right).$$

Thus, the boundary conditions (4.7) and (4.8) lead to

$$A_ke^{\lambda h_k}+B_ke^{-\lambda h_k}=A_{k+1}I_0\left(\frac{\lambda}{\varrho_{k+1}}\psi_{k+1}(h_k)\right)+B_{k+1}K_0\left(\frac{\lambda}{\varrho_{k+1}}\psi_{k+1}(h_k)\right)$$

and

$$\lambda\sigma_k^{\circ}\left(A_k e^{\lambda h_k} - B_k e^{-\lambda h_k}\right)$$
$$= \lambda\sigma_{k+1}^{\bullet}\left(A_{k+1} I_1\left(\frac{\lambda}{\varrho_{k+1}}\psi_{k+1}(h_k)\right) - B_{k+1} K_1\left(\frac{\lambda}{\varrho_{k+1}}\psi_{k+1}(h_k)\right)\right).$$

Hence, A_{k+1} and B_{k+1} can also be written in terms of A_k and B_k as

$$A_{k+1} = M_{k+1}^{(11)} A_k + M_{k+1}^{(12)} B_k$$

and

$$B_{k+1} = M_{k+1}^{(21)} A_k + M_{k+1}^{(22)} B_k,$$

where all the coefficients $M_{k+1}^{(ij)}$ are given by

$$M_{k+1}^{(11)} = \frac{\lambda e^{\lambda h_k}}{m_{k+1}}\left(\sigma_k^{\circ} K_0\left(\frac{\lambda}{\varrho_{k+1}}\psi_{k+1}(h_k)\right) + \sigma_{k+1}^{\bullet} K_1\left(\frac{\lambda}{\varrho_{k+1}}\psi_{k+1}(h_k)\right)\right),$$

$$M_{k+1}^{(12)} = \frac{\lambda e^{-\lambda h_k}}{m_{k+1}}\left(\sigma_{k+1}^{\bullet} K_1\left(\frac{\lambda}{\varrho_{k+1}}\psi_{k+1}(h_k)\right) - \sigma_k^{\circ} K_0\left(\frac{\lambda}{\varrho_{k+1}}\psi_{k+1}(h_k)\right)\right),$$

$$M_{k+1}^{(21)} = \frac{\lambda e^{\lambda h_k}}{m_{k+1}}\left(\sigma_{k+1}^{\bullet} I_1\left(\frac{\lambda}{\varrho_{k+1}}\psi_{k+1}(h_k)\right) - \sigma_k^{\circ} I_0\left(\frac{\lambda}{\varrho_{k+1}}\psi_{k+1}(h_k)\right)\right),$$

$$M_{k+1}^{(22)} = \frac{\lambda e^{-\lambda h_k}}{m_{k+1}}\left(\sigma_k^{\circ} I_0\left(\frac{\lambda}{\varrho_{k+1}}\psi_{k+1}(h_k)\right) + \sigma_{k+1}^{\bullet} I_1\left(\frac{\lambda}{\varrho_{k+1}}\psi_{k+1}(h_k)\right)\right).$$

Thus, for $0 \le k \le s-1$, the downward recurrence can be defined by

$$\begin{bmatrix} A_{k+1} \\ B_{k+1} \end{bmatrix} = \Gamma_{k+1} \begin{bmatrix} A_k \\ B_k \end{bmatrix}, \tag{4.12}$$

where the propagator matrix is

$$\Gamma_{k+1} = \begin{bmatrix} M_{k+1}^{(11)} & M_{k+1}^{(12)} \\ M_{k+1}^{(21)} & M_{k+1}^{(22)} \end{bmatrix}.$$

The coefficients $M_{k+1}^{(ij)}$, in the general case, can be rewritten as

$$M_{k+1}^{(11)} = \frac{\lambda}{m_{k+1}}\left(\sigma_k^{\circ}\zeta_k' K_0\left(\frac{\lambda}{\varrho_{k+1}}\psi_{k+1}(h_k)\right) + \sigma_{k+1}^{\bullet}\zeta_k K_1\left(\frac{\lambda}{\varrho_{k+1}}\psi_{k+1}(h_k)\right)\right),$$

$$M_{k+1}^{(12)} = \frac{\lambda}{m_{k+1}}\left(\sigma_{k+1}^{\bullet}\xi_k K_1\left(\frac{\lambda}{\varrho_{k+1}}\psi_{k+1}(h_k)\right) - \sigma_k^{\circ}\xi_k' K_0\left(\frac{\lambda}{\varrho_{k+1}}\psi_{k+1}(h_k)\right)\right),$$

$$M_{k+1}^{(21)} = \frac{\lambda}{m_{k+1}}\left(\sigma_{k+1}^{\bullet}\zeta_k I_1\left(\frac{\lambda}{\varrho_{k+1}}\psi_{k+1}(h_k)\right) - \sigma_k^{\circ}\zeta_k' I_0\left(\frac{\lambda}{\varrho_{k+1}}\psi_{k+1}(h_k)\right)\right),$$

$$M_{k+1}^{(22)} = \frac{\lambda}{m_{k+1}}\left(\sigma_k^{\circ}\xi_k' I_0\left(\frac{\lambda}{\varrho_{k+1}}\psi_{k+1}(h_k)\right) + \sigma_{k+1}^{\bullet}\xi_k I_1\left(\frac{\lambda}{\varrho_{k+1}}\psi_{k+1}(h_k)\right)\right),$$

where

$$\zeta_k = \begin{cases} I_0\left(\left(\lambda/\varrho_k\right)\psi_k\left(h_k\right)\right) & \text{if } 1 \le k \le s-1, \\ e^{\lambda h_k} & \text{if } k = 0, \end{cases}$$

$$\zeta_k' = \begin{cases} I_1\left(\left(\lambda/\varrho_k\right)\psi_k\left(h_k\right)\right) & \text{if } 1 \le k \le s-1, \\ e^{\lambda h_k} & \text{if } k = 0, \end{cases}$$

and

$$\xi_k = \begin{cases} K_0\left(\left(\lambda/\varrho_k\right)\psi_k\left(h_k\right)\right) & \text{if } 1 \le k \le s-1, \\ e^{-\lambda h_k} & \text{if } k = 0, \end{cases}$$

$$\xi_k' = \begin{cases} K_1\left(\left(\lambda/\varrho_k\right)\psi_k\left(h_k\right)\right) & \text{if } 1 \le k \le s-1, \\ e^{-\lambda h_k} & \text{if } k = 0. \end{cases}$$

4.4.2 Upward Recurrence

In a way similar to that of Section 4.4.1 but working in the opposite direction, the objective is to establish a linear equation with arbitrary constants A_k and B_k, incorporating the physical and geometric parameters of the layers and interfaces below layer k. This section involves only equations with arbitrary constants A_k and B_k for $k = s+1, s+2, \ldots, n$. If $s < n-1$, for $s+1 \le k \le n-1$, the electric potentials in layers k and $k+1$ can be written as

$$\tilde{V}_k\left(\lambda, z\right) = A_k I_0\left(\frac{\lambda}{\varrho_k}\psi_k\left(z\right)\right) + B_k K_0\left(\frac{\lambda}{\varrho_k}\psi_k\left(z\right)\right)$$

and

$$\tilde{V}_{k+1}\left(\lambda, z\right) = A_{k+1} I_0\left(\frac{\lambda}{\varrho_{k+1}}\psi_{k+1}\left(z\right)\right) + B_{k+1} K_0\left(\frac{\lambda}{\varrho_{k+1}}\psi_{k+1}\left(z\right)\right).$$

Using the boundary conditions (4.7) and (4.8), we obtain

$$A_k I_0\left(\frac{\lambda}{\varrho_k}\psi_k\left(h_k\right)\right) + B_k K_0\left(\frac{\lambda}{\varrho_k}\psi_k\left(h_k\right)\right) \\ = A_{k+1} I_0\left(\frac{\lambda}{\varrho_{k+1}}\psi_{k+1}\left(h_k\right)\right) + B_{k+1} K_0\left(\frac{\lambda}{\varrho_{k+1}}\psi_{k+1}\left(h_k\right)\right)$$

and

$$\lambda\sigma_k^{\circ}\left(A_k I_1\left(\frac{\lambda}{\varrho_k}\psi_k\left(h_k\right)\right) - B_k K_1\left(\frac{\lambda}{\varrho_k}\psi_k\left(h_k\right)\right)\right) \\ = \lambda\sigma_{k+1}^{\bullet}\left(A_{k+1} I_1\left(\frac{\lambda}{\varrho_{k+1}}\psi_{k+1}\left(h_k\right)\right) - B_{k+1} K_1\left(\frac{\lambda}{\varrho_{k+1}}\psi_{k+1}\left(h_k\right)\right)\right).$$

Hence, A_k and B_k can be written in terms of A_{k+1} and B_{k+1} as

$$A_k = N_{k+1}^{(11)} A_{k+1} + N_{k+1}^{(12)} B_{k+1}$$

and

$$B_k = N_{k+1}^{(21)} A_{k+1} + N_{k+1}^{(22)} B_{k+1},$$

where all the coefficients $N_{k+1}^{(ij)}$ are given by

$$N_{k+1}^{(11)} = \frac{\lambda}{m_k} \left(\sigma_k^{\circ} K_1 \left(\frac{\lambda}{\varrho_k} \psi_k \left(h_k \right) \right) I_0 \left(\frac{\lambda}{\varrho_{k+1}} \psi_{k+1} \left(h_k \right) \right) \right. \\ \left. + \sigma_{k+1}^{\bullet} K_0 \left(\frac{\lambda}{\varrho_k} \psi_k \left(h_k \right) \right) I_1 \left(\frac{\lambda}{\varrho_{k+1}} \psi_{k+1} \left(h_k \right) \right) \right),$$

$$N_{k+1}^{(12)} = \frac{\lambda}{m_k} \left(\sigma_k^{\circ} K_1 \left(\frac{\lambda}{\varrho_k} \psi_k \left(h_k \right) \right) K_0 \left(\frac{\lambda}{\varrho_{k+1}} \psi_{k+1} \left(h_k \right) \right) \right. \\ \left. - \sigma_{k+1}^{\bullet} K_0 \left(\frac{\lambda}{\varrho_k} \psi_k \left(h_k \right) \right) K_1 \left(\frac{\lambda}{\varrho_{k+1}} \psi_{k+1} \left(h_k \right) \right) \right),$$

$$N_{k+1}^{(21)} = \frac{\lambda}{m_k} \left(\sigma_k^{\circ} I_1 \left(\frac{\lambda}{\varrho_k} \psi_k \left(h_k \right) \right) I_0 \left(\frac{\lambda}{\varrho_{k+1}} \psi_{k+1} \left(h_k \right) \right) \right. \\ \left. - \sigma_{k+1}^{\bullet} I_0 \left(\frac{\lambda}{\varrho_k} \psi_k \left(h_k \right) \right) I_1 \left(\frac{\lambda}{\varrho_{k+1}} \psi_{k+1} \left(h_k \right) \right) \right),$$

$$N_{k+1}^{(22)} = \frac{\lambda}{m_k} \left(\sigma_k^{\circ} I_1 \left(\frac{\lambda}{\varrho_k} \psi_k \left(h_k \right) \right) K_0 \left(\frac{\lambda}{\varrho_{k+1}} \psi_{k+1} \left(h_k \right) \right) \right. \\ \left. + \sigma_{k+1}^{\bullet} I_0 \left(\frac{\lambda}{\varrho_k} \psi_k \left(h_k \right) \right) K_1 \left(\frac{\lambda}{\varrho_{k+1}} \psi_{k+1} \left(h_k \right) \right) \right).$$

Thus, for $s+1 \leq k \leq n-1$, the upward recurrence can be defined by

$$\begin{bmatrix} A_k \\ B_k \end{bmatrix} = \Theta_{k+1} \begin{bmatrix} A_{k+1} \\ B_{k+1} \end{bmatrix}, \tag{4.13}$$

where the propagator matrix is

$$\Theta_{k+1} = \begin{bmatrix} N_{k+1}^{(11)} & N_{k+1}^{(12)} \\ N_{k+1}^{(21)} & N_{k+1}^{(22)} \end{bmatrix}.$$

4.4.3 Solution for an n-layered Earth

We now consider an n-layered earth model. Each layer k of ground, where $1 \leq k \leq n$ and $n \geq 2$, has a linearly varying conductivity as given in (4.10). A region of air, denoted by layer 0, has a constant conductivity. A point source of direct current is deliberately located at the interface $z = h_s$ of layer s and layer $s+1$, where $1 \leq s \leq n-1$, for simplifying the mathematics. The downward recurrence (4.12) can be applied to obtain

$$\begin{bmatrix} A_s \\ B_s \end{bmatrix} = \prod_{j=s}^{1} \Gamma_j \begin{bmatrix} A_0 \\ B_0 \end{bmatrix}. \tag{4.14}$$

Similarly, the upward recurrence (4.13) yields

$$\begin{bmatrix} A_{s+1} \\ B_{s+1} \end{bmatrix} = \Theta^* \begin{bmatrix} A_n \\ B_n \end{bmatrix}, \tag{4.15}$$

where

$$\Theta^* = \begin{cases} \prod_{j=s+2}^{n} \Theta_j & \text{if } s < n-1, \\ \mathbf{I}_2 & \text{if } s = n-1. \end{cases}$$

On the boundary plane $z = h_s$, the boundary condition (4.7) is used again, and so we have

$$\begin{aligned} A_s I_0 \left(\frac{\lambda}{\varrho_s} \psi_s(h_s) \right) &+ B_s K_0 \left(\frac{\lambda}{\varrho_s} \psi_s(h_s) \right) \\ &= A_{s+1} I_0 \left(\frac{\lambda}{\varrho_{s+1}} \psi_{s+1}(h_s) \right) + B_{s+1} K_0 \left(\frac{\lambda}{\varrho_{s+1}} \psi_{s+1}(h_s) \right). \end{aligned} \tag{4.16}$$

Moreover, the boundary condition (4.9) requires

$$\begin{aligned} \lim_{h \to 0} \Bigg(\int_{\phi=0}^{2\pi} \int_{r=0}^{\xi} & \left(\sigma_s \frac{\partial \tilde{V}_s}{\partial z} \right) \Bigg|_{z=h_s-h} r dr d\phi \\ & - \int_{\phi=0}^{2\pi} \int_{r=0}^{\xi} \left(\sigma_{s+1} \frac{\partial \tilde{V}_{s+1}}{\partial z} \right) \Bigg|_{z=h_s+h} r dr d\phi \Bigg) = I. \end{aligned} \tag{4.17}$$

Replacing k by s and $s+1$ in (4.11), equation (4.17) then becomes

$$\begin{aligned} \int_{r=0}^{\xi} \int_{\lambda=0}^{\infty} \Bigg(\sigma_s^{\circ} & \left(A_s I_1 \left(\frac{\lambda}{\varrho_s} \psi_s(h_s) \right) - B_s K_1 \left(\frac{\lambda}{\varrho_s} \psi_s(h_s) \right) \right) \\ & - \sigma_{s+1}^{\bullet} \left(A_{s+1} I_1 \left(\frac{\lambda}{\varrho_{s+1}} \psi_{s+1}(h_s) \right) - B_{s+1} K_1 \left(\frac{\lambda}{\varrho_{s+1}} \psi_{s+1}(h_s) \right) \right) \Bigg) \\ & \qquad \times 2\pi \lambda r J_0(\lambda r) \, d\lambda dr = I. \end{aligned}$$

Using the integral (Watson [67])

$$\int \lambda r J_0(\lambda r) \, dr = r J_1(\lambda r),$$

we obtain

$$\begin{aligned} \int_0^{\infty} \Bigg(\sigma_s^{\circ} & \left(A_s I_1 \left(\frac{\lambda}{\varrho_s} \psi_s(h_s) \right) - B_s K_1 \left(\frac{\lambda}{\varrho_s} \psi_s(h_s) \right) \right) \\ & - \sigma_{s+1}^{\bullet} \left(A_{s+1} I_1 \left(\frac{\lambda}{\varrho_{s+1}} \psi_{s+1}(h_s) \right) - B_{s+1} K_1 \left(\frac{\lambda}{\varrho_{s+1}} \psi_{s+1}(h_s) \right) \right) \Bigg) \\ & \qquad \times 2\pi \xi J_1(\lambda \xi) \, d\lambda = I. \end{aligned}$$

Inverting the above equation yields

$$2\pi\left(\sigma_s^{\circ}\left(A_s I_1\left(\frac{\lambda}{\varrho_s}\psi_s(h_s)\right)-B_s K_1\left(\frac{\lambda}{\varrho_s}\psi_s(h_s)\right)\right)\right.$$
$$\left.-\sigma_{s+1}^{\bullet}\left(A_{s+1} I_1\left(\frac{\lambda}{\varrho_{s+1}}\psi_{s+1}(h_s)\right)-B_{s+1} K_1\left(\frac{\lambda}{\varrho_{s+1}}\psi_{s+1}(h_s)\right)\right)\right)=I. \quad (4.18)$$

Thus, from equations (4.16) and (4.18), A_s and B_s can be written in terms of A_{s+1} and B_{s+1} as

$$A_s = N_{s+1}^{(11)} A_{s+1} + N_{s+1}^{(12)} B_{s+1} + \frac{I\lambda}{2\pi m_s} K_0\left(\frac{\lambda}{\varrho_s}\psi_s(h_s)\right)$$

and

$$B_s = N_{s+1}^{(21)} A_{s+1} + N_{s+1}^{(22)} B_{s+1} - \frac{I\lambda}{2\pi m_s} I_0\left(\frac{\lambda}{\varrho_s}\psi_s(h_s)\right),$$

where all the coefficients $N_{s+1}^{(ij)}$ are determined from the entries of the propagator matrix in Section 4.4.2 by replacing k with s. These can be rewritten in matrix form as

$$\begin{bmatrix} A_s \\ B_s \end{bmatrix} = \Theta_{s+1}\begin{bmatrix} A_{s+1} \\ B_{s+1} \end{bmatrix} + \frac{I\lambda}{2\pi m_s}\begin{bmatrix} K_0\left((\lambda/\varrho_s)\,\psi_s(h_s)\right) \\ -I_0\left((\lambda/\varrho_s)\,\psi_s(h_s)\right) \end{bmatrix}. \quad (4.19)$$

Substituting equations (4.14) and (4.15) into (4.19), we obtain

$$\prod_{j=s}^{1}\Gamma_j\begin{bmatrix} A_0 \\ B_0 \end{bmatrix} = \Theta_{s+1}\Theta^*\begin{bmatrix} A_n \\ B_n \end{bmatrix} + \frac{I\lambda}{2\pi m_s}\begin{bmatrix} K_0\left((\lambda/\varrho_s)\,\psi_s(h_s)\right) \\ -I_0\left((\lambda/\varrho_s)\,\psi_s(h_s)\right) \end{bmatrix}. \quad (4.20)$$

To guarantee the convergence of the electric potential V_0 when z tends to minus infinity, we must take

$$B_0 = 0.$$

Similarly, when z tends to infinity, the convergence of the electric potential V_n can be guaranteed by taking

$$A_n = 0.$$

Hence, equation (4.20) becomes

$$\prod_{j=s}^{1}\Gamma_j\begin{bmatrix} A_0 \\ 0 \end{bmatrix} = \Theta_{s+1}\Theta^*\begin{bmatrix} 0 \\ B_n \end{bmatrix} + \frac{I\lambda}{2\pi m_s}\begin{bmatrix} K_0\left((\lambda/\varrho_s)\,\psi_s(h_s)\right) \\ -I_0\left((\lambda/\varrho_s)\,\psi_s(h_s)\right) \end{bmatrix}.$$

This can be rewritten as a system of two linear equations in terms of the unknowns A_0 and B_n as

$$\begin{bmatrix} F_{11} & -G_{12} \\ F_{21} & -G_{22} \end{bmatrix}\begin{bmatrix} A_0 \\ B_n \end{bmatrix} = \frac{I\lambda}{2\pi m_s}\begin{bmatrix} K_0\left((\lambda/\varrho_s)\,\psi_s(h_s)\right) \\ -I_0\left((\lambda/\varrho_s)\,\psi_s(h_s)\right) \end{bmatrix},$$

where F_{ij} and G_{ij} are determined by

$$\prod_{j=s}^{1}\Gamma_j = \begin{bmatrix} F_{11} & F_{12} \\ F_{21} & F_{22} \end{bmatrix}, \qquad \Theta_{s+1}\Theta^* = \begin{bmatrix} G_{11} & G_{12} \\ G_{21} & G_{22} \end{bmatrix}.$$

Similar to Section 2.5, we can prove that the coefficient matrix of the above system is nonsingular (see also Chen and Oldenburg [11, 12]). By virtue of Cramer's rule, the system has a unique solution

$$A_0 = \frac{I\lambda}{2\pi m_s} \frac{G_{12}\, I_0\left(\left(\lambda/\varrho_s\right)\psi_s\left(h_s\right)\right) + G_{22}\, K_0\left(\left(\lambda/\varrho_s\right)\psi_s\left(h_s\right)\right)}{F_{11}G_{22} - F_{21}G_{12}},$$

$$B_n = \frac{I\lambda}{2\pi m_s} \frac{F_{11}\, I_0\left(\left(\lambda/\varrho_s\right)\psi_s\left(h_s\right)\right) + F_{21}\, K_0\left(\left(\lambda/\varrho_s\right)\psi_s\left(h_s\right)\right)}{F_{11}G_{22} - F_{21}G_{12}}.$$

As A_0, B_0, A_n and B_n are determined, so A_k and B_k, where $k \neq 0$ and n, can be obtained from the upward and downward recurrences as shown in equations (4.12) and (4.13).

4.5 Response of a Ground Layer Having Binomially Varying Conductivity

For each layer k, where $1 \leq k \leq n$ and $n \geq 2$, the variation of conductivity is denoted by

$$\sigma_k\left(z\right) = c_k\left(1 + d_k z\right)^{p_k}, \tag{4.21}$$

where c_k, p_k and $d_k \neq 0$ are constants, which preserve $\sigma_k\left(z\right) > 0$. Hence, the equation for the electric potential in layer k can be simplified by substituting equation (4.21) into (2.5) and we obtain

$$\frac{\partial^2 \tilde{V}_k}{\partial z^2} + \frac{d_k p_k}{1 + d_k z} \frac{\partial \tilde{V}_k}{\partial z} - \lambda^2 \tilde{V}_k = 0.$$

The solution to the above equation has been found by Lal [36] and given as

$$\tilde{V}_k\left(\lambda, z\right) = \tilde{\psi}_k^{\gamma_k}\left(z\right)\left(C_k I_{-\gamma_k}\left(\frac{\lambda}{\tilde{\varrho}_k}\tilde{\psi}_k\left(z\right)\right) + D_k K_{-\gamma_k}\left(\frac{\lambda}{\tilde{\varrho}_k}\tilde{\psi}_k\left(z\right)\right)\right),$$

where

$$\tilde{\varrho}_k = d_k, \qquad \tilde{\psi}_k\left(z\right) = 1 + \tilde{\varrho}_k z, \qquad \gamma_k = \frac{1 - p_k}{2},$$

C_k and D_k are arbitrary constants, which can be determined by using the boundary conditions. Thus, the electric potential in layer k is

$$V_k\left(r, z\right) = \int_0^\infty \tilde{\psi}_k^{\gamma_k}\left(z\right)\left(C_k I_{-\gamma_k}\left(\frac{\lambda}{\tilde{\varrho}_k}\tilde{\psi}_k\left(z\right)\right) + D_k K_{-\gamma_k}\left(\frac{\lambda}{\tilde{\varrho}_k}\tilde{\psi}_k\left(z\right)\right)\right) J_0\left(\lambda r\right) d\lambda. \tag{4.22}$$

4.5.1 Downward Recurrence

The objective is to establish a linear equation with arbitrary constants C_k and D_k, incorporating the physical and geometric parameters of the layers and interfaces above layer k. This section involves only equations with arbitrary constants C_k and D_k for $k = 0, 1, \ldots, s$. If $1 \leq k \leq s-1$, then the electric potentials in layers k and $k+1$ can be written as

$$\tilde{V}_k(\lambda, z) = \tilde{\psi}_k^{\gamma_k}(z)\left(C_k I_{-\gamma_k}\left(\frac{\lambda}{\tilde{\varrho}_k}\tilde{\psi}_k(z)\right) + D_k K_{-\gamma_k}\left(\frac{\lambda}{\tilde{\varrho}_k}\tilde{\psi}_k(z)\right)\right)$$

and

$$\tilde{V}_{k+1}(\lambda, z) = \tilde{\psi}_{k+1}^{\gamma_{k+1}}(z)\left(C_{k+1} I_{-\gamma_{k+1}}\left(\frac{\lambda}{\tilde{\varrho}_{k+1}}\tilde{\psi}_{k+1}(z)\right) + D_{k+1} K_{-\gamma_{k+1}}\left(\frac{\lambda}{\tilde{\varrho}_{k+1}}\tilde{\psi}_{k+1}(z)\right)\right).$$

Using the boundary conditions (4.7) and (4.8), we obtain

$$\begin{aligned}\tilde{\psi}_k^{\gamma_k}(h_k)&\left(C_k I_{-\gamma_k}\left(\frac{\lambda}{\tilde{\varrho}_k}\tilde{\psi}_k(h_k)\right) + D_k K_{-\gamma_k}\left(\frac{\lambda}{\tilde{\varrho}_k}\tilde{\psi}_k(h_k)\right)\right)\\ &= \tilde{\psi}_{k+1}^{\gamma_{k+1}}(h_k)\left(C_{k+1} I_{-\gamma_{k+1}}\left(\frac{\lambda}{\tilde{\varrho}_{k+1}}\tilde{\psi}_{k+1}(h_k)\right) + D_{k+1} K_{-\gamma_{k+1}}\left(\frac{\lambda}{\tilde{\varrho}_{k+1}}\tilde{\psi}_{k+1}(h_k)\right)\right)\end{aligned}$$

and

$$\begin{aligned}\lambda c_k \tilde{\psi}_k^{\upsilon_k}(h_k)&\left(C_k I_{\upsilon_k}\left(\frac{\lambda}{\tilde{\varrho}_k}\tilde{\psi}_k(h_k)\right) - D_k K_{\upsilon_k}\left(\frac{\lambda}{\tilde{\varrho}_k}\tilde{\psi}_k(h_k)\right)\right)\\ &= \lambda c_{k+1}\tilde{\psi}_{k+1}^{\upsilon_{k+1}}(h_k)\left(C_{k+1} I_{\upsilon_{k+1}}\left(\frac{\lambda}{\tilde{\varrho}_{k+1}}\tilde{\psi}_{k+1}(h_k)\right) - D_{k+1} K_{\upsilon_{k+1}}\left(\frac{\lambda}{\tilde{\varrho}_{k+1}}\tilde{\psi}_{k+1}(h_k)\right)\right),\end{aligned}$$

where

$$\upsilon_j = \frac{1+p_j}{2}.$$

Hence, C_{k+1} and D_{k+1} can be written in terms of C_k and D_k as

$$C_{k+1} = \tilde{M}_{k+1}^{(11)} C_k + \tilde{M}_{k+1}^{(12)} D_k$$

and

$$D_{k+1} = \tilde{M}_{k+1}^{(21)} C_k + \tilde{M}_{k+1}^{(22)} D_k,$$

where all the coefficients $\tilde{M}_{k+1}^{(ij)}$ are given by

$$\tilde{M}_{k+1}^{(11)} = \frac{\lambda}{\tilde{\varrho}_{k+1} c_{k+1}} \tilde{\psi}_k^{\gamma_k}(h_k)\, \tilde{\psi}_{k+1}^{\gamma_{k+1}}(h_k) \times \left(\sigma_k^{\circ} I_{\upsilon_k}\left(\frac{\lambda}{\tilde{\varrho}_k}\tilde{\psi}_k(h_k)\right) K_{-\gamma_{k+1}}\left(\frac{\lambda}{\tilde{\varrho}_{k+1}}\tilde{\psi}_{k+1}(h_k)\right) + \sigma_{k+1}^{\bullet} I_{-\gamma_k}\left(\frac{\lambda}{\tilde{\varrho}_k}\tilde{\psi}_k(h_k)\right) K_{\upsilon_{k+1}}\left(\frac{\lambda}{\tilde{\varrho}_{k+1}}\tilde{\psi}_{k+1}(h_k)\right)\right),$$

$$\tilde{M}_{k+1}^{(12)} = \frac{\lambda}{\tilde{\varrho}_{k+1} c_{k+1}} \tilde{\psi}_k^{\gamma_k}(h_k)\, \tilde{\psi}_{k+1}^{\gamma_{k+1}}(h_k) \times \left(\sigma_{k+1}^{\bullet} K_{-\gamma_k}\left(\frac{\lambda}{\tilde{\varrho}_k}\tilde{\psi}_k(h_k)\right) K_{\upsilon_{k+1}}\left(\frac{\lambda}{\tilde{\varrho}_{k+1}}\tilde{\psi}_{k+1}(h_k)\right) - \sigma_k^{\circ} K_{\upsilon_k}\left(\frac{\lambda}{\tilde{\varrho}_k}\tilde{\psi}_k(h_k)\right) K_{-\gamma_{k+1}}\left(\frac{\lambda}{\tilde{\varrho}_{k+1}}\tilde{\psi}_{k+1}(h_k)\right)\right),$$

$$\tilde{M}_{k+1}^{(21)} = \frac{\lambda}{\tilde{\varrho}_{k+1} c_{k+1}} \tilde{\psi}_k^{\gamma_k}(h_k)\, \tilde{\psi}_{k+1}^{\gamma_{k+1}}(h_k) \times \left(\sigma_{k+1}^{\bullet} I_{-\gamma_k}\left(\frac{\lambda}{\tilde{\varrho}_k}\tilde{\psi}_k(h_k)\right) I_{\upsilon_{k+1}}\left(\frac{\lambda}{\tilde{\varrho}_{k+1}}\tilde{\psi}_{k+1}(h_k)\right) - \sigma_k^{\circ} I_{\upsilon_k}\left(\frac{\lambda}{\tilde{\varrho}_k}\tilde{\psi}_k(h_k)\right) I_{-\gamma_{k+1}}\left(\frac{\lambda}{\tilde{\varrho}_{k+1}}\tilde{\psi}_{k+1}(h_k)\right)\right),$$

$$\tilde{M}_{k+1}^{(22)} = \frac{\lambda}{\tilde{\varrho}_{k+1} c_{k+1}} \tilde{\psi}_k^{\gamma_k}(h_k)\, \tilde{\psi}_{k+1}^{\gamma_{k+1}}(h_k) \times \left(\sigma_k^{\circ} K_{\upsilon_k}\left(\frac{\lambda}{\tilde{\varrho}_k}\tilde{\psi}_k(h_k)\right) I_{-\gamma_{k+1}}\left(\frac{\lambda}{\tilde{\varrho}_{k+1}}\tilde{\psi}_{k+1}(h_k)\right) + \sigma_{k+1}^{\bullet} K_{-\gamma_k}\left(\frac{\lambda}{\tilde{\varrho}_k}\tilde{\psi}_k(h_k)\right) I_{\upsilon_{k+1}}\left(\frac{\lambda}{\tilde{\varrho}_{k+1}}\tilde{\psi}_{k+1}(h_k)\right)\right).$$

Similarly, if $k = 0$, then we have

$$\tilde{V}_k(\lambda, z) = A_k e^{\lambda z} + B_k e^{-\lambda z}$$

and

$$\tilde{V}_{k+1}(\lambda, z) = \tilde{\psi}_{k+1}^{\gamma_{k+1}}(z) \left(C_{k+1} I_{-\gamma_{k+1}}\left(\frac{\lambda}{\tilde{\varrho}_{k+1}}\tilde{\psi}_{k+1}(z)\right) + D_{k+1} K_{-\gamma_{k+1}}\left(\frac{\lambda}{\tilde{\varrho}_{k+1}}\tilde{\psi}_{k+1}(z)\right)\right).$$

Thus, the boundary conditions (4.7) and (4.8) lead to

$$A_k e^{\lambda h_k} + B_k e^{-\lambda h_k} = \tilde{\psi}_{k+1}^{\gamma_{k+1}}(h_k)\left(C_{k+1} I_{-\gamma_{k+1}}\left(\frac{\lambda}{\tilde{\varrho}_{k+1}}\tilde{\psi}_{k+1}(h_k)\right) + D_{k+1} K_{-\gamma_{k+1}}\left(\frac{\lambda}{\tilde{\varrho}_{k+1}}\tilde{\psi}_{k+1}(h_k)\right)\right)$$

and

$$\lambda\sigma_k^{\circ}\left(A_k e^{\lambda h_k} - B_k e^{-\lambda h_k}\right) = \lambda c_{k+1}\tilde{\psi}_{k+1}^{\upsilon_{k+1}}(h_k)\left(C_{k+1} I_{\upsilon_{k+1}}\left(\frac{\lambda}{\tilde{\varrho}_{k+1}}\tilde{\psi}_{k+1}(h_k)\right) - D_{k+1} K_{\upsilon_{k+1}}\left(\frac{\lambda}{\tilde{\varrho}_{k+1}}\tilde{\psi}_{k+1}(h_k)\right)\right).$$

Hence, C_{k+1} and D_{k+1} can also be written in terms of C_k and D_k as

$$C_{k+1} = \tilde{M}_{k+1}^{(11)} C_k + \tilde{M}_{k+1}^{(12)} D_k$$

and

$$D_{k+1} = \tilde{M}_{k+1}^{(21)} C_k + \tilde{M}_{k+1}^{(22)} D_k,$$

where all the coefficients $\tilde{M}_{k+1}^{(ij)}$ are given by

$$\tilde{M}_{k+1}^{(11)} = \frac{\lambda e^{\lambda h_k}}{\tilde{\varrho}_{k+1} c_{k+1}}\tilde{\psi}_{k+1}^{\gamma_{k+1}}(h_k)\left(\sigma_k^{\circ} K_{-\gamma_{k+1}}\left(\frac{\lambda}{\tilde{\varrho}_{k+1}}\tilde{\psi}_{k+1}(h_k)\right) + \sigma_{k+1}^{\bullet} K_{\upsilon_{k+1}}\left(\frac{\lambda}{\tilde{\varrho}_{k+1}}\tilde{\psi}_{k+1}(h_k)\right)\right),$$

$$\tilde{M}_{k+1}^{(12)} = \frac{\lambda e^{-\lambda h_k}}{\tilde{\varrho}_{k+1} c_{k+1}}\tilde{\psi}_{k+1}^{\gamma_{k+1}}(h_k)\left(\sigma_{k+1}^{\bullet} K_{\upsilon_{k+1}}\left(\frac{\lambda}{\tilde{\varrho}_{k+1}}\tilde{\psi}_{k+1}(h_k)\right) - \sigma_k^{\circ} K_{-\gamma_{k+1}}\left(\frac{\lambda}{\tilde{\varrho}_{k+1}}\tilde{\psi}_{k+1}(h_k)\right)\right),$$

$$\tilde{M}_{k+1}^{(21)} = \frac{\lambda e^{\lambda h_k}}{\tilde{\varrho}_{k+1} c_{k+1}}\tilde{\psi}_{k+1}^{\gamma_{k+1}}(h_k)\left(\sigma_{k+1}^{\bullet} I_{\upsilon_{k+1}}\left(\frac{\lambda}{\tilde{\varrho}_{k+1}}\tilde{\psi}_{k+1}(h_k)\right) - \sigma_k^{\circ} I_{-\gamma_{k+1}}\left(\frac{\lambda}{\tilde{\varrho}_{k+1}}\tilde{\psi}_{k+1}(h_k)\right)\right),$$

$$\tilde{M}_{k+1}^{(22)} = \frac{\lambda e^{-\lambda h_k}}{\tilde{\varrho}_{k+1} c_{k+1}}\tilde{\psi}_{k+1}^{\gamma_{k+1}}(h_k)\left(\sigma_k^{\circ} I_{-\gamma_{k+1}}\left(\frac{\lambda}{\tilde{\varrho}_{k+1}}\tilde{\psi}_{k+1}(h_k)\right) + \sigma_{k+1}^{\bullet} I_{\upsilon_{k+1}}\left(\frac{\lambda}{\tilde{\varrho}_{k+1}}\tilde{\psi}_{k+1}(h_k)\right)\right).$$

Thus, for $0 \leq k \leq s-1$, the downward recurrence can be defined by

$$\begin{bmatrix} C_{k+1} \\ D_{k+1} \end{bmatrix} = \tilde{\Gamma}_{k+1} \begin{bmatrix} C_k \\ D_k \end{bmatrix}, \tag{4.23}$$

where the propagator matrix is

$$\tilde{\Gamma}_{k+1} = \begin{bmatrix} \tilde{M}_{k+1}^{(11)} & \tilde{M}_{k+1}^{(12)} \\ \tilde{M}_{k+1}^{(21)} & \tilde{M}_{k+1}^{(22)} \end{bmatrix}.$$

The coefficients $\tilde{M}_{k+1}^{(ij)}$, in the general case, can be rewritten as

$$\begin{aligned} \tilde{M}_{k+1}^{(11)} = \frac{\lambda}{\tilde{\varrho}_{k+1} c_{k+1}} \tilde{\psi}_{k+1}^{\gamma_{k+1}} (h_k) \Bigg(& \sigma_k^{\circ} \tilde{\zeta}_k' K_{-\gamma_{k+1}} \left(\frac{\lambda}{\tilde{\varrho}_{k+1}} \tilde{\psi}_{k+1} (h_k) \right) \\ & + \sigma_{k+1}^{\bullet} \tilde{\zeta}_k K_{\upsilon_{k+1}} \left(\frac{\lambda}{\tilde{\varrho}_{k+1}} \tilde{\psi}_{k+1} (h_k) \right) \Bigg), \end{aligned}$$

$$\begin{aligned} \tilde{M}_{k+1}^{(12)} = \frac{\lambda}{\tilde{\varrho}_{k+1} c_{k+1}} \tilde{\psi}_{k+1}^{\gamma_{k+1}} (h_k) \Bigg(& \sigma_{k+1}^{\bullet} \tilde{\xi}_k K_{\upsilon_{k+1}} \left(\frac{\lambda}{\tilde{\varrho}_{k+1}} \tilde{\psi}_{k+1} (h_k) \right) \\ & - \sigma_k^{\circ} \tilde{\xi}_k' K_{-\gamma_{k+1}} \left(\frac{\lambda}{\tilde{\varrho}_{k+1}} \tilde{\psi}_{k+1} (h_k) \right) \Bigg), \end{aligned}$$

$$\begin{aligned} \tilde{M}_{k+1}^{(21)} = \frac{\lambda}{\tilde{\varrho}_{k+1} c_{k+1}} \tilde{\psi}_{k+1}^{\gamma_{k+1}} (h_k) \Bigg(& \sigma_{k+1}^{\bullet} \tilde{\zeta}_k I_{\upsilon_{k+1}} \left(\frac{\lambda}{\tilde{\varrho}_{k+1}} \tilde{\psi}_{k+1} (h_k) \right) \\ & - \sigma_k^{\circ} \tilde{\zeta}_k' I_{-\gamma_{k+1}} \left(\frac{\lambda}{\tilde{\varrho}_{k+1}} \tilde{\psi}_{k+1} (h_k) \right) \Bigg), \end{aligned}$$

$$\begin{aligned} \tilde{M}_{k+1}^{(22)} = \frac{\lambda}{\tilde{\varrho}_{k+1} c_{k+1}} \tilde{\psi}_{k+1}^{\gamma_{k+1}} (h_k) \Bigg(& \sigma_k^{\circ} \tilde{\xi}_k' I_{-\gamma_{k+1}} \left(\frac{\lambda}{\tilde{\varrho}_{k+1}} \tilde{\psi}_{k+1} (h_k) \right) \\ & + \sigma_{k+1}^{\bullet} \tilde{\xi}_k I_{\upsilon_{k+1}} \left(\frac{\lambda}{\tilde{\varrho}_{k+1}} \tilde{\psi}_{k+1} (h_k) \right) \Bigg), \end{aligned}$$

where

$$\tilde{\zeta}_k = \begin{cases} \tilde{\psi}_k^{\gamma_k} (h_k) \, I_{-\gamma_k} \left((\lambda/\varrho_k) \, \psi_k (h_k) \right) & \text{if } 1 \leq k \leq s-1, \\ e^{\lambda h_k} & \text{if } k = 0, \end{cases}$$

$$\tilde{\zeta}_k' = \begin{cases} \tilde{\psi}_k^{\gamma_k} (h_k) \, I_{\upsilon_k} \left((\lambda/\varrho_k) \, \psi_k (h_k) \right) & \text{if } 1 \leq k \leq s-1, \\ e^{\lambda h_k} & \text{if } k = 0, \end{cases}$$

and

$$\tilde{\xi}_k = \begin{cases} \tilde{\psi}_k^{\gamma_k} (h_k) \, K_{-\gamma_k} \left((\lambda/\varrho_k) \, \psi_k (h_k) \right) & \text{if } 1 \leq k \leq s-1, \\ e^{-\lambda h_k} & \text{if } k = 0, \end{cases}$$

$$\tilde{\xi}_k' = \begin{cases} \tilde{\psi}_k^{\gamma_k} (h_k) \, K_{\upsilon_k} \left((\lambda/\varrho_k) \, \psi_k (h_k) \right) & \text{if } 1 \leq k \leq s-1, \\ e^{-\lambda h_k} & \text{if } k = 0. \end{cases}$$

4.5.2 Upward Recurrence

In a way similar to that of Section 4.5.1 but working in the opposite direction, the objective is to establish a linear equation with arbitrary constants C_k and D_k, incorporating the physical and geometric parameters of the layers and interfaces below layer k. This section involves only equations with arbitrary constants C_k and D_k for $k = s+1, s+2, \ldots, n$. If $s < n-1$, for $s+1 \leq k \leq n-1$, the electric potentials in layers k and $k+1$ can be written as

$$\tilde{V}_k(\lambda, z) = \tilde{\psi}_k^{\gamma_k}(z)\left(C_k I_{-\gamma_k}\left(\frac{\lambda}{\tilde{\varrho}_k}\tilde{\psi}_k(z)\right) + D_k K_{-\gamma_k}\left(\frac{\lambda}{\tilde{\varrho}_k}\tilde{\psi}_k(z)\right)\right)$$

and

$$\tilde{V}_{k+1}(\lambda, z) = \tilde{\psi}_{k+1}^{\gamma_{k+1}}(z)\left(C_{k+1} I_{-\gamma_{k+1}}\left(\frac{\lambda}{\tilde{\varrho}_{k+1}}\tilde{\psi}_{k+1}(z)\right) + D_{k+1} K_{-\gamma_{k+1}}\left(\frac{\lambda}{\tilde{\varrho}_{k+1}}\tilde{\psi}_{k+1}(z)\right)\right).$$

Using the boundary conditions (4.7) and (4.8), we obtain

$$\tilde{\psi}_k^{\gamma_k}(h_k)\left(C_k I_{-\gamma_k}\left(\frac{\lambda}{\tilde{\varrho}_k}\tilde{\psi}_k(h_k)\right) + D_k K_{-\gamma_k}\left(\frac{\lambda}{\tilde{\varrho}_k}\tilde{\psi}_k(h_k)\right)\right) = \tilde{\psi}_{k+1}^{\gamma_{k+1}}(h_k)\left(C_{k+1} I_{-\gamma_{k+1}}\left(\frac{\lambda}{\tilde{\varrho}_{k+1}}\tilde{\psi}_{k+1}(h_k)\right) + D_{k+1} K_{-\gamma_{k+1}}\left(\frac{\lambda}{\tilde{\varrho}_{k+1}}\tilde{\psi}_{k+1}(h_k)\right)\right)$$

and

$$\lambda c_k \tilde{\psi}_k^{\upsilon_k}(h_k)\left(C_k I_{\upsilon_k}\left(\frac{\lambda}{\tilde{\varrho}_k}\tilde{\psi}_k(h_k)\right) - D_k K_{\upsilon_k}\left(\frac{\lambda}{\tilde{\varrho}_k}\tilde{\psi}_k(h_k)\right)\right) = \lambda c_{k+1} \tilde{\psi}_{k+1}^{\upsilon_{k+1}}(h_k)\left(C_{k+1} I_{\upsilon_{k+1}}\left(\frac{\lambda}{\tilde{\varrho}_{k+1}}\tilde{\psi}_{k+1}(h_k)\right) - D_{k+1} K_{\upsilon_{k+1}}\left(\frac{\lambda}{\tilde{\varrho}_{k+1}}\tilde{\psi}_{k+1}(h_k)\right)\right).$$

Hence, C_k and D_k can be written in terms of C_{k+1} and D_{k+1} as

$$C_k = \tilde{N}_{k+1}^{(11)} C_{k+1} + \tilde{N}_{k+1}^{(12)} D_{k+1}$$

and

$$D_k = \tilde{N}_{k+1}^{(21)} C_{k+1} + \tilde{N}_{k+1}^{(22)} D_{k+1},$$

where all the coefficients $\tilde{N}_{k+1}^{(ij)}$ are given by

$$\tilde{N}_{k+1}^{(11)} = \frac{\lambda}{\tilde{\varrho}_k c_k}\tilde{\psi}_k^{\gamma_k}(h_k)\,\tilde{\psi}_{k+1}^{\gamma_{k+1}}(h_k) \times \left(\sigma_k^{\circ} K_{\upsilon_k}\left(\frac{\lambda}{\tilde{\varrho}_k}\tilde{\psi}_k(h_k)\right) I_{-\gamma_{k+1}}\left(\frac{\lambda}{\tilde{\varrho}_{k+1}}\tilde{\psi}_{k+1}(h_k)\right) + \sigma_{k+1}^{\bullet} K_{-\gamma_k}\left(\frac{\lambda}{\tilde{\varrho}_k}\tilde{\psi}_k(h_k)\right) I_{\upsilon_{k+1}}\left(\frac{\lambda}{\tilde{\varrho}_{k+1}}\tilde{\psi}_{k+1}(h_k)\right)\right),$$

$$\tilde{N}_{k+1}^{(12)} = \frac{\lambda}{\tilde{\varrho}_k c_k} \tilde{\psi}_k^{\gamma_k}(h_k)\, \tilde{\psi}_{k+1}^{\gamma_{k+1}}(h_k) \times \left(\sigma_k^{\circ} K_{\upsilon_k}\left(\frac{\lambda}{\tilde{\varrho}_k}\tilde{\psi}_k(h_k)\right) K_{-\gamma_{k+1}}\left(\frac{\lambda}{\tilde{\varrho}_{k+1}}\tilde{\psi}_{k+1}(h_k)\right) - \sigma_{k+1}^{\bullet} K_{-\gamma_k}\left(\frac{\lambda}{\tilde{\varrho}_k}\tilde{\psi}_k(h_k)\right) K_{\upsilon_{k+1}}\left(\frac{\lambda}{\tilde{\varrho}_{k+1}}\tilde{\psi}_{k+1}(h_k)\right)\right),$$

$$\tilde{N}_{k+1}^{(21)} = \frac{\lambda}{\tilde{\varrho}_k c_k} \tilde{\psi}_k^{\gamma_k}(h_k)\, \tilde{\psi}_{k+1}^{\gamma_{k+1}}(h_k) \times \left(\sigma_k^{\circ} I_{\upsilon_k}\left(\frac{\lambda}{\tilde{\varrho}_k}\tilde{\psi}_k(h_k)\right) I_{-\gamma_{k+1}}\left(\frac{\lambda}{\tilde{\varrho}_{k+1}}\tilde{\psi}_{k+1}(h_k)\right) - \sigma_{k+1}^{\bullet} I_{-\gamma_k}\left(\frac{\lambda}{\tilde{\varrho}_k}\tilde{\psi}_k(h_k)\right) I_{\upsilon_{k+1}}\left(\frac{\lambda}{\tilde{\varrho}_{k+1}}\tilde{\psi}_{k+1}(h_k)\right)\right),$$

$$\tilde{N}_{k+1}^{(22)} = \frac{\lambda}{\tilde{\varrho}_k c_k} \tilde{\psi}_k^{\gamma_k}(h_k)\, \tilde{\psi}_{k+1}^{\gamma_{k+1}}(h_k) \times \left(\sigma_k^{\circ} I_{\upsilon_k}\left(\frac{\lambda}{\tilde{\varrho}_k}\tilde{\psi}_k(h_k)\right) K_{-\gamma_{k+1}}\left(\frac{\lambda}{\tilde{\varrho}_{k+1}}\tilde{\psi}_{k+1}(h_k)\right) + \sigma_{k+1}^{\bullet} I_{-\gamma_k}\left(\frac{\lambda}{\tilde{\varrho}_k}\tilde{\psi}_k(h_k)\right) K_{\upsilon_{k+1}}\left(\frac{\lambda}{\tilde{\varrho}_{k+1}}\tilde{\psi}_{k+1}(h_k)\right)\right).$$

Thus, for $s+1 \le k \le n-1$, the upward recurrence can be defined by

$$\begin{bmatrix} C_k \\ D_k \end{bmatrix} = \tilde{\Theta}_{k+1} \begin{bmatrix} C_{k+1} \\ D_{k+1} \end{bmatrix}, \tag{4.24}$$

where the propagator matrix is

$$\tilde{\Theta}_{k+1} = \begin{bmatrix} \tilde{N}_{k+1}^{(11)} & \tilde{N}_{k+1}^{(12)} \\ \tilde{N}_{k+1}^{(21)} & \tilde{N}_{k+1}^{(22)} \end{bmatrix}.$$

4.5.3 Solution for an n-layered Earth

We now consider an n-layered earth model. Each layer k of ground, where $1 \le k \le n$ and $n \ge 2$, has a binomially varying conductivity as given in (4.21). A region of air, denoted by layer 0, has a constant conductivity. A point source of direct current is deliberately located at the interface $z = h_s$ of layer s and layer $s+1$, where $1 \le s \le n-1$, for simplifying the mathematics. The downward recurrence (4.23) can be applied to obtain

$$\begin{bmatrix} C_s \\ D_s \end{bmatrix} = \prod_{j=s}^{1} \tilde{\Gamma}_j \begin{bmatrix} C_0 \\ D_0 \end{bmatrix}. \tag{4.25}$$

Similarly, the upward recurrence (4.24) yields

$$\begin{bmatrix} C_{s+1} \\ D_{s+1} \end{bmatrix} = \tilde{\Theta}^* \begin{bmatrix} C_n \\ D_n \end{bmatrix}, \tag{4.26}$$

where

$$\tilde{\Theta}^{*}=\begin{cases}\prod_{j=s+2}^{n}\tilde{\Theta}_{j} & \text{if } s<n-1,\\ \mathbf{I}_{2} & \text{if } s=n-1.\end{cases}$$

On the boundary plane $z = h_s$, the boundary condition (4.7) is used again, and so we have

$$\begin{aligned}\tilde{\psi}_{s}^{\gamma_{s}}(h_{s})\left(C_{s}I_{-\gamma_{s}}\left(\frac{\lambda}{\tilde{\varrho}_{s}}\tilde{\psi}_{s}(h_{s})\right)+D_{s}K_{-\gamma_{s}}\left(\frac{\lambda}{\tilde{\varrho}_{s}}\tilde{\psi}_{s}(h_{s})\right)\right)\\ =\tilde{\psi}_{s+1}^{\gamma_{s+1}}(h_{s})\left(C_{s+1}I_{-\gamma_{s+1}}\left(\frac{\lambda}{\tilde{\varrho}_{s+1}}\tilde{\psi}_{s+1}(h_{s})\right)\right.\\ \left.+D_{s+1}K_{-\gamma_{s+1}}\left(\frac{\lambda}{\tilde{\varrho}_{s+1}}\tilde{\psi}_{s+1}(h_{s})\right)\right).\end{aligned}\tag{4.27}$$

Moreover, the boundary condition (4.9) requires

$$\begin{aligned}\lim_{h\to0}\left(\int_{\phi=0}^{2\pi}\int_{r=0}^{\xi}\left(\sigma_{s}\frac{\partial\tilde{V}_{s}}{\partial z}\right)\Bigg|_{z=h_{s}-h}rdrd\phi\right.\\ \left.-\int_{\phi=0}^{2\pi}\int_{r=0}^{\xi}\left(\sigma_{s+1}\frac{\partial\tilde{V}_{s+1}}{\partial z}\right)\Bigg|_{z=h_{s}+h}rdrd\phi\right)=I.\end{aligned}\tag{4.28}$$

Replacing k by s and $s+1$ in (4.22), equation (4.28) then becomes

$$\begin{aligned}\int_{r=0}^{\xi}\int_{\lambda=0}^{\infty}\left(c_{s}\tilde{\psi}_{s}^{\upsilon_{s}}(h_{s})\left(C_{s}I_{\upsilon_{s}}\left(\frac{\lambda}{\tilde{\varrho}_{s}}\tilde{\psi}_{s}(h_{s})\right)-D_{s}K_{\upsilon_{s}}\left(\frac{\lambda}{\tilde{\varrho}_{s}}\tilde{\psi}_{s}(h_{s})\right)\right)\right.\\ -c_{s+1}\tilde{\psi}_{s+1}^{\upsilon_{s+1}}(h_{s})\left(C_{s+1}I_{\upsilon_{s+1}}\left(\frac{\lambda}{\tilde{\varrho}_{s+1}}\tilde{\psi}_{s+1}(h_{s})\right)\right.\\ \left.\left.-D_{s+1}K_{\upsilon_{s+1}}\left(\frac{\lambda}{\tilde{\varrho}_{s+1}}\tilde{\psi}_{s+1}(h_{s})\right)\right)\right)2\pi\lambda rJ_{0}(\lambda r)\,d\lambda dr=I.\end{aligned}$$

Using the integral

$$\int\lambda rJ_{0}(\lambda r)\,dr=rJ_{1}(\lambda r),$$

we obtain

$$\begin{aligned}\int_{0}^{\infty}\left(c_{s}\tilde{\psi}_{s}^{\upsilon_{s}}(h_{s})\left(C_{s}I_{\upsilon_{s}}\left(\frac{\lambda}{\tilde{\varrho}_{s}}\tilde{\psi}_{s}(h_{s})\right)-D_{s}K_{\upsilon_{s}}\left(\frac{\lambda}{\tilde{\varrho}_{s}}\tilde{\psi}_{s}(h_{s})\right)\right)\right.\\ -c_{s+1}\tilde{\psi}_{s+1}^{\upsilon_{s+1}}(h_{s})\left(C_{s+1}I_{\upsilon_{s+1}}\left(\frac{\lambda}{\tilde{\varrho}_{s+1}}\tilde{\psi}_{s+1}(h_{s})\right)\right.\\ \left.\left.-D_{s+1}K_{\upsilon_{s+1}}\left(\frac{\lambda}{\tilde{\varrho}_{s+1}}\tilde{\psi}_{s+1}(h_{s})\right)\right)\right)2\pi\xi J_{1}(\lambda\xi)\,d\lambda=I.\end{aligned}$$

Inverting the above equation yields

$$2\pi \left(c_s \tilde{\psi}_s^{\upsilon_s}(h_s) \left(C_s I_{\upsilon_s} \left(\frac{\lambda}{\tilde{\varrho}_s} \tilde{\psi}_s(h_s) \right) - D_s K_{\upsilon_s} \left(\frac{\lambda}{\tilde{\varrho}_s} \tilde{\psi}_s(h_s) \right) \right) - c_{s+1} \tilde{\psi}_{s+1}^{\upsilon_{s+1}}(h_s) \left(C_{s+1} I_{\upsilon_{s+1}} \left(\frac{\lambda}{\tilde{\varrho}_{s+1}} \tilde{\psi}_{s+1}(h_s) \right) - D_{s+1} K_{\upsilon_{s+1}} \left(\frac{\lambda}{\tilde{\varrho}_{s+1}} \tilde{\psi}_{s+1}(h_s) \right) \right) \right) = I. \quad (4.29)$$

Thus, from equations (4.27) and (4.29), C_s and D_s can be written in terms of C_{s+1} and D_{s+1} as

$$C_s = \tilde{N}_{s+1}^{(11)} C_{s+1} + \tilde{N}_{s+1}^{(12)} D_{s+1} + \frac{I\lambda}{2\pi c_s \tilde{\varrho}_s} \tilde{\psi}_s^{\gamma_s}(h_s) K_{-\gamma_s} \left((\lambda/\tilde{\varrho}_s) \tilde{\psi}_s(h_s) \right)$$

and

$$D_s = \tilde{N}_{s+1}^{(21)} C_{s+1} + \tilde{N}_{s+1}^{(22)} D_{s+1} - \frac{I\lambda}{2\pi c_s \tilde{\varrho}_s} \tilde{\psi}_s^{\gamma_s}(h_s) I_{-\gamma_s} \left((\lambda/\tilde{\varrho}_s) \tilde{\psi}_s(h_s) \right),$$

where all the coefficients $\tilde{N}_{s+1}^{(ij)}$ are determined from the entries of the propagator matrix in Section 4.5.2 by replacing k with s. These can be rewritten in matrix form as

$$\begin{bmatrix} C_s \\ D_s \end{bmatrix} = \tilde{\Theta}_{s+1} \begin{bmatrix} C_{s+1} \\ D_{s+1} \end{bmatrix} + \tilde{\psi}_s^{\gamma_s}(h_s) \frac{I\lambda}{2\pi c_s \tilde{\varrho}_s} \begin{bmatrix} K_{-\gamma_s} \left((\lambda/\tilde{\varrho}_s) \tilde{\psi}_s(h_s) \right) \\ -I_{-\gamma_s} \left((\lambda/\tilde{\varrho}_s) \tilde{\psi}_s(h_s) \right) \end{bmatrix}. \quad (4.30)$$

Substituting equations (4.25) and (4.26) into (4.30), we obtain

$$\prod_{j=s}^{1} \tilde{\Gamma}_j \begin{bmatrix} C_0 \\ D_0 \end{bmatrix} = \tilde{\Theta}_{s+1} \tilde{\Theta}^* \begin{bmatrix} C_n \\ D_n \end{bmatrix} + \tilde{\psi}_s^{\gamma_s}(h_s) \frac{I\lambda}{2\pi c_s \tilde{\varrho}_s} \begin{bmatrix} K_{-\gamma_s} \left((\lambda/\tilde{\varrho}_s) \tilde{\psi}_s(h_s) \right) \\ -I_{-\gamma_s} \left((\lambda/\tilde{\varrho}_s) \tilde{\psi}_s(h_s) \right) \end{bmatrix}. \quad (4.31)$$

To guarantee the convergence of the electric potential V_0 when z tends to minus infinity, we must take

$$D_0 = 0.$$

Similarly, when z tends to infinity, the convergence of the electric potential V_n can be guaranteed by taking

$$C_n = 0.$$

Hence, equation (4.31) becomes

$$\prod_{j=s}^{1} \tilde{\Gamma}_j \begin{bmatrix} C_0 \\ 0 \end{bmatrix} = \tilde{\Theta}_{s+1} \tilde{\Theta}^* \begin{bmatrix} 0 \\ D_n \end{bmatrix} + \tilde{\psi}_s^{\gamma_s}(h_s) \frac{I\lambda}{2\pi c_s \tilde{\varrho}_s} \begin{bmatrix} K_{-\gamma_s} \left((\lambda/\tilde{\varrho}_s) \tilde{\psi}_s(h_s) \right) \\ -I_{-\gamma_s} \left((\lambda/\tilde{\varrho}_s) \tilde{\psi}_s(h_s) \right) \end{bmatrix}.$$

This can be rewritten as a system of two linear equations in terms of the unknowns C_0 and D_n as

$$\begin{bmatrix} \tilde{F}_{11} & -\tilde{G}_{12} \\ \tilde{F}_{21} & -\tilde{G}_{22} \end{bmatrix} \begin{bmatrix} C_0 \\ D_n \end{bmatrix} = \tilde{\psi}_s^{\gamma_s}(h_s) \frac{I\lambda}{2\pi c_s \tilde{\varrho}_s} \begin{bmatrix} K_{-\gamma_s} \left((\lambda/\tilde{\varrho}_s) \tilde{\psi}_s(h_s) \right) \\ -I_{-\gamma_s} \left((\lambda/\tilde{\varrho}_s) \tilde{\psi}_s(h_s) \right) \end{bmatrix},$$

where $\tilde{F}_{ij}$ and $\tilde{G}_{ij}$ are determined by

$$\prod_{j=s}^{1} \tilde{\Gamma}_j = \begin{bmatrix} \tilde{F}_{11} & \tilde{F}_{12} \\ \tilde{F}_{21} & \tilde{F}_{22} \end{bmatrix}, \qquad \tilde{\Theta}_{s+1}\tilde{\Theta}^* = \begin{bmatrix} \tilde{G}_{11} & \tilde{G}_{12} \\ \tilde{G}_{21} & \tilde{G}_{22} \end{bmatrix}.$$

Similar to Section 2.5, we can prove that the coefficient matrix of the above system is nonsingular (see also Chen and Oldenburg [11, 12]). By virtue of Cramer's rule, the system has a unique solution

$$C_0 = \tilde{\psi}_s^{\gamma_s}(h_s)\, \frac{I\lambda}{2\pi c_s \tilde{\varrho}_s} \frac{\tilde{G}_{12}\, I_{-\gamma_s}\left((\lambda/\tilde{\varrho}_s)\,\tilde{\psi}_s(h_s)\right) + \tilde{G}_{22}\, K_{-\gamma_s}\left((\lambda/\tilde{\varrho}_s)\,\tilde{\psi}_s(h_s)\right)}{\tilde{F}_{11}\tilde{G}_{22} - \tilde{F}_{21}\tilde{G}_{12}},$$

$$D_n = \tilde{\psi}_s^{\gamma_s}(h_s)\, \frac{I\lambda}{2\pi c_s \tilde{\varrho}_s} \frac{\tilde{F}_{11}\, I_{-\gamma_s}\left((\lambda/\tilde{\varrho}_s)\,\tilde{\psi}_s(h_s)\right) + \tilde{F}_{21}\, K_{-\gamma_s}\left((\lambda/\tilde{\varrho}_s)\,\tilde{\psi}_s(h_s)\right)}{\tilde{F}_{11}\tilde{G}_{22} - \tilde{F}_{21}\tilde{G}_{12}}.$$

As C_0, D_0, C_n and D_n are determined, so C_k and D_k, where $k \neq 0$ and n, can be obtained from the upward and downward recurrences as shown in equations (4.23) and (4.24).

4.6 Numerical Experiments and Inversion Processes

In our inverse model examples, we simulate array data of the electric potential from our forward models of practical interest. Two types of ground structures are used to investigate the conductivity profiles. Chave's algorithm is used for numerically calculating the inverse Hankel transform of the electric potential solutions. The special functions are computed by using the Numerical Recipes source codes. The electric current of 1 ampere is used in our computations. The Newton-Raphson and quasi-Newton methods in optimization are applied to find the conductivity parameters of the ground.

4.6.1 Sample Tests

We firstly consider the electric potential data obtained from the models of two simple cases. Both of the test ground models have two layers. The conductivity in the region of air is approximately equal to zero. The overburden of these models has a constant conductivity denoted by a with thickness h, whereas the host has a linearly varying conductivity denoted by $\sigma(z) = a + m(z - h)$ with infinite depth. The values of the model parameters are given in Table 4.1. The buried depth of the current source for our entire models is 10 metres. The parameter a is a conductivity of the earth's surface, which can be assumed to be known from the measurement. This implies that the first example model has only one unknown parameter, namely, m. The iterative procedure using the Newton-Raphson method is applied to estimate this unknown parameter, whereas the unknown parameters m and h of the second model are estimated by using the quasi-Newton optimization technique. We start the iterative processes to find the values of the model parameters with initial guess values $m = 0.01$ S·m^{-2} and $h = 10$ m. The optimal result of the first model is close to the true value with misfit less than 10^{-15} A·m^{-1} after using only 5 iterations (see Table 4.2). Figure 4.2 shows the convergence of inversion for the second model. After using 19 iterations, the method leads to the optimal result with misfit less than 10^{-8} A·m^{-1}.

Table 4.1: Model parameters used in our sample tests.

	Parameters		
Model	a (S·m^{-1})	m (S·m^{-2})	h (m)
1	0.1692857143	0.0261904761	10
2	0.1692857143	0.0261904761	15

Table 4.2: Successive iterations for finding a conductivity parameter of the first model in our sample tests.

Iteration	Parameter m (S·m^{-2})	Misfit (A·m^{-1})
0	$1.000000000000000 \times 10^{-2}$	$4.749162622332120 \times 10^{-2}$
1	$2.033955876743766 \times 10^{-2}$	$1.293418643404850 \times 10^{-2}$
2	$2.552178316744411 \times 10^{-2}$	$1.330168906724910 \times 10^{-3}$
3	$2.618214527566087 \times 10^{-2}$	$1.636837440359377 \times 10^{-5}$
4	$2.619047481445817 \times 10^{-2}$	$2.525438450070918 \times 10^{-9}$
5	$2.619047610000015 \times 10^{-2}$	$1.539218879220922 \times 10^{-16}$

4.6.2 Interpretations of Simulated Real Data

We now consider the real data of electric potential obtained from the simulation models. The electric potentials are generated by the forward problems of the first and second models in our sample tests. Random errors up to 3% are superimposed on the scaled electric potentials to simulate the set of real data. The iterative procedures using the Newton-Raphson and quasi-Newton methods are also applied to estimate the model parameters of conductivity variations for the first and second models, respectively. The optimal result of the first model example is close to the true value with percentage error less than only 2.3% after using 19 iterations. The graphs of the true and estimated conductivity models are plotted as shown in Figure 4.3. The method for the second model leads to the optimal values of the parameters h and m in which the percentage errors are less than 4.3% and 8.0%, respectively, after using 23 iterations. Figure 4.4 shows the true and estimated conductivity models for the second model example.

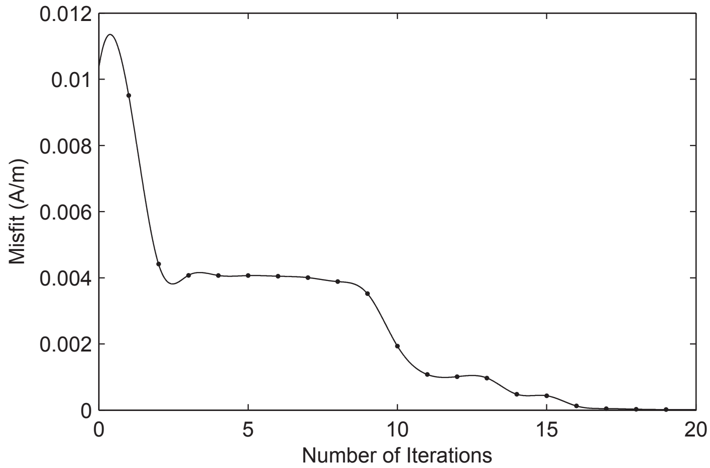

Figure 4.2: Misfit versus number of iterations for the second model in our sample tests.

4.7 Discussions

Analytical solutions of the electric potential resulting from a buried current source are derived by using upward and downward recurrences. The recurrence relations (4.12) and (4.13) are applied to determine a solution for the problem of a multilayered earth with layers having linearly varying conductivities, whereas the recurrence relations (4.23) and (4.24) are used for a binomial conductivity profile. These relations are applicable to general cases in which the layers have constant, linearly or binomially varying conductivities. Our solutions can be used to interpret hole-to-hole, hole-to-surface and conventional surface array data (the buried depth of the current source is assumed to be zero).

Inverse problems via the use of optimization techniques are introduced for finding the conductivity parameters of the ground. Two types of ground structures are used to investigate the conductivity profiles. The first ground model has only one unknown parameter of the conductivity variation. The iterative procedure using the Newton-Raphson method is applied to estimate this unknown parameter, whereas all the unknown parameters of the second model are estimated by using the quasi-Newton optimization technique. The optimal result of the first model in our sample tests converges very fast to the true value with misfit less than 10^{-15} $A{\cdot}m^{-1}$ after using only 5 iterations. The optimal result of the second model is also close to the true value with misfit less than 10^{-8} $A{\cdot}m^{-1}$ after using 19 iterations. These illustrate the advantage in using the Newton-Raphson and quasi-Newton methods which give the results much better than using another method of inversion (e.g., Oldenburg [44], Vozoff and Jupp [65]). Moreover, in the interpretations of simulated real data, the optimal result of the first model converges to the true value with percentage error less than only 2.3% after using 19 iterations. The graphs of the true and estimated conductivity models are plotted as shown in Figure 4.3. We see that the graph of the estimated model is close to the true model. After using 23 iterations, the inversion method for the second model leads to the optimal

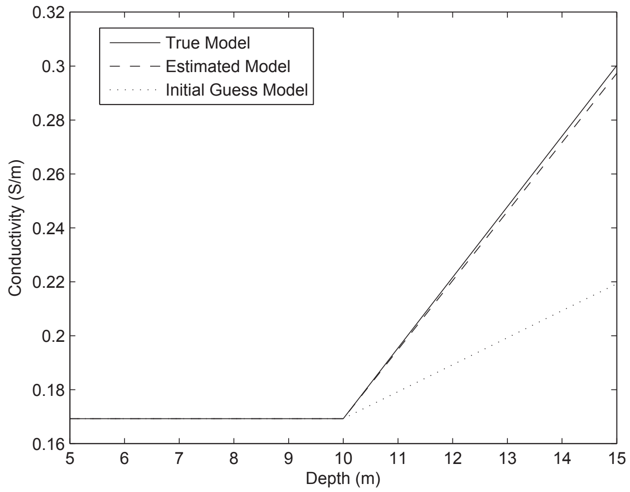

Figure 4.3: Graphs of conductivity σ against depth z for our first model example.

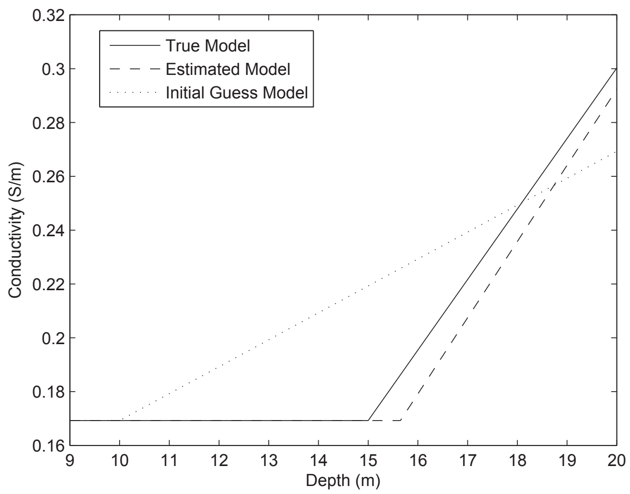

Figure 4.4: Graphs of conductivity σ against depth z for our second model example.

values of the conductivity parameters in which the percentage errors are less than 4.3% and 8.0%. Figure 4.4 shows the true and estimated conductivity models for the second model example. The graph of the estimated model is also close to the true model. The inversion methods lead to very good results and have high speed of convergence. This shows the robustness of our models and procedures. We note that, since the number of unknown parameters in the first model is less than the unknown parameters in the second model example, not surprisingly, the convergence of inversion for the first model is faster than the inversion for the second model. Moreover, the optimal result of the first model should also be better than the result of the second model example.

4.8 Summary and Conclusions

The problem of a buried current source and a buried receiver in a transitional medium is studied in this chapter. We derive analytical solutions of the electric potential resulting from a direct current point source located anywhere within two types of multilayered earth structures including layers having linearly varying conductivities and layers having binomially varying conductivities. The Hankel transform is introduced to our problems and analytical results are obtained. Our solutions are achieved by solving a boundary value problem in the wave number domain and then transforming the solution back to the spatial domain. The propagator matrix technique is used to formulate upward and downward recurrences for solving the problems. One of these relations is generalized in all cases where the layers have constant, linearly or binomially varying conductivities. Our solutions can be used to interpret hole-to-hole, hole-to-surface and conventional surface array data. The inversion processes, using the Newton-Raphson and quasi-Newton methods, are conducted to estimate the conductivity variation parameters. The methods also perform very good results and have high speed of convergence.

Chapter 5

Regularized Solution of Inverse Problem for DC Magnetic Field from a Multilayered Earth

5.1 Introduction

The electrical resistivity method was first applied by Conrad Schlumberger in 1912. The purpose of resistivity sounding is to investigate the change of formation resistivity with depth. The inverse problem in resistivity interpretation was reported as early as the 1930s. Slichter [53] presented a method of interpretation of resistivity data over a layered earth using Hankel's Fourier-Bessel inversion formula. The method gives a unique solution if the resistivity is a continuous function of electrode spacings. In practice, resistivity measurements are limited to a small number of readings taken at discrete electrode spacings, and thus, a unique resistivity response does not exist. Vozoff [53] tested Slichter's method on field and synthetic data generated for three-layered and four-layered earth models. The method becomes unstable if the data are noisy. Zohdy [75] proposed a method of direct resistivity interpretation which is valid for noisy data as well. Unfortunately, none of these earlier investigations deal with existence, uniqueness, construction and stability, which are important concerns and must be dealt with in any inverse problem.

In the late 1960s and early 1970s, Backus and Gilbert [4, 5, 6] introduced a linear inverse theory for geophysical problems. They thoroughly discussed model resolution, least squares fit of the data, and solution uniqueness. The method is valid even for noisy or insufficient data, and they quantified the trade-off between resolution and stability for solutions to inverse problems. The Backus-Gilbert approach, as do many others, suffers from the difficulty in estimating the degree of smoothness for all admissible models, this is required to calculate the greatest deviation between the estimated and true models. Following Backus and Gilbert's work, generalized linear inverse theory was described by Wiggins [68] and Jackson [29] in terms of linear algebra. They described classical solutions to inverse problems and resolution of model parameters in terms of matrix algebra.

The method of generalized linear inverse theory for the resistivity problem was introduced initially by Inman et al. [28]. They described the linearization of inverse resistivity problems and minimization in a least squares manner to find the best possible solution. They also discussed important information such as the noise level (random error) associated with data, the eigenvalues and eigenvectors of the system matrix, which are essential to study model parameter resolution. They did not discuss the singularity of the system metrix that arises with small but nonzero eigenvalues, which was experienced by Inman [27], Jupp and Vozoff [33], Vozoff and Jupp [65] in many resistivity problems. Thus, because of its ill-conditioned nature, the generalized linear inverse method is unstable for geophysical inverse problems which have a nearly singular system matrix. Only very simple resistivity structures do not produce a system matrix which is nearly singular.

Fortunately, Hoerl and Kennard [23, 24] showed that linear estimation from non-orthogonal data (i.e., nearly singular data) could be refined or improved by using biased estimators, this technique has been named ridge regression. Marquardt [42] established the similarities between the generalized inverse method and ridge regression method, and proved the suitability of ridge regression methods for problems with small eigenvalues. Because most common resistivity problems involve small eigenvalues, Inman [27] introduced ridge regression for inversion of resistivity data. Hoversten et al. [25] studied five different least squares inversion techniques and their speeds of convergence over horizontally layered resistivity structures. They showed that, of the five methods studied, ridge regression requires the fewest number of iterations to reach a desired minimum. A critical review of least squares inversion techniques and their application to layered geophysical problems has been done by Lines and Treitel [39].

Previously, one of the central problems in inversion theory was a solution of minimization problem for different functionals. This problem can be solved directly in the linear case of a forward operator. However, in the general case of a nonlinear operator, the solution can only be found iteratively. There are many different approaches to the construction of the iterative processes for functional minimization. One of the most widely used techniques for optimization is based on gradient-type methods. The formal solution of ill-posed inverse problem could result in unstable, unrealistic models. Regularization theory provides guidance for overcoming this difficulty. The foundations of regularization theory were developed in numerous publications by Andrei N. Tikhonov. Pous et al. [47] proposed an iterative technique for inverting one-dimensional resistivity data, where an error function is minimized. They tried to resolve equivalence in the resistivity data, and were able to obtain a more realistic model by using a regularization process.

In this study, we adapt and apply a regularization technique to inverse problems arising in geoelectrical resistivity sounding based on the measurement of static magnetic fields. The proposed method is the regularized conjugate gradient (RCG) method which is used to interpret magnetic field data gathered from a horizontally stratified layered earth. The L-curve criterion is applied to determine a suitable value of the regularization parameter. A comparison of this inversion scheme with conventional conjugate gradient (CG) and Levenberg-Marquardt (LM) methods on a test model is also presented.

5.2 Forward Problem

The forward problem expressed in terms of integral expression for magnetic field due to a direct current source on a horizontally stratified layered earth with all layers possessing constant conductivities was described and discussed in Chapter 2. The azimuthal component of the magnetic field, denoted by H_k, in the k-th layer is given as follows:

$$H_k\left(r,z\right)=\int_0^{\infty}\left(A_k e^{-\lambda z}+B_k e^{\lambda z}\right)J_1\left(\lambda r\right)d\lambda, \tag{5.1}$$

where A_k and B_k are undetermined coefficients that can be efficiently calculated through a recursive scheme presented in Section 2.3, and J_1 is the Bessel function of the first kind of order one. Equation (5.1) can be integrated by a quadrature and continued fraction expansion technique (e.g., Chave [10]).

5.3 Regularized Inversion Scheme

The main objective in our inversion method is to obtain a geologically interpretable model that can adequately reproduce observations. This is accomplished by posing the inverse problem as an optimization problem in which an objective function of the earth model is minimized.

5.3.1 Regularized Conjugate Gradient Method

Let us consider a geophysical inverse problem described by the operator equation

$$\mathbf{d}=A\left(\mathbf{m}\right),$$

where $\mathbf{m}$ is a model vector, $\mathbf{d}$ is an observed data vector and A is a nonlinear operator. In the framework of general regularization theory, a solution of inverse problem can be reduced to minimization of the Tikhonov parametric functional, namely

$$\min\mathcal{F}_\alpha\left(\mathbf{m}\right), \tag{5.2}$$

where

$$\mathcal{F}_\alpha\left(\mathbf{m}\right)=\left\|A\left(\mathbf{m}\right)-\mathbf{d}\right\|^2+\alpha\left\|\mathbf{m}\right\|^2,$$

α is a regularization parameter and $\|\cdot\|$ denotes the Euclidean norm. The regularized least squares problem (5.2) can be solved by applying a nonlinear conjugate gradient method. This technique generates a sequence $\mathbf{m}_k$ for $k\geq 1$, starting from an initial guess $\mathbf{m}_0$ and using the recurrence

$$\mathbf{m}_{k+1}=\mathbf{m}_k+\lambda_k\mathbf{h}_k,$$

where λ_k is a positive step size obtained by a line search, and $\mathbf{h}_k$ is a search direction generated by the rule

$$\mathbf{h}_0 = -\mathbf{g}_0, \qquad \mathbf{h}_{k+1} = -\mathbf{g}_{k+1} + \gamma_k \mathbf{h}_k,$$

where $\mathbf{g}_k = \nabla \mathcal{F}_\alpha (\mathbf{m}_k)$ and γ_k is an update parameter which can be determined by using the Fletcher-Reeves formula

$$\gamma_k = \frac{\mathbf{g}_{k+1}^\mathsf{T} \, \mathbf{g}_{k+1}}{\mathbf{g}_k^\mathsf{T} \, \mathbf{g}_k},$$

or the Polak-Ribiére formula

$$\gamma_k = \frac{(\mathbf{g}_{k+1} - \mathbf{g}_k)^\mathsf{T} \, \mathbf{g}_{k+1}}{\mathbf{g}_k^\mathsf{T} \, \mathbf{g}_k}.$$

5.3.2 Choice of the Regularization Parameter

There are several heuristic ways to proceed in order to select the regularization parameter, but the criterion based on the L-curve construction (Hansen [20], Hansen and O'Leary [22]) is certainly the most used. The method offers a convenient way to display regularized information as a function of the regularization parameter. The L-curve is a parametric plot of the norm of a regularized solution versus the norm of the corresponding residual. The idea of the L-curve criterion is to choose a regularization parameter related to the characteristic L-shaped corner of the L-curve which corresponds to a good balance between minimization of these two quantities. The L-curve's corner is defined as a point on the curve

$$(\mathcal{R}(\alpha), \mathcal{S}(\alpha)) = (\log \|A(\mathbf{m}_\alpha) - \mathbf{d}\|, \log \|\mathbf{m}_\alpha\|),$$

which has a maximum curvature. The curvature κ is usually given by the formula

$$\kappa(\alpha) = \frac{\mathcal{R}'\mathcal{S}'' - \mathcal{R}''\mathcal{S}'}{\left((\mathcal{R}')^2 + (\mathcal{S}')^2\right)^{3/2}},$$

where the differentiation is with respect to α.

5.4 Numerical Experiments

In our inverse model example, we simulate the reflection of magnetic radiation data from the forward model of practical interest. The model of a simple case for the ground structure is used to investigate the conductivity profile. The algorithm for regularized inversion is applied to find the model parameters of conductivity variation.

5.4.1 RCG Solution

As a sample test, we consider the synthesis model of a 2-layered earth. The overburden for our model has a constant conductivity σ_1 with thickness h over the host medium having constant conductivity σ_2 with infinite depth. The values of the model parameters are given in Table 5.1. The magnetic field data are generated by the forward problem of the example model for our sample test. Random errors up to 3% are superimposed on the scaled magnetic fields to simulate the set of real data. The parameter σ_1 is a conductivity of the earth's surface, which can be assumed to be known from the measurement. The iterative procedure using the regularized conjugate gradient method is applied to estimate the unknown parameters h and σ_2. We start the iterative process to find the values of the model parameters with initial guess values $h = 1$ m and $\sigma_2 = 0.01\ \mathrm{S{\cdot}m^{-1}}$. The suite of RCG solutions is obtained for a range of 20 values of α, ranging between approximately 2.3×10^{-15} and 5.3×10^{-17} after using 12 iterations. The L-curve of the model norm versus the data misfit is plotted as shown in Figure 5.1. As the regularization parameter α decreases, the curve moves from the lower right to the upper left. Figure 5.2 shows the curvature κ of the L-curve as a function of the regularization parameter α. The optimal value for α is located at the point of maximum curvature of the L-curve. The solution best satisfying the L-curve criterion corresponds to $\alpha = 1.1827196 \times 10^{-16}$ in which the misfit norm is roughly 2.4489561×10^{-7} (see Figure 5.3). Figure 5.4 shows the RCG solution for our sample test in comparison with the initial and true models.

Table 5.1: Model parameters used in our sample test.

Model Parameters		
σ_1 $(\mathrm{S{\cdot}m^{-1}})$	σ_2 $(\mathrm{S{\cdot}m^{-1}})$	h (m)
0.1	0.25	5

5.4.2 Comparison of Inversion Schemes

The regularization scheme for the inversion of magnetic field data is compared with conventional conjugate gradient and Levenberg-Marquardt methods in terms of the final model obtained from the same starting model, and the number of iterations taken to attain the final model parameters. The usefulness of the scheme proposed here is demonstrated by Table 5.2 which compares the results obtained from three inversion schemes tested on the example model in Section 5.4.1.

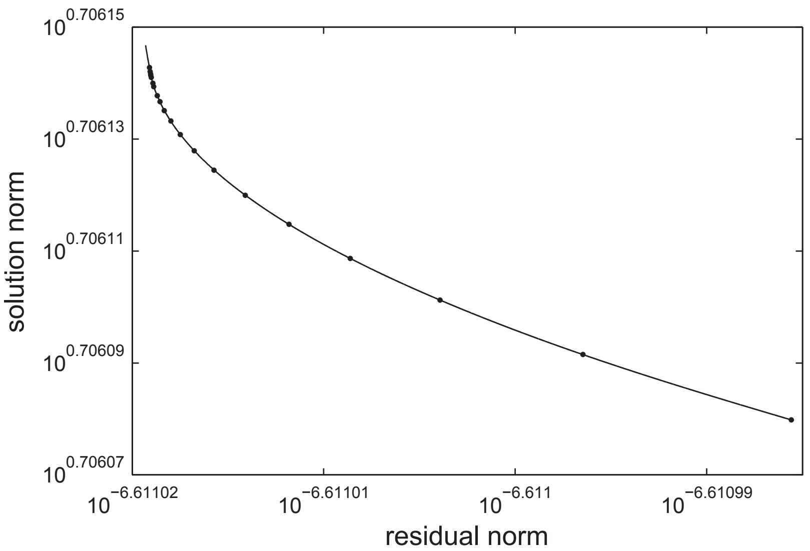

Figure 5.1: L-curve of solution norm versus corresponding residual norm.

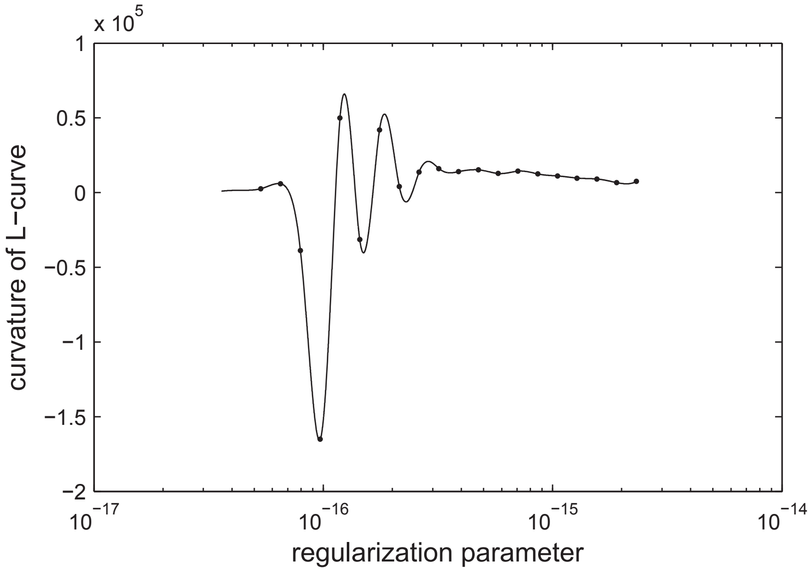

Figure 5.2: Curvature κ of L-curve as a function of regularization parameter α.

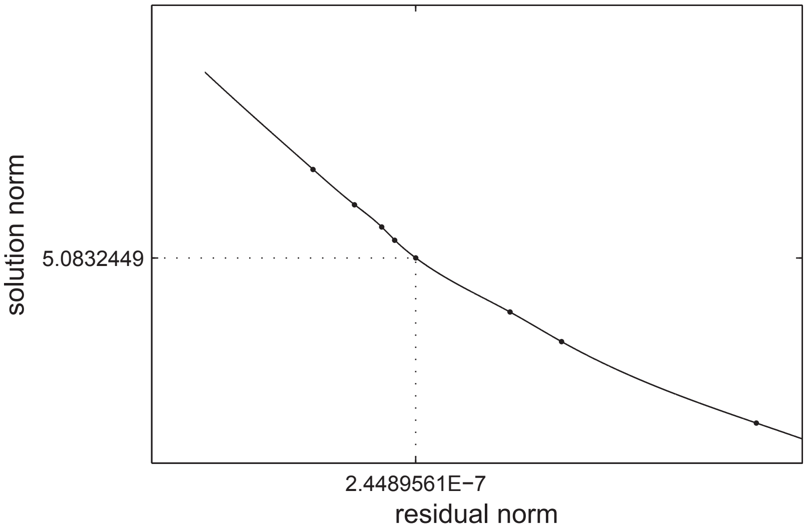

Figure 5.3: Characteristic L-shaped corner of L-curve as a point on curve with maximum curvature.

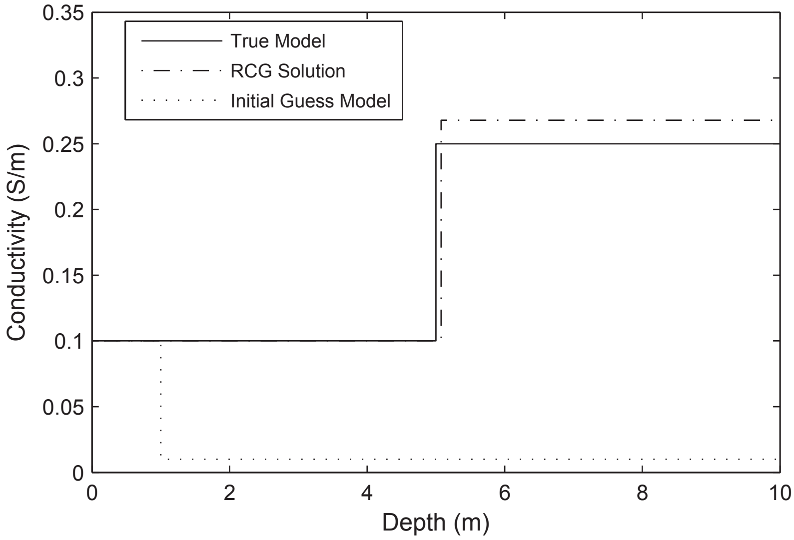

Figure 5.4: RCG solution shown in comparison with initial and true models.

Table 5.2: Comparison table of results obtained from three inversion schemes.

	Inversion Schemes		
	RCG	CG	LM
no. of iterations	12	13	17
h	5.0761858	5.0762371	5.0762391
% error in h	1.5237159	1.5247415	1.5247811
σ_2	2.6779874×10^{-1}	2.6780332×10^{-1}	2.6780341×10^{-1}
% error in σ_2	7.1194965	7.1213277	7.1213621
residual norm	2.4489561×10^{-7}	2.4489552×10^{-7}	2.4489552×10^{-7}
solution norm	5.0832449	5.0832963	5.0832983
error norm	7.8237271×10^{-2}	7.8288248×10^{-2}	7.8290194×10^{-2}

5.5 Discussions

A regularization technique can be applied to inverse problems arising in geoelectrical resistivity sounding. The model of a simple case for the ground structure is used to investigate the conductivity profile. The iterative scheme using the regularized conjugate gradient method is applied to estimate the model parameters of conductivity variation. The L-curve criterion is used to select an optimal value of the regularization parameter. The scheme has taken only 12 iterations to attain the true model parameters. The graphs of the true and estimated conductivity models are plotted as shown in Figure 5.4. We see that the graph of the estimated model is close to the true model. The inversion scheme leads to very good result and has high speed of convergence. A comparison of inversion results obtained from our scheme, conventional conjugate gradient and Levenberg-Marquardt methods on a test data set clearly demonstrates an edge over the other two stated schemes as far as the robustness is concerned (see Table 5.2). This illustrates the advantage in using the RCG method which gives the result much better than using another method of inversion.

5.6 Summary and Conclusions

An inversion scheme for nonlinear ill-posed problems arising in geoelectrical resistivity sounding is presented in this study. The proposed method is the regularized conjugate gradient method which is used to interpret magnetic field data gathered from a horizontally stratified layered earth. The L-curve criterion is applied to determine a suitable value of the regularization parameter. The final inverted model obtained is qualitatively in good agreement with the real model from synthetic data. A comparison of this scheme with conventional conjugate gradient and Levenberg-Marquardt methods on a test model is also presented, and our scheme is found to be more robust than the other two schemes. The example of using RCG scheme described here has been successfully applied for geophysical inversion of magnetic field data.

Chapter 6

Conclusions and Future Works

6.1 Conclusions of the Thesis

Of all the electrical prospecting methods, resistivity sounding is the simplest way to understand in principle. This thesis has been concerned about the problem of determining resistivity kernel function for a horizontally stratified layered earth. An inverse problem in resistivity interpretation has also been described and discussed in this study.

In the first part of this thesis, covering Chapters 2 and 3, we presented a new electrical method used for investigation of a multilayered earth structure. The method proposed here is based on the measurement of low-level, low-frequency static magnetic fields associated with noninductive current flow between two current electrodes on the earth's surface. In Chapter 2, we derived analytical solutions of the steady state magnetic field due to a direct current source on two types of multilayered earth structures including layers having constant conductivities and layers having exponentially varying conductivities. The Hankel transform was introduced to our problems and analytical results were obtained. Our solutions were achieved by solving a boundary value problem in the wave number domain and then transforming the solution back to the spatial domain. The propagator matrix technique was used to formulate recurrence relations for solving the problems. One of these relations is applicable to general cases in which the layers have either constant or exponentially varying conductivities. The effects of magnetic fields obtained from the DC and MMR methods were plotted and compared to show the behavior in response to different ground structures at many depths while some parameters were approximately given. The ground structures of rice paddy field and marine shrimp aquaculture farm were used to investigate the magnetic field responses. The magnetic fields obtained from different ground structures and methods of investigation are very much different, especially for the first 5 metres of source-receiver spacing. The curves of magnetic fields show some significance to the depth of overburden layer.

Recurrence relations used to calculate resistivity kernel functions of transitional ground structures were derived in Chapter 3. Two types of transitional zones were considered, including layers having linearly and binomially varying conductivities. One of these relations was generalized in all cases where the layers have constant, linearly or binomially varying conductivities. An inverse problem via the use of the Newton-Raphson optimization technique was introduced for finding a conductivity parameter of the ground. The method led to very good results and had high speed of convergence.

In the second part (Chapter 4) of this study, we discussed the problem of a buried current source and a buried receiver in a transitional medium. Analytical solutions of the electric potential resulting from a direct current point source located anywhere within multilayered earth structures were developed for this problem. The propagator matrix technique was also applied to make upward and downward recurrences for solving the problems. Our solutions can be used to interpret hole-to-hole, hole-to-surface and conventional surface array data. The inversion processes, using the Newton-Raphson and quasi-Newton methods, were conducted to estimate the conductivity variation parameters.

The last part of the thesis, Chapter 5, presented an inversion scheme for nonlinear ill-posed problems arising in geoelectrical resistivity sounding. The proposed method is the regularized conjugate gradient method which is used to interpret magnetic field data gathered from a horizontally stratified layered earth. The L-curve criterion was applied to select an optimal value of the regularization parameter. The final inverted model obtained is qualitatively in good agreement with the real model from synthetic data. A comparison of inversion results obtained from our scheme, conventional conjugate gradient and Levenberg-Marquardt methods on a test data set was also presented. This clearly demonstrates an edge over the other two stated schemes as far as the robustness is concerned. The scheme has been successfully used for geophysical inversion of magnetic field data.

6.2 Future Works

Even though the work presented in this thesis provides interesting ideas about the solutions to the forward and inverse problems in geoelectrical resistivity sounding, the issues that we dealt with suggest numerous avenues for possible extensions and future works. In the area of electrical resistivity methods described in this thesis, the following outline is a list of interesting future directions that require further investigation:

- On the magnetometric resistivity method, analytical solution of the magnetic field response from a multilayered earth containing buried electrodes can be derived by using the boundary conditions described in Chapters 2 and 4.
- The above solution should be developed for a non-uniform layered medium such as an exponentially varying conductivity structure. The case of a transitional medium should also be considered.

- In regularization process, stabilizing operator can be shaped to meet a smooth solution requirement, and its preferable implementations are the derivative of the first or second order of the solution.

Bibliography

[1] L. Alfano, Geoelectrical prospecting with underground electrodes, *Geophys. Prosp.* **10**(3)(1962), 290–303.

[2] I. Ali and S. Kalla, A generalized Hankel transform and its use for solving certain partial differential equations, *J. Austral. Math. Soc. Ser. B* **41**(1)(1999), 105–117.

[3] R. C. Aster, B. Borchers and C. H. Thurber, *Parameter Estimation and Inverse Problems*, International Geophysics Vol. 90, Elsevier Academic Press, 2005.

[4] G. Backus and F. Gilbert, Numerical applications of a formalism for geophysical inverse problems, *Geophys. J. R. astr. Soc.* **13**(1-3)(1967), 247–276.

[5] G. Backus and F. Gilbert, The resolving power of gross earth data, *Geophys. J. R. astr. Soc.* **16**(2)(1968), 169–205.

[6] G. Backus and F. Gilbert, Uniqueness in the inversion of inaccurate gross earth data, *Phil. Trans. R. Soc. A* **266**(1173)(1970), 123–192.

[7] B. Banerjee, B. J. Sengupta and B. P. Pal, Apparent resistivity of a multilayered earth with a layer having exponentiality varying conductivity, *Geophys. Prosp.* **28**(3)(1980), 435–452.

[8] B. Banerjee, B. J. Sengupta and B. P. Pal, Resistivity sounding on a multilayered earth containing transition layers, *Geophys. Prosp.* **28**(5)(1980), 750–758.

[9] F. Baumgartner, A new method for geoelectrical investigations underwater, *Geophys. Prosp.* **44**(1)(1996), 71–98.

[10] A. D. Chave, Numerical integration of related Hankel transforms by quadrature and continued fraction expansion, *Geophysics* **48**(12)(1983), 1671–1686.

[11] J. Chen and D. W. Oldenburg, Magnetic and electrical fields of direct currents in a layered earth, *Expl. Geophys.* **35**(2)(2004), 157–163.

[12] J. Chen and D. W. Oldenburg, A new formula to compute apparent resistivities from marine magnetometric resistivity data, *Geophysics* **71**(3)(2006), 73–81.

[13] J. J. Daniels, Interpretation of buried electrode resistivity data using a layered earth model, *Geophysics* **43**(5)(1978), 988–1001.

[14] A. Doicu, T. Trautmann and F. Schreier, *Numerical Regularization for Atmospheric Inverse Problems*, Springer-Praxis Books in Environmental Sciences, Springer-Verlag, 2010.

[15] R. N. Edwards, A downhole magnetometric resistivity technique for electrical sounding beneath a conductive surface layer, *Geophysics* **53**(4)(1988), 528–536.

[16] R. N. Edwards and E. C. Howell, A field test of the magnetometric resistivity (MMR) method, *Geophysics* **41**(6)(1976), 1170–1183.

[17] R. N. Edwards, H. Lee and M. N. Nabighian, On the theory of magnetometric resistivity (MMR) methods, *Geophysics* **43**(6)(1978), 1176–1203.

[18] R. N. Edwards and M. N. Nabighian, The magnetometric resistivity method, in M. N. Nabighian, ed., *Electromagnetic Methods in Applied Geophysics, Vol. 2: Application Parts A and B*, Investigations in Geophysics No. 3, Soc. Expl. Geophys., Tulsa, 1991, pp. 47–104.

[19] R. Fletcher, *Practical Methods of Optimization*, 2nd ed., John Wiley & Sons, 1987.

[20] P. C. Hansen, Analysis of discrete ill-posed problems by means of the L-curve, *SIAM Rev.* **34**(4)(1992), 561–580.

[21] P. C. Hansen, *Rank-Deficient and Discrete Ill-Posed Problems: Numerical Aspects of Linear Inversion*, Monographs on Mathematical Modeling and Computation, SIAM, Philadelphia, 1998.

[22] P. C. Hansen and D. P. O'Leary, The use of the L-curve in the regularization of discrete ill-posed problems, *SIAM J. Sci. Comput.* **14**(6)(1993), 1487–1503.

[23] A. E. Hoerl and R. W. Kennard, Ridge regression: biased estimation for nonorthogonal problems, *Technometrics* **12**(1)(1970), 55–67.

[24] A. E. Hoerl and R. W. Kennard, Ridge regression: applications to nonorthogonal problems, *Technometrics* **12**(1)(1970), 69–82.

[25] G. M. Hoversten, A. Dey and H. F. Morrison, Comparison of five least-squares inversion techniques in resistivity sounding, *Geophys. Prosp.* **30**(5)(1982), 688–715.

[26] A. A. Inayat-Hussain, Magnetic fields of direct currents in horizontally stratified conductors, *J. Appl. Phys.* **65**(9)(1989), 3731-3732.

[27] J. R. Inman, Resistivity inversion with ridge regression, *Geophysics* **40**(5)(1975), 798–817.

[28] J. R. Inman, J. Ryu and S. H. Ward, Resistivity inversion, *Geophysics* **38**(6)(1973), 1088–1108.

[29] D. D. Jackson, Interpretation of inaccurate, insufficient and inconsistent data, *Geophys. J. R. astr. Soc.* **28**(2)(1972), 97–109.

[30] S. C. Jain, Resistivity sounding on a three-layer transitional model, *Geophys. Prosp.* **20**(2)(1972), 283–292.

[31] J. J. Jakosky, Method and apparatus for determining underground structure, *U.S. Patent No. 1906271*, 1933.

[32] J. J. Jakosky, *Exploration Geophysics*, 2nd ed., Trija Pub. Co., Los Angeles, 1950.

[33] D. L. B. Jupp and K. Vozoff, Stable iterative methods for the inversion of geophysical data, *Geophys. J. R. astr. Soc.* **42**(3)(1975), 957–976.

[34] H.-S. Kim and K. Lee, Response of a multilayered earth with layers having exponentially varying resistivities, *Geophysics* **61**(1)(1996), 180–191.

[35] O. Koefoed, Resistivity sounding on an earth model containing transition layers with linear change of resistivity with depth, *Geophys. Prosp.* **27**(4)(1979), 862–868.

[36] T. Lal, Apparent resistivity over a three layer earth with an inhomogeneous interstratum, *Pure Appl. Geophys.* **82**(1)(1970), 259–269.

[37] T. J. Lee and R. Ignetik, Transient electromagnetic response of a halfspace with exponential conductivity profile and its applications to salinity mapping, *Expl. Geophys.* **25**(1)(1994), 39–51.

[38] K. Levenberg, A method for the solution of certain non-linear problems in least squares, *Quart. Appl. Math.* **2**(2)(1944), 164–168.

[39] L. R. Lines and S. Treitel, A review of least-squares inversion and its application to geophysical problems, *Geophys. Prosp.* **32**(2)(1984), 159–186.

[40] K. Mallick and A. Roy, Resistivity sounding on a two-layer earth with transitional boundary, *Geophys. Prosp.* **16**(4)(1968), 436–446.

[41] D. W. Marquardt, An algorithm for least-squares estimation of nonlinear parameters, *SIAM J. Appl. Math.* **11**(2)(1963), 431–441.

[42] D. W. Marquardt, Generalized inverses, ridge regression, biased linear estimation, and nonlinear estimation, *Technometrics* **12**(3)(1970), 591–612.

[43] M. N. Nabighian, G. L. Oppliger, R. N. Edwards, B. B. H. Lo and S. J. Cheesman, Cross-hole magnetometric resistivity (MMR), *Geophysics* **49**(8)(1984), 1313–1326.

[44] D. W. Oldenburg, The interpretation of direct current resistivity measurements, *Geophysics* **43**(3)(1978), 610–625.

[45] D. Patella, Resistivity sounding on a multi-layered earth with transitional layers, Part I: Theory, *Geophys. Prosp.* **25**(4)(1977), 699–729.

[46] D. Patella, Resistivity sounding on a multi-layered earth with transitional layers, Part II: Theoretical and field examples, *Geophys. Prosp.* **26**(1)(1978), 130–156.

[47] J. Pous, A. Marcuello and P. Queralt, Inversion with an alternative error function in resistivity measurements, *Geoexpl.* **23**(4)(1985), 527–536.

[48] W. H. Press, S. A. Teukolsky, W. T. Vetterling and B. P. Flannery, *Numerical Recipes in Fortran 77: The Art of Scientific Computing*, Fortran Numerical Recipes Vol. 1, 2nd ed., Cambridge Univ. Press, 1992.

[49] S. S. Raghuwanshi and B. Singh, Resistivity sounding on a horizontally stratified multi-layered earth, *Geophys. Prosp.* **34**(3)(1986), 409–423.

[50] H. K. Sato, Potential field from a dc current source arbitrarily located in a nonuniform layered medium, *Geophysics* **65**(6)(2000), 1726–1732.

[51] H. O. Seigel, The magnetic induced polarization (MIP) method, *Geophysics* **39**(3)(1974), 321–339.

[52] H. O. Seigel and A. W. Howland-Rose, Magnetic induced-polarization method, in J. B. Fink, B. K. Sternberg, E. O. McAlister, W. G. Wieduwilt and S. H. Ward, eds., *Induced Polarization: Applications and Case Histories*, Investigations in Geophysics No. 4, Soc. Expl. Geophys., Tulsa, 1990, pp. 23–56.

[53] L. B. Slichter, The interpretation of the resistivity prospecting method for horizontal structures, *Physics* **4**(9)(1933), 307–322.

[54] W. Sripanya, N. Chumchob and S. Yooyuanyong, Regularized inverse problem of magnetic field from a layered earth structure, *Pioneer J. Adv. Appl. Math.* (accepted).

[55] W. Sripanya and S. Yooyuanyong, Mathematical inverse problem of electric potential in a heterogeneous layered earth containing buried electrodes, *J. Math. Sci. Adv. Appl.* **7**(1)(2011), 37–56.

[56] W. Sripanya and S. Yooyuanyong, Mathematical inverse problem of magnetic field for transitional ground profile, *Pioneer J. Math. Math. Sci.* **2**(1)(2011), 17–29.

[57] W. Sripanya and S. Yooyuanyong, Mathematical modelling of magnetic field soundings for soil salinity profile, *Thai J. Math.* (submitted).

[58] C. H. Stoyer and J. R. Wait, Resistivity probing of an "exponential" earth with a homogeneous overburden, *Geoexpl.* **15**(1)(1977), 11–18.

[59] A. Tarantola, *Inverse Problem Theory and Methods for Model Parameter Estimation*, SIAM, Philadelphia, 2005.

[60] W. M. Telford, L. P. Geldart and R. E. Sheriff, *Applied Geophysics*, 2nd ed., Cambridge Univ. Press, 1990.

[61] A. N. Tikhonov and V. Y. Arsenin, *Solutions of Ill-Posed Problems*, V. H. Winston & Sons, Washington, 1977.

[62] D. Veitch, M. W. Asten and E. H. van Leeuwen, Electrical and magnetometric fields in a layered earth containing buried electrodes, *Geophysics* **55**(12)(1990), 1605–1612.

[63] C. R. Vogel, *Computational Methods for Inverse Problems*, Frontiers in Applied Mathematics, SIAM, Philadelphia, 2002.

[64] K. Vozoff, Numerical resistivity analysis: horizontal layers, *Geophysics* **23**(3)(1958), 536–556.

[65] K. Vozoff and D. L. B. Jupp, Joint inversion of geophysical data, *Geophys. J. R. astr. Soc.* **42**(3)(1975), 977–991.

[66] S. H. Ward and G. W. Hohmann, Electromagnetic theory for geophysical applications, in M. N. Nabighian, ed., *Electromagnetic Methods in Applied Geophysics, Vol. 1: Theory*, Investigations in Geophysics No. 3, Soc. Expl. Geophys., Tulsa, 1987, pp. 131-311.

[67] G. N. Watson, *A Treatise on the Theory of Bessel Functions*, 2nd ed., Cambridge Univ. Press, 1995.

[68] R. A. Wiggins, The general linear inverse problem: implication of surface waves and free oscillations for earth structure, *Rev. Geophys.* **10**(1)(1972), 251–285.

[69] S. Yooyuanyong, P. Lee and W. Sripanya, Soil salinity profile of marine shrimp aquaculture farm: a case study at Banglen, Nakornpathom, Thailand, *Thai J. Math.* **7**(3)(2009), 15–21.

[70] S. Yooyuanyong and W. Sripanya, Mathematical modelling of magnetometric resistivity sounding earth structures, *Thai J. Math.* **3**(2)(2005), 249–258.

[71] S. Yooyuanyong and W. Sripanya, Magnetic field of direct current in heterogeneous ground, *Songklanakarin J. Sci. Technol.* **29**(2)(2007), 565–573.

[72] S. Yooyuanyong and W. Sripanya, Analytical solutions of magnetic field response from multilayered earth structures, in Y. A. Hasan, N. M. Ali and A. I. M. Ismail, eds., *Proceedings of the 5th Asian Mathematical Conference, Vol. II: Applied Mathematics*, 2009, pp. 411–418.

[73] M. S. Zhdanov, *Geophysical Inverse Theory and Regularization Problems*, Methods in Geochemistry and Geophysics Vol. 36, Elsevier, 2002.

[74] M. S. Zhdanov, *Geophysical Electromagnetic Theory and Methods*, Methods in Geochemistry and Geophysics Vol. 43, Elsevier, 2009.

[75] A. A. R. Zohdy, *Automatic Interpretation of Schlumberger Sounding Curves, Using Modified Dar Zarrouk Functions*, New Techniques in Direct-Current Resistivity Exploration, U.S. Geol. Surv. Bull. No. 1313-E, U.S. Govt. Print. Off., Washington, 1975.

Publications of the Thesis

- S. Yooyuanyong and W. Sripanya, Analytical solutions of magnetic field response from multilayered earth structures, in Y. A. Hasan, N. M. Ali and A. I. M. Ismail, eds., *Proceedings of the 5th Asian Mathematical Conference, Vol. II: Applied Mathematics*, 2009, pp. 411–418.

- W. Sripanya and S. Yooyuanyong, Mathematical inverse problem of electric potential in a heterogeneous layered earth containing buried electrodes, *J. Math. Sci. Adv. Appl.* **7**(1)(2011), 37–56.

- W. Sripanya and S. Yooyuanyong, Mathematical inverse problem of magnetic field for transitional ground profile, *Pioneer J. Math. Math. Sci.* **2**(1)(2011), 17–29.

- W. Sripanya, N. Chumchob and S. Yooyuanyong, Regularized inverse problem of magnetic field from a layered earth structure, *Pioneer J. Adv. Appl. Math.* (accepted).

- W. Sripanya and S. Yooyuanyong, Mathematical modelling of magnetic field soundings for soil salinity profile, *Thai J. Math.* (submitted).

AMC 2009

This is to certify that

WARIN SRIPANYA

has presented a paper at the

5th Asian Mathematical Conference

*held on **June 22-26, 2009** at the **Putra World Trade Centre Kuala Lumpur, MALAYSIA***

Dean
School of Mathematical Sciences
(Conference Chairman)

UNIVERSITI SAINS MALAYSIA

Chiang Mai International Conference and Workshop-Applied Mathematics

4 - 7 January 2011

CMIC 2011

CONFIRMATION OF PARTICIPATION

Warin Sripanya and Suabsagun Yooyuanyong

The above–named attended the CMIC 2011 in Chiang Mai, 6 – 7 January 2011, and presented a talk entitled:

Mathematical modelling of magnetic field soundings for soil salinity profile

T. Chamkong

Head of the Department of Mathematics,
Faculty of Science, Chiang Mai University,
239 Huay Kaew Road, Muang District,
Chiang Mai, Thailand, 50200
Tel +66 53 943327
Fax +66 53 892280
http://math.science.cmu.ac.th/html/

Scientific Advances Publishers

Search

My Scientific Advances · Shopping Cart

Log In · Articles: 0

Home · Journals · Contact Us

Journal of Mathematical Sciences: Advances and Applications

Journal Menu

- About this Journal
- Aims and Scope
- Indexing and Reviews
- Frequency
- Managing Editor
- Editorial Board
- Author Guidelines
- Subscription
- Content

Article

Volume no :7, Issue no: 1, January (2011)

• MATHEMATICAL INVERSE PROBLEM OF ELECTRIC POTENTIAL IN A HETEROGENEOUS LAYERED EARTH CONTAINING BURIED ELECTRODES

PAGE: [37] - [56]
RECEIVED DATE: December 30, 2010
COMMUNICATED BY:
AUTHOR: Warin Sripanya and Suabsagun Yooyuanyong

• Abstract

We derive analytical solutions of the electric potential resulting from a direct current point source located anywhere within two types of multilayered earth structures including layers having linearly varying conductivities and layers having binomially varying conductivities. Our solutions are obtained by solving a boundary value problem in the wave number domain and then transforming the solution back to the spatial domain. The propagator matrix technique is used to formulate the upward-downward recurrences for solving the problems. One of these recurrences is applicable to general cases in which, the layers have constant, linearly or binomially varying conductivities. The equations derived for the electric potential can be used to interpret the hole-to-hole, hole-to-surface, and conventional surface array data. The inverse problems via the use of the Newton-Raphson and quasi-Newton optimization techniques are introduced for finding the conductivity parameters.

• Keywords

Hankel transform, inverse problem, electric potential, buried current source.

• Back · Add to cart

Pioneer Journal of Mathematics and Mathematical Sciences
Volume 2, Issue 1, Pages 17-29 (May 2011)

ISSN: 2230-9829

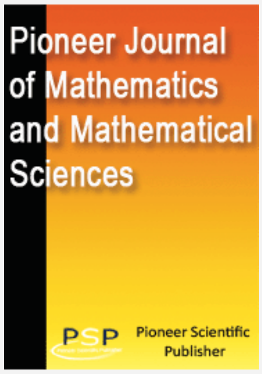

MATHEMATICAL INVERSE PROBLEM OF MAGNETIC FIELD FOR TRANSITIONAL GROUND PROFILE

Warin Sripanya and Suabsagun Yooyuanyong

Received March 12, 2011

Abstract

Magnetic field response due to the injection of electric current into the ground can be used to explore the earth structure. We derive analytical solutions of the steady state magnetic field due to a direct current source on two types of multilayered earth structures including layers having linearly varying conductivities and layers having binomially varying conductivities. Our solutions are obtained by solving a boundary value problem in the wave number domain and then transforming the solution in the wave number domain back to the spatial domain. The propagator matrix technique is used to formulate recurrence relations for solving the problems. One of these relations is applicable to general cases in which the layers have constant, linearly or binomially varying conductivities. An inverse problem via the use of the Newton-Raphson optimization technique is introduced for finding the conductivity parameter. The optimal result of our model is close to the true value after using only 3 iterations.

Keywords and phrases: Hankel transform, inverse problem, magnetic field, transitional layer.

Pioneer Scientific Publisher
Pioneer Research House, S 9/137A-4A Nai-Basti Pandeypur
Varanasi-221002, INDIA
http://www.pspchv.com

Acceptence

Pioneer Journal of Advances in Applied Mathematics

Reference no.: AAM 48-201111012 Date: December 27, 2011

To

Professor Suabsagun Yooyuanyong
Faculty of Science
Silpakorn University
Nakhon Pathom 73000, Thailand

Dear Professor Yooyuanyong

We are pleased to inform you that your paper entitled "*Regularized Inverse Problem of Magnetic Field from a Layered Earth Structure*" written jointly with Warin Sripanya and Noppadol Chumchob in the PJAAM has recommended and submitted by Professor V. Rai, Managing Editor of the Pioneer Journal of Advances in Applied Mathematics. Accordingly the Editorial Board is pleased to accept it for publication in the Pioneer Journal of Advances in Applied Mathematics.

Sincerely Yours

(A. K. Jaiswal)
(Executive Manager)

Curriculum Vitae

Name:	Warin Sripanya
Address:	10/6 M. 1, Lat Bua Khao, Ban Pong, Ratchaburi 70110.
Workplace:	Nakhon Pathom Rajabhat University 85 Malaiman Rd., Muang, Nakhon Pathom 73000.

Education

1996-2000	Bachelor of Science in Physics, Silpakorn University.
2001-2006	Master of Science in Mathematics, Silpakorn University.
2007-2012	Doctor of Philosophy in Mathematics, Silpakorn University.

Work Experience

2000-2001	Academic, The Institute for the Promotion of Teaching Science and Technology, Bangkok.
2011-Present	Lecturer, Faculty of Science and Technology, Nakhon Pathom Rajabhat University.